finalreport

Project code: B.MGS.0035

Prepared by: Richard Eckard, Brendan Cullen, The University of Melbourne

Val Snow, AgResearch, New Zealand

Date published: December 2008

ISBN: 978 0 734 04091 6

PUBLISHED BY

Meat & Livestock Australia Limited
Locked Bag 991
NORTH SYDNEY NSW 2059

Meat & Livestock Australia acknowledges the matching funds provided by the Australian Government to support the research and development detailed in this publication.

In submitting this report, you agree that Meat & Livestock Australia Limited may publish the report in whole or in part as it considers appropriate.

Climate change impacts on Australian grazing systems

Whole Farm Systems Analysis and Tools for the Australian and New Zealand Grazing Industries Project Report

December 2008

B Cullen[1], R Eckard[1], I Johnson[2], G Lodge[3], R Walker[4], R Rawnsley[5], K Dassanayake[1], K Christie[5], M McCaskill[6], S Clark[6], P Sanford[7], N Browne[6], K Sinclair[3], D Chapman[1], M Leiffering[8], V Snow[8], M Hovenden[9], M Perring[9]

[1] Melbourne School of Land and Environment, University of Melbourne
[2] IMJ Consultants, Armidale, NSW
[3] NSW Department of Primary Industries
[4] Queensland Department of Primary Industries and Fisheries
[5] Tasmanian Institute of Agricultural Research
[6] Victorian Department of Primary Industries
[7] Department of Agriculture and Food, WA
[8] AgResearch, New Zealand
[9] University of Tasmania

This page is intentionally left blank.

Summary

Climate change projections for Australia forecast increasing temperatures and changes to rainfall patterns. The aim of this work was to quantify the effects of climate change scenarios in 2030 and 2070 on pasture growth, species composition and water balance for a range of sites (cool temperate to subtropical) and pasture types, relative to an historical baseline climate. Six future climate scenarios were developed for each site by combining historical climate data with climate change projections for Low, Medium and High climate change scenarios in 2030 and 2070. The impact of the future climate scenarios on pasture production and water balance were modelled using the SGS Pasture Model and DairyMod. Detailed results for each site are presented. In general, climate change impacts on pasture production were predicted to be minor under the 2030 scenarios, associated with temperature increases of up to 1.2^{o}C and rainfall reductions up to 9%. However, under High climate change projections for 2070, with up to 4.4^{o}C warming and 30% annual rainfall declines, increased growth and a shift towards C_4 dominance was modelled in mixed C_3/C_4 swards in summer dominant rainfall regions or where irrigation was applied, while declines up to 19% of annual production of C_3 dominant pastures in southern Australia were predicted. In the C_3 dominant pastures, the decline in production was moderated by reduced drainage below the root zone, and employing deeper rooted plant systems was an effective means of mitigating some of the impact of lower rainfall. In areas where irrigation was used, the irrigation requirement increased by up to 10% (with no extension of the irrigation season), with the greatest increase in the northern Victorian dairying region. This is also an area where climate change is likely to cause a reduction in irrigation water availability.

Introduction

Climate change projections for Australia forecast increasing temperatures and changes to rainfall patterns, with elevated atmospheric CO_2 concentrations (CSIRO 2007). In a review of climate change issues for the Australian grazing industries, Howden *et al.* (2008) identified three areas of likely impact on the pasture resource base;

1. the amount and reliability of forage production, where overall impact will be determined by the combination of climatic effects and plant responses to elevated atmospheric CO_2,
2. forage quality, where the overall impact will be determined by changes in water-soluble carbohydrates and leaf N concentration, as well as the balance between C_3 and C_4 species, and
3. degradation process such as erosion and salinity, where changing rainfall amount and intensity will influence the risk of runoff and drainage events.

The impact of climate change will vary according to the regional change projections and characteristics of the farming system (eg. pasture species sown). Climate change projections for Australia indicate a general warming, but with different impacts on rainfall generally along a north-south gradient. In the subtropical regions, little change in annual rainfall is predicted but a shift in rainfall distribution to more summer dominance

is forecast, while in southern Australia annual rainfall declines are predicted with spring being the season most heavily affected (CSIRO 2007).

The objective of this paper was to quantify changes in pasture production, forage quality (as determined by the balance between C_3 and C_4 species) and degradation process (using the surrogates of runoff and drainage below the root zone for erosion and salinity respectively) in response to projected climatic changes. To do this, pasture systems were simulated along a north-south gradient, taking in a range of environments from tropical upland to cool temperate and a range of pasture types from C_4 to C_3 dominant. The specific aim of this study was to quantify the effects of climate change scenarios in 2030 and 2070 on pasture growth, species composition and water balance for a range of sites (from tropical to cool temperate climates) and pasture types, relative to an historical baseline climate. In addition, where large changes in pasture dry matter (DM) production were predicted, a second aim was to investigate the potential of an adaptation option to reduce the climate change impact, specifically by increasing plant rooting depth.

Materials and Methods

Sites and pasture systems simulations

Climate change impacts on pastoral systems were modelled at 13 sites across Australia, ranging from C_4 dominant pastures in tropical northern Queensland to C_3 pastures in the cool temperate environment of north western Tasmania. The site details, including location, climatic zone and pasture species, are shown in Table 1. All sites were in the medium-high rainfall zone, with Kyabram being the site with the lowest mean rainfall (470 mm, Table 1). The SGS Pasture model and DairyMod version 4.7.5 (Johnson *et al.* 2003; 2008) were used to simulate pasture growth rates based on the local conditions at each site. These models utilise the same equations for their soil and pasture growth components, and have previously been shown to adequately simulate pasture growth rates across a range of climatic zones (Cullen *et al.* 2008; White *et al.* 2008). All simulations were conducted without nutrient limitation and a consistent grazing management system was implemented. Grazing was applied using a 'put and take' system, whereby animal numbers were adjusted daily to maintain the pasture mass at 2 t DM/ha and removed when the mass was less than this target, so as not to bias scenarios by applying inappropriate grazing management.

Irrigated pasture systems were simulated at Malanda, Mutdapilly, Kyabram, Dookie and Elliott. The irrigation season was defined according to typical practice in each region. At Malanda irrigation was applied between 15 April and 30 November, at Mutdapilly from 15 April to 28 February, while at Dookie and Kyabram the irrigation season was from 15 August to 30 April. Irrigation was applied whenever required (ie. all year round) at Elliott.

Table 1. Descriptions of each site, including location, soil type (Isbell 1996), climatic zone, mean annual rainfall (1971-2000, mm) and pasture species simulated.

Site	Lat./Long.	Soil type	Climate	Rainfall	Pasture species[A]
Malanda	-17.35, 145.59	Krasnozem	Tropical	1733	Dryland – setaria Irrigated – setaria, ARG
Mutdapilly	-27.63, 152.71	Black vertosol	Subtropical	859	Dryland – Rhodes grass Irrigated – Sorghum, ARG
Kyogle	-28.62, 153.00	Clay loam	Subtropical	1177	Kikuyu, ARG
Barraba	-30.55, 150.65	Red chromosol	Subhumid	661	Native C_3, native C_4
Albany	-34.90, 117.80	Petroferric brown sodosol	Temperate	761	Kikuyu, subclover
Wagga Wagga	-35.10, 147.30	Red chromosol/leptic tenosol	Mediterranean	565	Phalaris, subclover, native C_4
Kyabram	-36.34, 145.06	Red-brown chromosol	Mediterranean	470	Irrigated – PRG, subclover, pasp. Dryland – PRG, subclover, pasp.
Dookie	-36.37, 145.70	Vertic calic red chromosol	Mediterranean	592	PRG, subclover, paspalum
Vasey	-37.40, 141.90	Yellow sodosol	Mediterranean	640	Phalaris, subclover, ARG
Hamilton	-37.83, 142.06	Brown chromosol	Temperate	689	PRG, subclover
Terang	-38.15, 142.55	Brown chromosol	Temperate	746	PRG, white clover
Ellinbank	-38.25, 145.93	red mesotrophic haplic ferrosol	Temperate	1078	PRG, white clover
Elliott	-41.08, 145.77	red mesotrophic haplic ferrosol	Cool temperate	1220	Dryland – PRG, white clover Irrigated – PRG, white clover

[A] ARG = annual ryegrass, PRG = perennial ryegrass

Table 2. Annual average temperature and rainfall change statistics for the six future climate scenarios at each site.

	2030 Low		2030 Medium		2030 High		2070 Low		2070 Medium		2070 High	
	Temp (°C)	Rain (%)	Temp (°C)	Rain (%)	Temp (°C)	Rain (%)	Temp (°C)	Rain (%)	Temp (°C)	Rain (%)	Temp (°C)	Rain (%)
Malanda	0.5	-1	0.8	-1.5	1	-1.9	1.1	-2.1	2.2	-4.2	3.6	-6.8
Mutdapilly	0.7	-0.2	1	-0.3	1.2	-0.4	1.3	-0.4	2.6	-0.8	4.3	-1.3
Kyogle	0.6	0.2	1	0.3	1.2	0.3	1.3	0.4	2.6	0.7	4.2	1.2
Barraba	0.7	0.8	1	1.2	1.2	1.4	1.4	1.6	2.7	3.2	4.4	5.2
Albany	0.5	-3.2	0.7	-4.7	0.9	-5.8	1	-6.5	2	-12.8	3.3	-20.9
Wagga Wagga	0.4	-4.6	0.6	-6.9	0.7	-8.4	0.8	-9.5	1.5	-18.6	2.5	-30.5
Kyabram	0.6	-3	0.8	-4.4	1	-5.4	1.2	-6.1	2.3	-11.9	3.7	-19.5
Dookie	0.6	-2.6	0.8	-3.9	1	-4.7	1.2	-5.3	2.3	-10.5	3.7	-17.2
Vasey	0.4	-4.4	0.7	-6.6	0.8	-8.1	0.9	-9.1	1.8	-17.9	2.9	-29.3
Hamilton	0.4	-4.5	0.6	-6.7	0.8	-8.2	0.9	-9.2	1.7	-18.2	2.8	-29.8
Ellinbank	0.5	-2.8	0.7	-4.2	0.9	-5.1	1	-5.7	2	-11.2	3.3	-18.4
Terang	0.4	-4.3	0.6	-6.5	0.8	-7.9	0.9	-8.9	1.7	-17.6	2.8	-28.8
Elliott	0.4	-3.1	0.6	-4.6	0.7	-5.6	0.8	-6.3	1.5	-12.3	2.5	-20.2

The climate scenarios developed for each site were modelled using the consistent nutrient, grazing and irrigation management rules outlined. The impact of climate scenarios on monthly and annual pasture production, and the water balance at each site was investigated.

Climate scenarios

An historical baseline climate and six future climate scenarios were used to compare the productivity of pasture systems. A 30-year climate 'baseline' (1971-2000) was used to capture inherent climate variability at each site. Although the period 1961-1990 is often used as the baseline for climate change impact analysis, the period 1971-2000 was adopted as the baseline in this study because it better reflects the recent climate, following the convention of Hennessy (2007). This 'baseline' was also used to create 30-year realisations of future climate scenarios. Six future climate scenarios were developed for each site by combining historical climate data with Low, Medium and High climate change projections for 2030 and 2070. A 10-year lead-in period, based on 1961-1970 historical climate data, was modelled prior to the each scenario to stabilise the initial conditions of the model.

For each site, historical climate data for the 30-year baseline and 10-year 'lead-in' period (1/1/1961-31/12/2000 in total) were obtained from the Bureau of Meteorology SILO database (http://www.nrw.qld.gov.au/silo/ppd/, Jeffery *et al.* 2001). Monthly average minimum and maximum temperature and rainfall over this 30-year baseline climate were tested for the presence of any linear annual trends (Anwar *et al.* 2007), however, few significant trends were observed (as measured by r^2 correlation), so de-trending of the data to 1990 was not performed. The lack of significant trends was probably due to the relatively short (ie. 30 year) dataset examined.

The monthly climate change statistics for mean temperature (^oC) and rainfall (%) changes were based on output from the CSIRO Mk3 global circulation model, obtained from the OzClim database (www.csiro.au/ozclim). The Low, Medium and High climate change impact scenarios were based on B1 emission scenario with low climate sensitivity, A1B emission scenario with medium climate sensitivity and A1FI emission scenario with high climate sensitivity respectively. The change in annual average temperature and rainfall change statistics for each site under the six future climate scenarios are shown in Table 2. The differences between the Low, Medium and High scenarios were smaller in 2030, with 0.4-1.2^{o}C temperature and -8-+1% rainfall changes, than in 2070, where the corresponding changes are 0.8-4.4^{o}C and -30-+5% rainfall (Table 2). The change statistics also differed according to region with slightly larger temperature increases in northern compared to southern Australia, but while there is little change in annual rainfall in northern Australia decreases of up to 30% were predicted in southern sites (Table 2). In addition, seasonal changes were also evident, with reduced spring rainfall and increased summer/autumn rainfall in northern sites, and in southern Australia the majority of the annual rainfall reductions were projected to occur in spring. A full summary of the monthly change statistics for each site is provided in Appendix 1. To

convert changes in mean temperature to changes in maximum and minimum temperature required by the models, minimum/maximum temperature scalar factors were used, based on Fig 5.10 (CSIRO 2007, p. 60). These scalar factors were in the range 0.85-1.15. Finally, annual change statistics for radiation and relative humidity were incorporated for each scenario by applying the changes from the nearest site reported in 'Appendix B – City Summaries' (CSIRO 2007, p. 130-136).

The daily historical baseline climate data was directly scaled according to the climate change statistic for each future climate scenario, adapting an approach applied in previous climate change impact analyses (eg. van Ittersum *et al.* 2003; Anwar *et al.* 2007). For example, the historical weather on the 1st of January 1971 at Ellinbank was a minimum temperature 10°C, maximum temperature 17°C and rainfall of 10.2 mm. In the 2070 High future scenario, the climate change statistics for January at Ellinbank were +3.7°C average temperature change, with a minimum temperature scalar of 0.9 and a maximum temperature scalar of 1, and a rainfall change of -17.9%. Therefore, weather on the 1st January 1971, scaled to the 2070 High future climate scenario (i.e. 1st January 2070) was minimum temperature 13.5°C, maximum temperature 20.9°C and rainfall 8.4 mm.

Two further rainfall scenarios were developed to reflect a change in the distribution of rainfall events, such that large rainfall events are increased in volume and small rainfall events become less important (CSIRO 2007). To simulate this change in rainfall distribution, two rainfall distribution treatments were created whereby rainfall events greater than the average event were scaled to increase by 10 and 20% respectively, with reductions to rainfall events less than the average made to keep the long-term average annual rainfall the same. For example, in the Ellinbank 'baseline' climate data the average rainfall event was 6.18 mm. To create the 'Rainfall distribution 10 and 20%' treatments, rain events greater than 6.18 mm were increased by 10% and 20%, with reductions of 33 and 66% for below average rainfall events imposed to keep the long-term average annual rainfall the same. Imposing this treatment did create a small increase in inter-annual rainfall variability.

In addition, climate change projections also suggest more 'extreme' events (CSIRO 2007). This was simulated by increasing the inter-annual rainfall variability. This was achieved by making the wettest 7 years in the 30-year baseline wetter by increasing rainfall by 10 and 20% and making the driest 7 years in the baseline climate were made drier by 10 and 20%, to create the 'Inter-annual 10 and 20%' treatments. The 'Inter-annual 10%' treatment was applied to the 'Rainfall distribution 10%' data-set and the 'Inter-annual 20%' treatment was applied to the 'Rainfall distribution 20%' data-set so that both rainfall distribution and inter-annual variability was altered. These treatments produced a small increase in mean rainfall but a large increase in inter-annual rainfall variability.

Appendix 1 provides a step-by-step guide to creating the climate scenarios and documents the monthly climate change statistics applied for each scenario and site.

The baseline scenarios used an atmospheric CO_2 concentration of 380 ppm. This was increased in the 2030 Low, Medium and High climate change scenarios to 429, 446 and 455 ppm CO_2 respectively, and in the 2070 scenarios to 525, 581 and 716 ppm CO_2 (IPCC 2001).

Photosynthesis, nitrogen and canopy conductance responses to CO_2

The three principal physiological plant responses to elevated CO_2 concentration are:

- An increase in leaf photosynthetic potential;
- A decrease in plant nitrogen content; and
- A decrease in stomatal, and therefore canopy, conductance (Long *et al.* 2004).

While mechanistic approaches are possible to describe these responses (eg. Johnson *et al.* 1995), we have used simple empirical scaling functions in this whole-system simulation model.

The response of leaf photosynthetic potential, P_{mx} mg CO_2 (m^2 leaf)$^{-1}$, is defined by

$$P_{mx} = P_{mx,amb}\left(\frac{C}{C+K_P}\right)\left(\frac{C_{amb}+K_P}{C_{amb}}\right) \qquad (1)$$

where C , ppm, is atmospheric CO_2 concentration, C_{amb} is the current ambient level, taken to be 380 ppm, K_P ,ppm, is a constant, and $P_{mx,amb}$ is the value of P_{mx} at ambient CO_2. Equation (1) is a simple Michalis-Menten type response, also referred to as a rectangular hyberbola (Thornley and Johnson, 2000). The term in the second bracket is constant and is there to impose the constraint $P_{mx}(C = C_{amb}) = P_{mx,amb}$.

The response of plant nitrogen level, f_N , kg N (kg dry weight)$^{-1}$, to CO_2 concentrations is described by

$$f_N = f_{N,amb}\left[\lambda + (1-\lambda)\frac{(K_N - C_{amb})^{\alpha}}{(K_N - C_{amb})^{\alpha} + (C - C_{amb})^{\alpha}}\right] \qquad (2a)$$

where α is a curvature coefficient, and K_N , ppm, and λ are scaling parameters. According to this equation,

$$f_N(C = C_{amb}) = f_{N,amb}$$

$$f_N(C = K) = f_{N,amb}\frac{1+\lambda}{2} \qquad (2b)$$

$$f_N(C \to \infty) = \lambda f_{N,amb}$$

The first of these confirms that $f_{N,amb}$ is the value of f_N at ambient CO_2; the third that this is reduced by the factor λ at saturating CO_2 while the second shows that, when $C = K$, f_N is the average of the value at ambient and saturated CO_2.

Canopy conductance, which is the sum of leaf stomatal conductances in the canopy, declines in response to CO_2 as described by

$$g_c = g_{c,mn} + \left(g_{c,mx} - g_{c,mn}\right)\frac{\left(1-g_{c,mn}\right)C_{amb}^{\beta}}{\left(g_{c,mx}-1\right)C^{\beta} + \left(1-g_{c,mn}\right)C_{amb}^{\beta}} \qquad (3a)$$

where β is a curvature coefficient and $g_{c,mn}$ and $g_{c,mx}$ are values such that

$$g_c\left(C=0\right) = g_{c,mn}$$

$$g_c\left(C\to\infty\right) = g_{c,mx}$$

$$g_c\left(C=C_{amb}\right) = 1$$

These simple and versatile functions allow the flexibility within the model to explore the consequences of different responses to elevated CO_2. In this study, increased leaf photosynthetic potential was defined using a CO_2 scale parameter of 700 for C_3 species and 150 for C_4 species, giving the responses shown in Figure 1, relative to 380 ppm CO_2. For plant N content, a scale parameter of 600 was used with a minimum value of 0.7 for C_3 species and 0.85 for C_4 species, giving the responses to increasing CO_2 shown in Figure 2. The canopy conductance response was defined using a maximum value of 1.25, a minimum value of 0.2 and a scale factor of 2.5. The shape of this canopy conductance response to increasing atmospheric CO_2 is shown in Figure 3. Using these parameters, the modelled responses for leaf photosynthetic potential, plant N content and stomatal conductance at 550 ppm CO_2 were compared with experimental results from free air CO_2 enhancement (FACE) studies and biomass multipliers used in other crop models in Table 3. While care must be taken in directly comparing the model responses with the experimental results, because the responses measured are relative to different baseline and elevated CO_2 concentrations, this demonstrates that the CO_2 effects implemented in the model were within the ranges that have been measured (Table 3).

The impact of elevated CO_2 concentrations on annual pasture production was tested by comparing the baseline scenario (380 ppm) with a simulation using the same weather but atmospheric CO_2 at 550 ppm. The yield response to increasing atmospheric CO_2 was dependant on the site and pasture type, with the largest responses (19-28% increases) generally occurring in C_3 dominant pastures in southern Australia (Table 4). C_4 pasture types had the lowest response (7-8%), while mixed C_3/C_4 pastures were intermediate (8-19%). These modelled production increases are consistent with comparable results from FACE experiments, particularly where soil nutrients were non-limiting. For example, Lüsher *et al.* (2006) measured 7-32% increases in annual DM production at 600 ppm CO_2 in an N fertilized, mixed perennial ryegrass/white clover pasture in Switzerland with the higher responses at higher levels of soil fertility, and Long *et al.* (2004) reported DM increases of 17-22% and -2-+12% for C_3 and C_4 species respectively, with similar findings published by Ainsworth and Long (2005). The production increases simulated at 550 ppm CO_2 in this study were higher than the biomass multipliers used in crop models such as DSSAT-CERES and EPIC/CropSyst, ie. 11-19% for C_3 species and 4-8% for C_4

species (Tubiello *et al.* 2007), but the magnitude of the difference between responses for C_3 and C_4 species was similar. It is important to note that the CO_2 responses modelled in this study were under non-limiting soil nutrient conditions, and that lower responses are expected when there are other limiting factors, for example N (Lüsher *et al.* 2006; Newton *et al.* 2006).

Table 3. Comparison of model parameters and responses to elevated CO_2 (550 ppm vs relative to a baseline of 380 ppm) for leaf photosynthetic potential, plant N concentration and canopy conductance with results from FACE studies where a similar degree of CO_2 elevation was used.

Plant trait	Model response	FACE experimental response
Leaf photosynthetic potential	C_3: 25%	30-40% (Ainsworth and Long 2005)
		Grasses 30-42, Crops 10-22% (Long *et al.* 2004)
	C_4: 10%	2-20% (Ainsworth and Long 2005)
		Grasses -12 to 10, Crops 7-32% (Long *et al.* 2004)
Plant N content	C_3: -11%	-10 to -18% (Long *et al.* 2004; Ainsworth and Long 2005)
		-3 to -10 (Barbehenn *et al.* 2004)[1]
	C_4: -6%	-10 to -18% (Long *et al.* 2004; Ainsworth and Long 2005)
		0 to -8 (Barbehenn *et al.* 2004) [1]
Canopy conductance	-21%	-10 to -35% (Long *et al.* 2004)
		-18 to -22% (Ainsworth and Long 2005)

[1] linear interpolation between 370 and 740 ppm CO_2 for individual species mean responses

Table 4. Mean annual yield response (% change) for baseline scenarios at 550 compared to 380 ppm CO_2 at each site.

Site	Pasture species	Yield response (%)
Malanda	Dryland – setaria	7.1
	Irrigated – setaria, ARG	8.4
Mutdapilly	Dryland – Rhodes	8.2
	Irrigated – Sorghum, ARG	11.1
Kyogle	Kikuyu, ARG	9.8
Barraba	Native C_3, C_4	16.7
Albany	Kikuyu, sub	14.8
Wagga Wagga	Phalaris, sub, native C_4	27.9
Kyabram	Irrigated – PRG, sub, pasp.	18.2
	Dryland – PRG, sub, pasp.	24.0
Dookie	PRG, sub, pasp.	19.5
Vasey	Phalaris, sub, annuals	27.8
Hamilton	PRG, sub	25.2
Terang	PRG, white clover	23.3
Ellinbank	PRG, white clover	23.6
Elliott	Dryland – PRG, white clover	19.4
	Irrigated – PRG, white clover	25.5

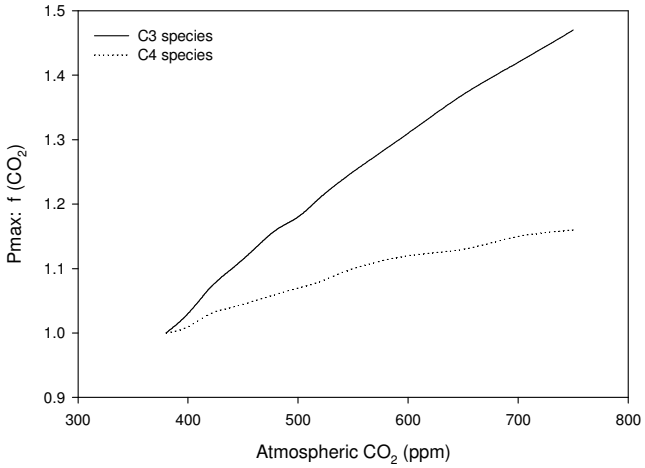

Figure 1. Leaf photosynthetic potential for C_3 and C_4 species in response to increasing atmospheric CO_2 concentration.

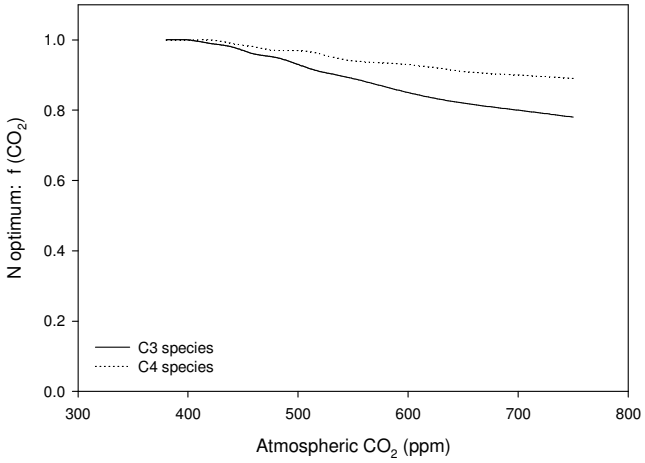

Figure 2. Plant nitrogen content in response to increasing atmospheric CO_2 concentration.

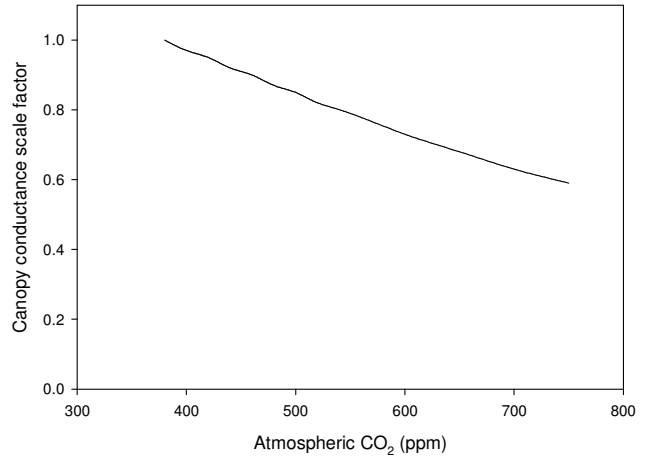

Figure 3. Canopy conductance scale factor in response to increasing atmospheric CO_2 concentration.

Modelling plant adaptation strategies

The effect of increasing the root depth of perennial ryegrass on pasture production under the 2070 High future climate scenario was modelled at a high (Ellinbank, 1078 mm/year) and medium rainfall site (Terang, 746 mm/year) in southern Victoria. The original root distribution with a maximum root depth of 40 cm and 50% of roots in the top 10 cm, was compared to two successively deeper root systems, that being maximum is 60 cm with 50% roots in top 15 cm, and maximum is 80 cm with 50% roots in top 20 cm. Changing root depth had a minimal effect the biomass of roots, with mean annual root mass predicted to be 0.48, 0.50 and 0.51 t DM/ha for the three root distributions at Ellinbank and 0.44, 0.46 and 0.47 t DM/ha at Terang. No other plant characteristics were altered.

Statistical analysis

No formal statistical analysis was applied to the modelled pasture growth rates because of correlations in the input climate data. Trends are presented across a range of future climate scenarios, and discussed in the context of pasture growth rate variability, with distribution (eg. for annual yields) shown when appropriate.

Results

Climate change impacts

The impact of Low, Medium and High climate change scenarios on pasture production, species composition (for simulations with mixed C_3/C_4 pastures only) and water balance are shown for all sites in Figures 4-78. A summary of all scenario effects on average annual production is provided in Table 5.

A brief summary of each site is provided here:

Malanda. The annual DM yield of dryland Setaria pastures was predicted to increase by up to 12% in the 2070 High scenario when CO_2 was included in the simulation (Table 5). Pasture growth rates were predicted to increase in the February-October period, with little change during the remainder of the year (Figs 4-5). Little change was also evident in the water balance (Fig 6), however there was an indication that changes in rainfall variability could reduce pasture growth (Fig 7). The impacts of the future climate scenarios on the irrigated pasture system at Malanda were similar, with increases in annual production simulated of up to 15% (Table 5). Increased winter/spring production was evident when CO_2 was included in the simulation (Figs 8-9), due to an increase in annual ryegrass growth rate (Fig 10). The small change in annual rainfall meant that there were only minor changes in the water balance (Fig 11). There was no the effect of changes in rainfall distribution on annual irrigated pasture production (Fig 12).

Mutdapilly. Dryland Rhodes grass annual production at Mutdapilly was increased by up to 18% under the 2070 High scenario (Table 5). A change in the seasonal growth pattern was predicted in the 2070 scenarios, with more growth in February-August but less in October-December (Fig 14 a,b), reflecting a re-distribution of rainfall from spring to summer/autumn and warmer winter temperatures (see Appendix 1, Table A4). Little change was expected in the water balance (Fig 15), and on pasture growth due to rainfall variability (Fig 16). In the irrigated sorghum/annual ryegrass system, the main effect was CO_2 stimulating increased annual ryegrass production in early winter, but with an earlier finish under the 2070 scenarios (Fig 17-19). The increase in irrigation inputs required were small (16 and 28 mm over the baseline for the 2030 and 2070 High scenarios, Fig 20). There was little impact of changed rainfall variability on irrigated pasture production (Fig 21).

Kyogle. Mean annual yield was predicted to increase by up to 9% for kikuyu/annual ryegrass pastures under future climate scenarios at Kyogle (Table 5). Little change in the seasonal growth pattern was modelled in 2030 (Fig 22), but changes during Spring were predicted in 2070 (Fig 23) due to an earlier finish to annual ryegrass and start of kikuyu (Fig 24). Again there was little change in the water balance (Fig 25) and little effect of increased rainfall variability on annual pasture production (Fig 26).

Barraba. Pasture production at Barraba was predicted to increase under all of the climate change scenarios investigated, by up to 52% in the 2070 High with CO_2 scenario (Table 5). December-April was the period of the largest growth increase (Figs 27-28) reflecting an earlier start to the C_4 spring growing season, a marked increase in growth of C_4 species in summer/autumn and of C_3 species in early winter, but an earlier decline in C_3 growth during spring (Fig 29). There was little impact of scenarios on the water balance (Fig 30) or of rainfall variability treatments on annual pasture production (Fig 31).

Albany. Climate scenarios up to 2070 Medium increased production at Albany by up to 29% but the increase was less (8%) under the 2070 High scenario (Figs 32-33, Table 5). Warming stimulated kikuyu to commence growth earlier in spring, and improved subclover early winter growth but resulted in an earlier finish to its growing season (Fig 34). Under the 2070 High scenario the spring growing season of kikuyu was shortened due to declining Spring rainfall (see Appendix 1, Table A7). The increases in production under the moderate climate change scenarios were made despite declining rainfall, compensated for in part by a reduction in drainage (Fig 35). There was little effect of changing rainfall variability on annual pasture growth (Fig 36).

Wagga Wagga. Under low climate change impact with CO_2 scenarios, small increases in annual production of up to 12% were predicted at Wagga Wagga, however with higher levels of climate change impact substantial declines were simulated, up to 17% in the 2070 High with CO_2 scenario (Table 5). Although winter growth rates were stimulated by CO_2, the shortening of the spring growing season led to overall production declines (Figs 37-38). Drainage was reduced to zero under the 2070 High scenario (Fig 39). There was little impact of the rainfall variability treatments on annual production (Fig 40).

Kyabram and Dookie. Annual production of irrigated perennial ryegrass, subclover and paspalum pastures in northern Victoria increased by up to 28% in the 2070 High scenario with CO_2 (Table 5). Increased summer production (Figs 41-42 for Kyabram, Figs 50-51 for Dookie), due to earlier growth of paspalum and higher summer growth rates, more than compensated for declining perennial ryegrass production in spring (Fig 43 for Kyabram, Fig 52 for Dookie). Average irrigation water requirements increased by 36-46 mm under the 2030 High scenario and approximately 71-79 mm/year under the 2070 High scenario compared to the baseline scenario, without changing the length of the irrigation season (Fig 44 for Kyabram, Fig 53 for Dookie). Again, rainfall variability treatments had little effect on pasture production (Fig 45 for Kyabram, Fig 54 for Dookie).

Dryland pasture production at Kyabram showed increases of up to 8% in the 2070 Low future climate scenario but reductions up to 26% in the 2070 High scenario when CO_2 was included in the simulation (Table 5). Winter and early spring growth rates were increased, due to CO_2, but this was counteracted by a progressively shorter spring season (Figs 46-47). Drainage declined under the lower rainfall scenarios (Fig 48) and rainfall variability treatments had little effect on pasture production (Figs 49).

Vasey. When CO_2 was included in the simulation, the low climate change impact scenarios increased annual production up to 21%, however under the 2070 High scenario the increase was 15% (Table 5). This was due to the stimulation of winter and early spring growth rates, by warmer temperatures and CO_2, counteracted by a progressively shorter spring season (Figs 55-56). Drainage declined markedly under the lower rainfall scenarios (Fig 57). Again, rainfall variability treatments had little effect on annual pasture production (Figs 58).

Hamilton and Terang. When CO_2 was included in the simulation, the low climate change impact scenarios showed increases of up to 12% in annual production, however under the 2070 High scenario production declines up to 15% were predicted (Table 5). This was due to the stimulation of winter and early spring growth rates, by warmer temperatures and CO_2, counteracted by a progressively shorter spring season (Figs 59-60 for Hamilton and Figs 63-64 for Terang). The amount of through drainage, and to a lesser extent runoff, declined under the lower rainfall scenarios (Fig 61 for Hamilton and Fig 65 for Terang). Again, rainfall variability treatments had little effect on pasture production (Fig 62 for Hamilton and Fig 66 for Terang).

Ellinbank. When CO_2 was included in the simulation, the low climate change impact scenarios showed small increases of up to 8% in annual production, however under the 2070 High scenario production declined by 18% (Table 5). This was due to the stimulation of winter and early spring growth rates, by elevated CO_2 levels, counteracted by a progressively shorter spring season (Figs 67-68). The amount of through drainage declined under the lower rainfall scenarios (Fig 69). Again, rainfall variability treatments had little effect on pasture production (Figs 70).

Elliott. Both dryland and irrigated simulations showed increased production under climate change scenarios with CO_2 included (Table 5). In the dryland simulation the increase was highest in the 2070 Low scenario (16%), with similar responses predicted for each of the 2070 scenarios in the irrigated system (Table 5). In the dryland simulation the increase was due to the stimulation of winter and early spring growth rates, by CO_2, counteracted by a small reduction in late spring and summer growth (Figs 71-72). In the irrigated simulation, higher winter and spring growth rates were counteracted by lower summer production, caused by high temperatures (Figs 75-76). Drainage was reduced in these pasture systems (Figs 73 and 77), with a 6% increase in irrigation requirements in the 2030 and 2070 High scenarios compared to the baseline (Fig 77). Again, rainfall variability treatments had little effect on annual pasture production (Figs 74 and 78).

Adaptation strategy

Increasing root depth from 40 to 60 then 80 cm at Ellinbank and Terang increased the spring growth rates (Fig 79). Mean total pasture production increased from 10.5 to 11.6 and 12.3 t DM/ha at Ellinbank and from 10.1 to 10.9 and 11.4 t DM/ha in the 40, 60 and 80 cm treatments and the Ellinbank and Terang sites, however production was still less than under baseline conditions (12.9 and 12.0 at Ellinbank and Terang respectively). Mean annual drainage was reduced under the deeper rooted systems, from 270 to 252 and 237 mm under the 40, 60 and 80 cm treatments at Ellinbank, and 31 to 20 and 7 mm for the corresponding treatments at Terang.

Table 5. Mean annual baseline yield (t DM/ha) and % change from baseline for each site – **without** (top line) and **with** (lower line) CO_2 effects included in the simulations

Site	Baseline production (t DM/ha)	% change from Baseline					
		2030 Low	2030 Medium	2030 High	2070 Low	2070 Medium	2070 High
Malanda – dryland	23.9	0.9	1.3	1.4	1.5	2.0	0.5
		4.4	4.5	5.8	8.3	10.1	12.3
Malanda – irrigated	25.3	1.4	1.8	2.2	2.4	3.8	3.7
		5.5	7.1	7.7	10.1	12.3	15.4
Mutdapilly – dryland	15.4	-0.3	-0.3	-0.5	-0.5	0.4	1.7
		2.6	3.6	3.9	7.4	10.7	18.7
Mutdapilly – irrigated	28.1	0	0	0.1	-0.5	-2.3	-6.5
		4.9	6.2	6.9	9.8	8.2	10.0
Kyogle	24.3	0	0.1	0	-0.3	-1.6	-5.2
		3.8	4.8	5.2	8.2	8.6	9.4
Barraba	4.0	5.9	9.9	8.8	13.7	23.9	30.0
		13.4	17.8	16.9	27.2	41.7	52.9
Albany	8.9	8.2	11.3	12.8	14.4	13.2	-11.3
		13.7	18.4	20.2	27.4	29.0	8.6
Wagga	7.0	-4.8	-7.5	-8.9	-10.0	-23.7	-42.6
Wagga		5.8	5.8	5.4	12.4	1.0	-17.8
Kyabram – irrigated	16.4	2.1	2.8	4.6	2.7	4.5	11.1
		8.9	10.4	12.9	17.4	20.5	27.3
Kyabram – dryland	5.4	-4.6	-7.2	-9.2	-10.7	-23.2	-38.5
		4.8	4.2	3.0	8.2	-4.3	-18.8
Dookie	16.2	1.0	2.0	3.6	1.9	4.3	8.7
		10.1	13.2	15.9	18.7	22.0	28.6
Vasey	7.1	-0.4	-1.5	-1.6	-2.6	-7.8	-19.6
		10.7	12.6	13.9	21.4	19.6	15.2
Hamilton	10.1	-4.3	-6.7	-7.8	-9.0	-20.1	-38.8
		5.8	5.7	5.9	12.2	3.6	-10.9
Terang	12.0	-4.3	-7.0	-8.3	-10.1	-22.6	-41.1
		4.9	4.4	4.2	9.4	-0.9	-15.5
Ellinbank	12.9	-4.6	-7.2	-8.6	-10.9	-23.9	-43.7
		4.9	4.5	4.2	8.9	-2.5	-18.7
Elliott – dryland	12.5	-3.2	-4.0	-4.6	-5.3	-11.2	-20.9
		6.9	8.8	9.5	16.9	15.3	14.6
Elliott – irrigated	22.0	-0.4	-0.5	-0.2	-1.4	-4.9	-11.3
		8.0	10.4	11.6	16.6	16.5	16.7

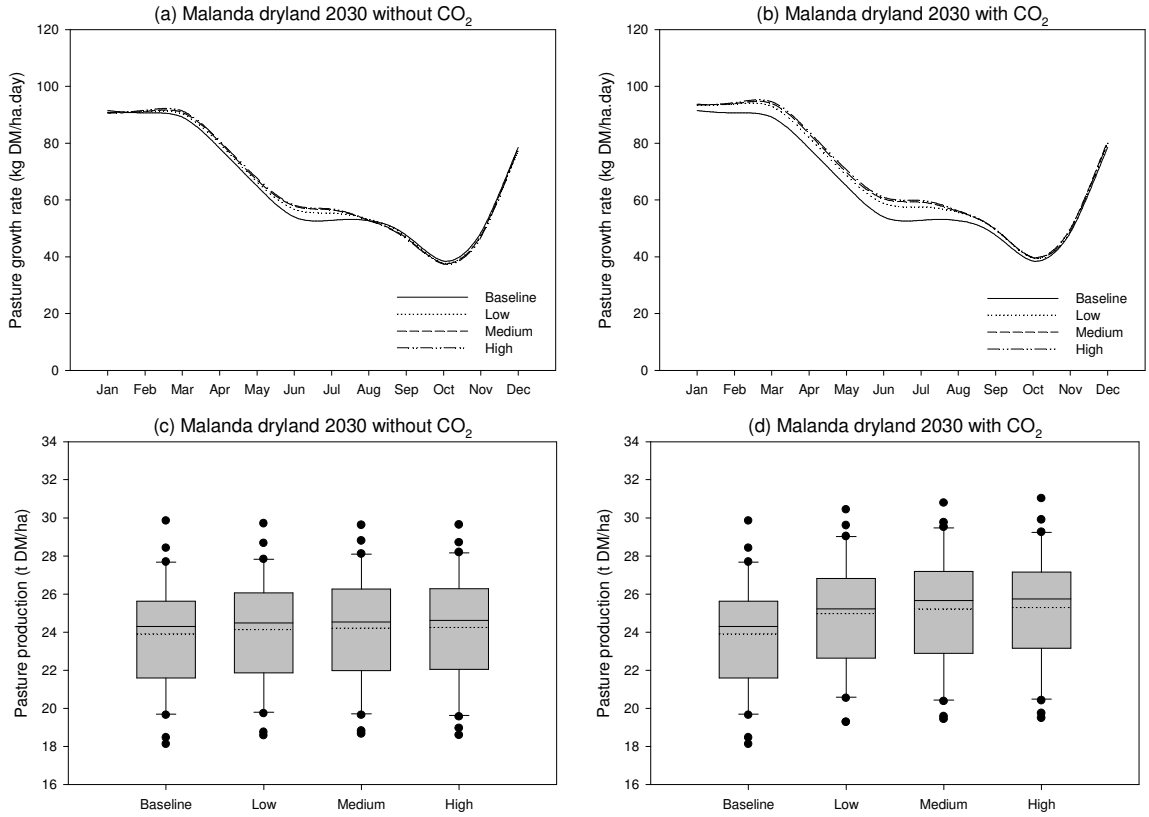

Figure 4. Dryland pasture production at Malanda in 2030. Mean monthly growth rates (a) without CO_2 and (b) with CO_2, and annual production (c) without CO_2 and (d) with CO_2.

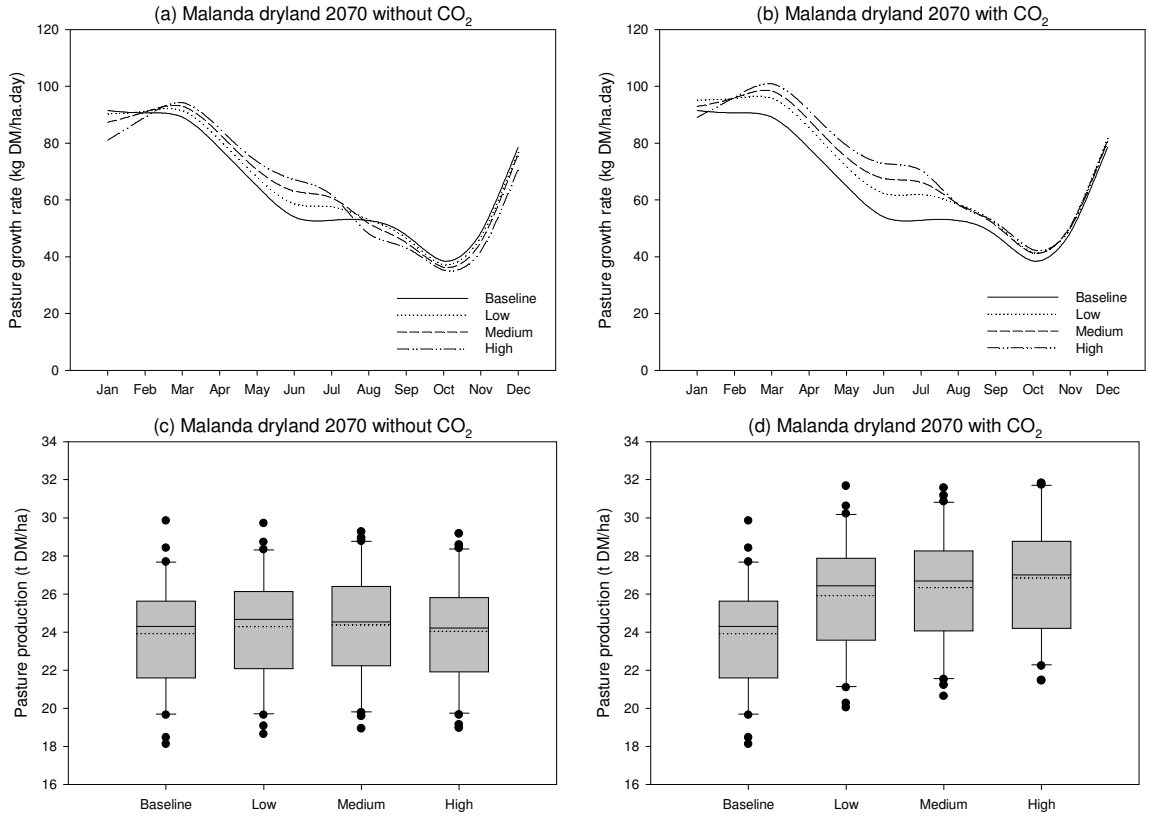

Figure 5. Dryland pasture production at Malanda in 2070. Mean monthly growth rates (a) without CO_2 and (b) with CO_2, and annual production (c) without CO_2 and (d) with CO_2.

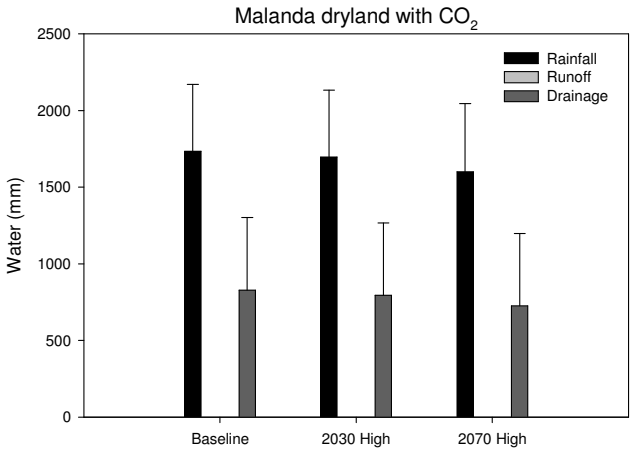

Figure 6. Rainfall, runoff and drainage for dryland pasture at Malanda under baseline, 2030 High and 2070 High scenarios. CO_2 is included in these simulations (vertical bars indicate one SD).

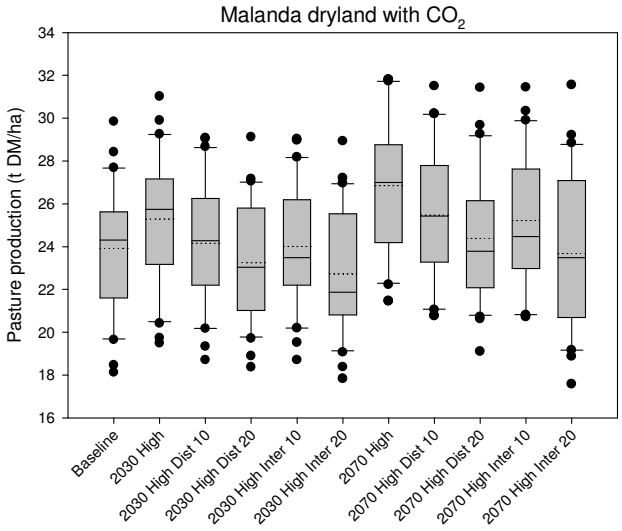

Figure 7. Annual dryland pasture production at Malanda for the baseline, 2030 and 2070 High scenarios including the rainfall distribution treatments.

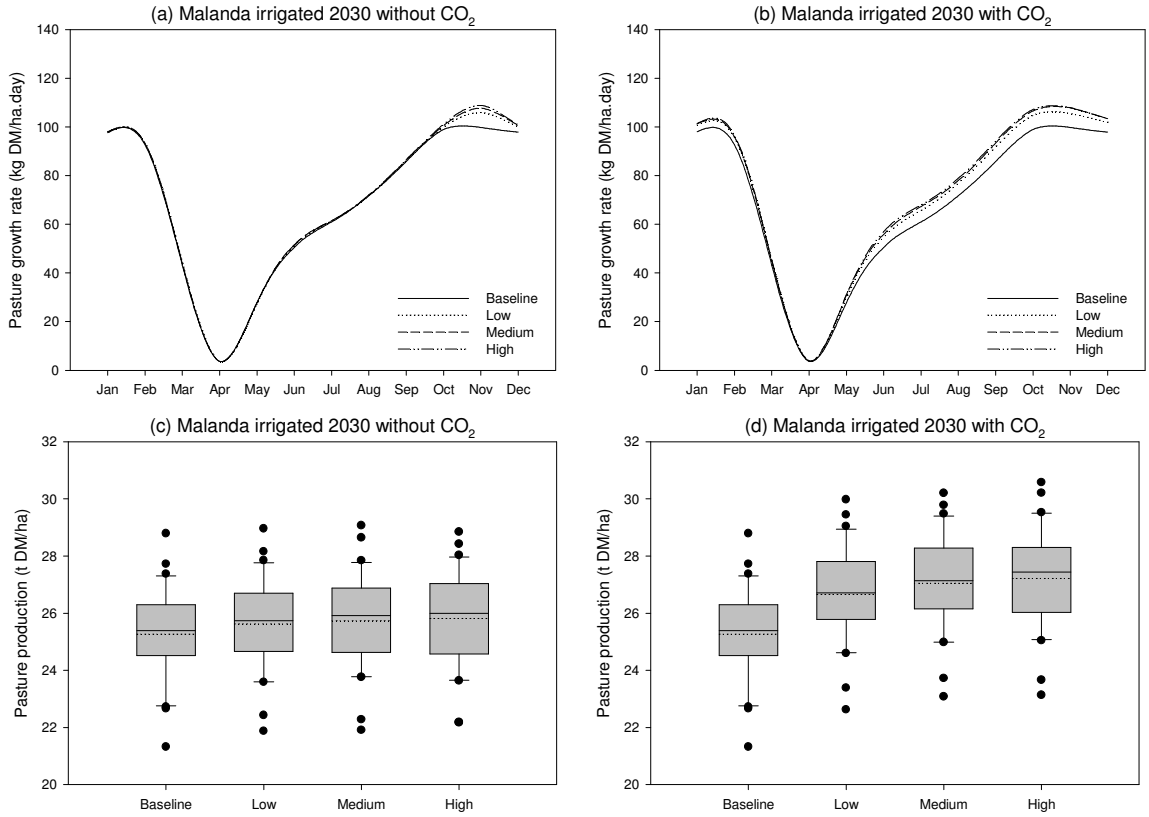

Figure 8. Irrigated pasture production at Malanda in 2030. Mean monthly growth rates (a) without CO_2 and (b) with CO_2, and annual production (c) without CO_2 and (d) with CO_2.

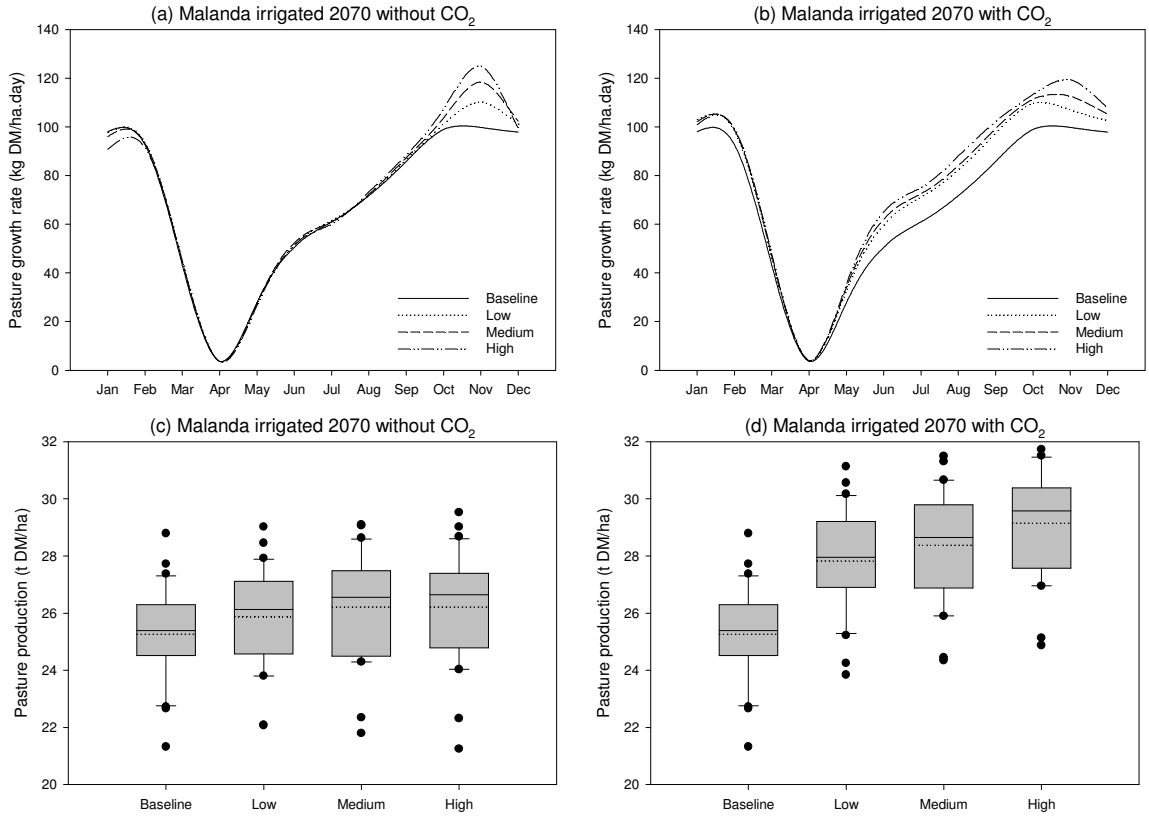

Figure 9. Irrigated pasture production at Malanda in 2070. Mean monthly growth rates (a) without CO_2 and (b) with CO_2, and annual production (c) without CO_2 and (d) with CO_2.

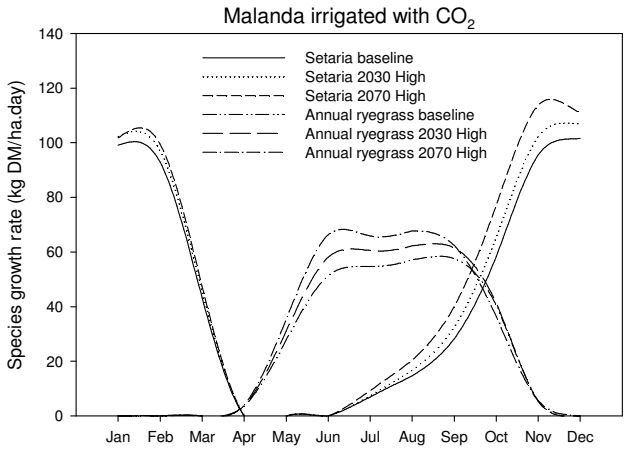

Figure 10. Growth rates of Setaria and irrigated annual ryegrass under baseline, 2030 High and 2070 High scenarios at Malanda. CO_2 is included in these simulations.

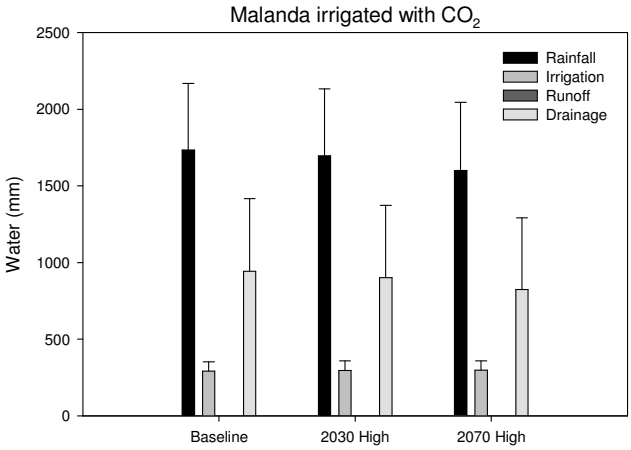

Figure 11. Rainfall, irrigation, runoff and drainage of irrigated pasture at Malanda under baseline, 2030 High and 2070 High scenarios. CO_2 is included in these simulations (vertical bars indicate one SD).

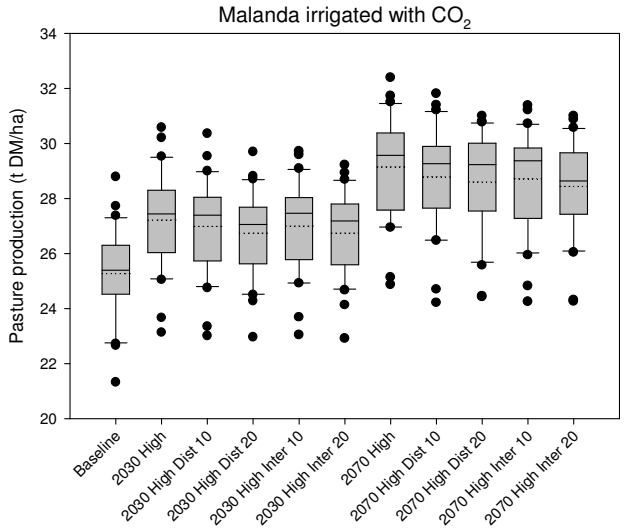

Figure 12. Annual irrigated pasture production at Malanda for the baseline, 2030 and 2070 High scenarios including the rainfall distribution treatments.

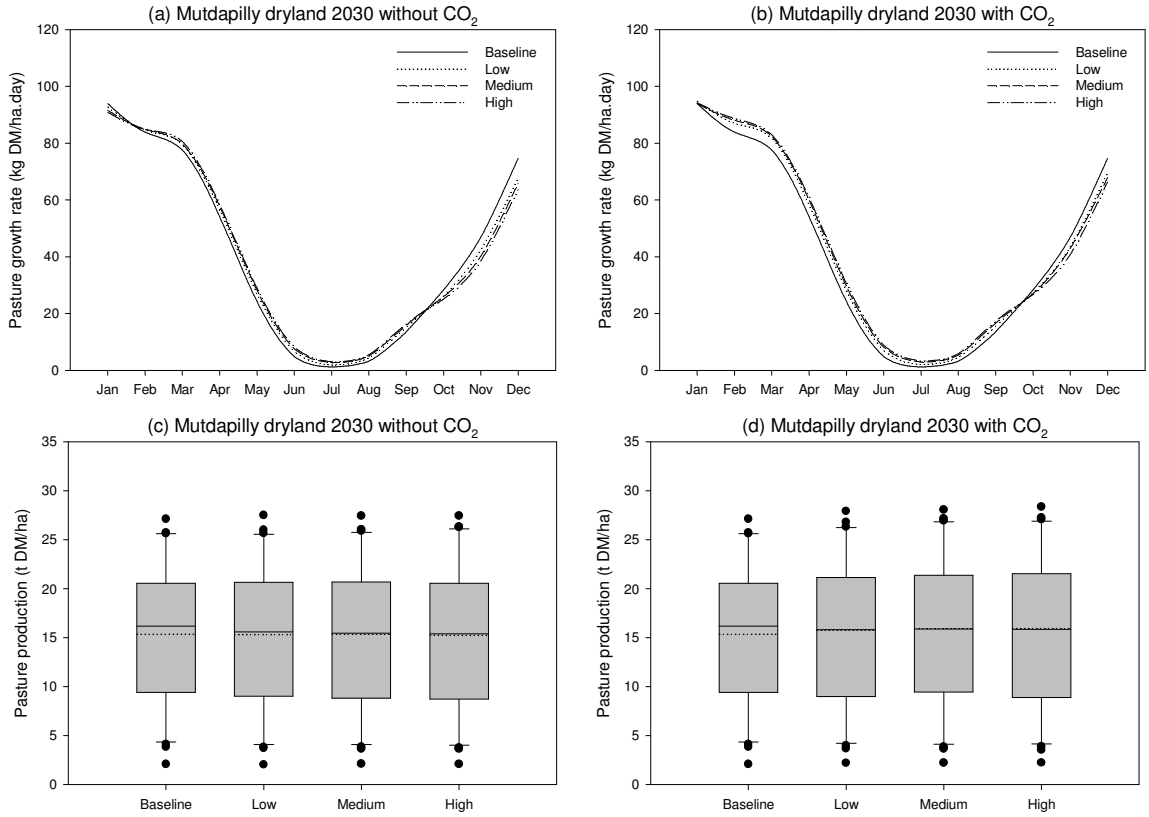

Figure 13. Dryland pasture production at Mutdapilly in 2030. Mean monthly growth rates (a) without CO_2 and (b) with CO_2, and annual production (c) without CO_2 and (d) with CO_2.

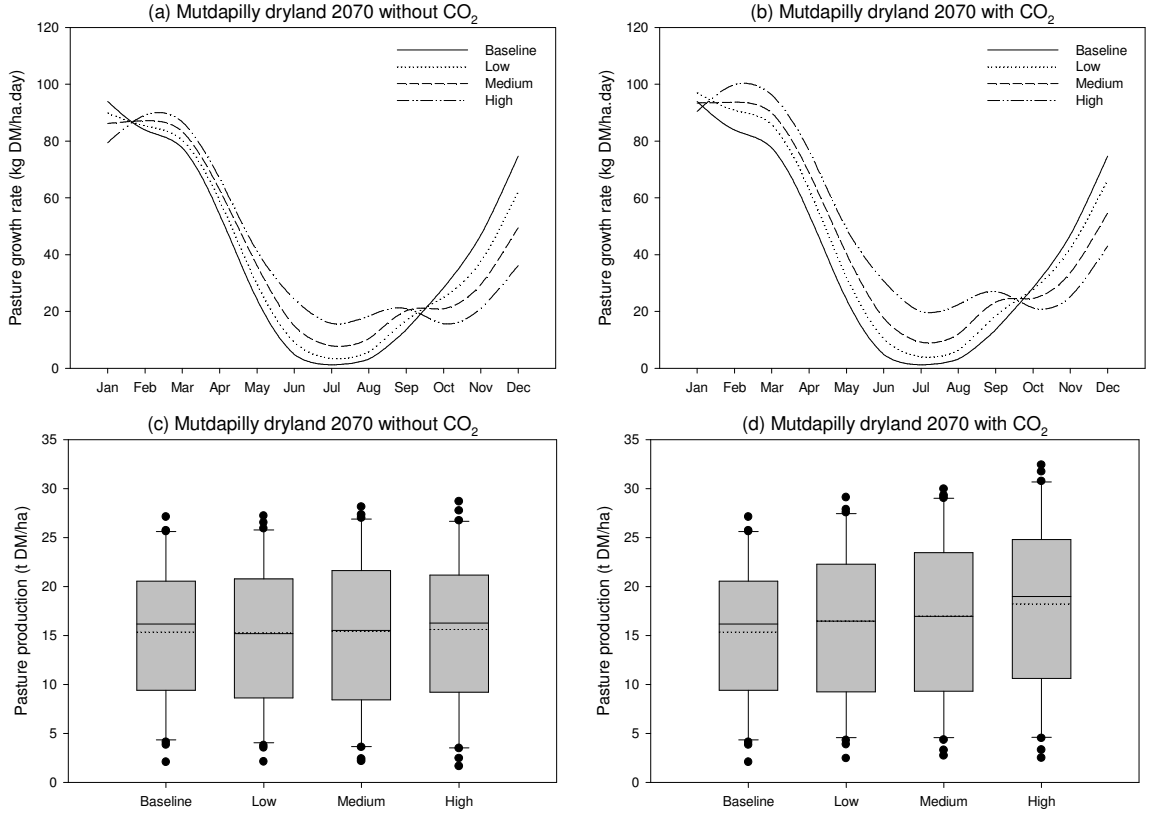

Figure 14. Dryland pasture production at Mutdapilly in 2030. Mean monthly growth rates (a) without CO_2 and (b) with CO_2, and annual production (c) without CO_2 and (d) with CO_2.

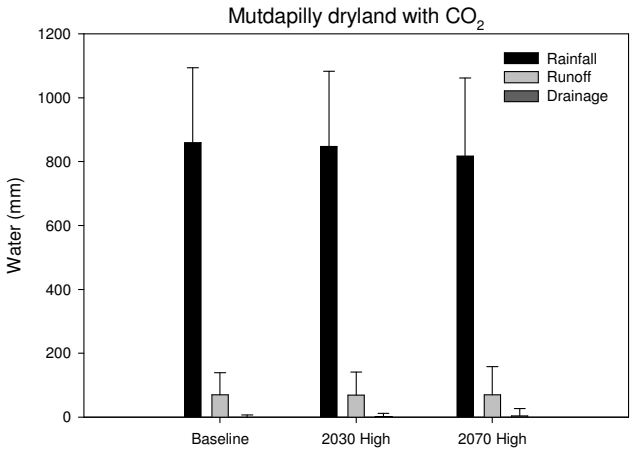

Figure 15. Rainfall, runoff and drainage for dryland pasture at Mutdapilly under baseline, 2030 High and 2070 High scenarios. CO_2 is included in these simulations (vertical bars indicate one SD).

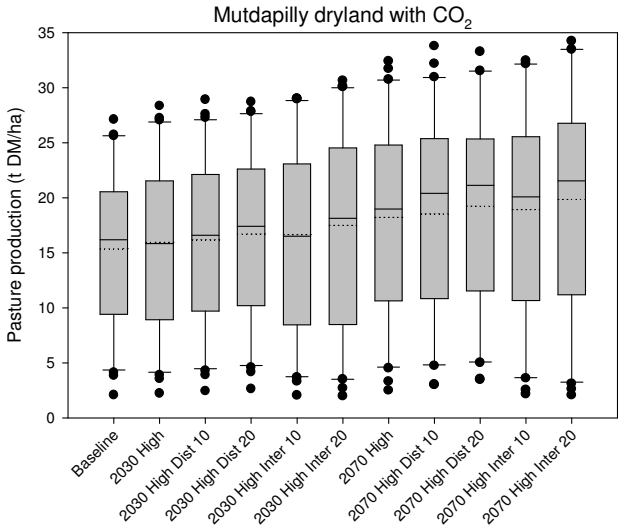

Figure 16. Annual dryland pasture production at Mutdapilly for the baseline, 2030 and 2070 High scenarios including the rainfall distribution treatments.

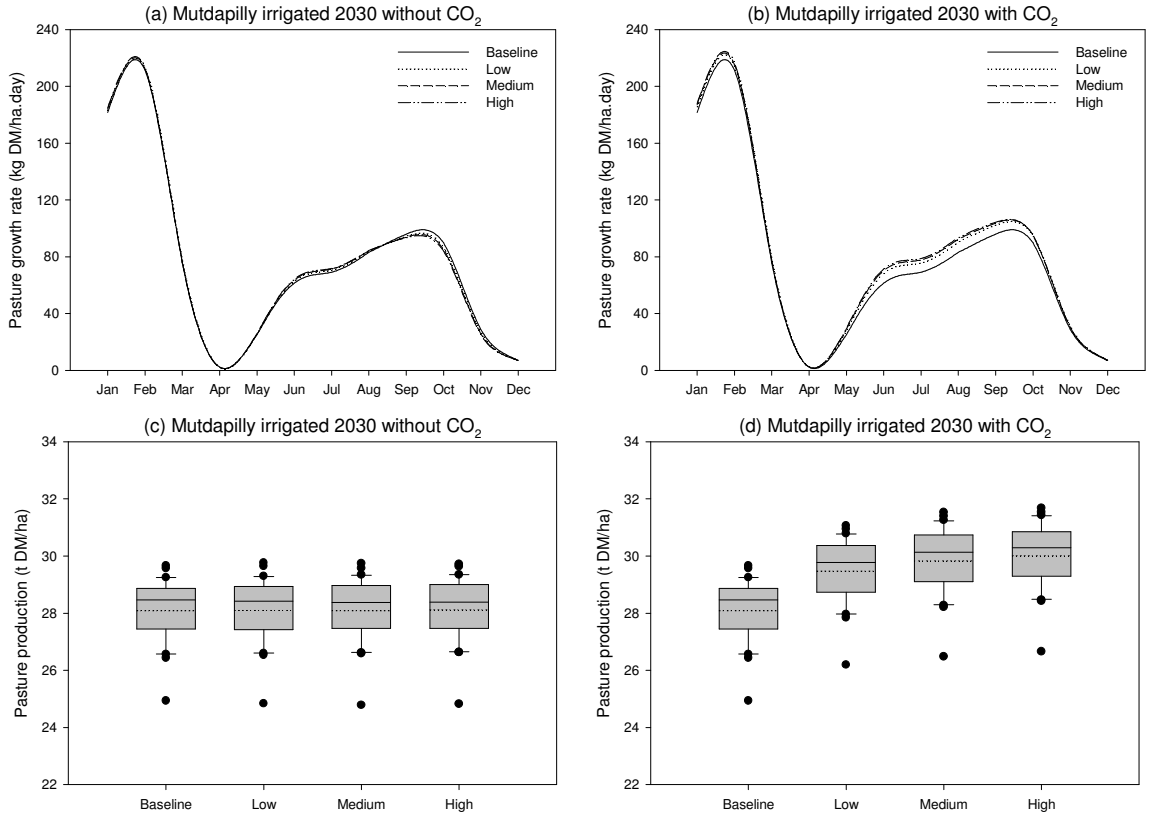

Figure 17. Irrigated pasture production at Mutdapilly in 2030. Mean monthly growth rates (a) without CO2 and (b) with CO_2, and annual production (c) without CO_2 and (d) with CO_2.

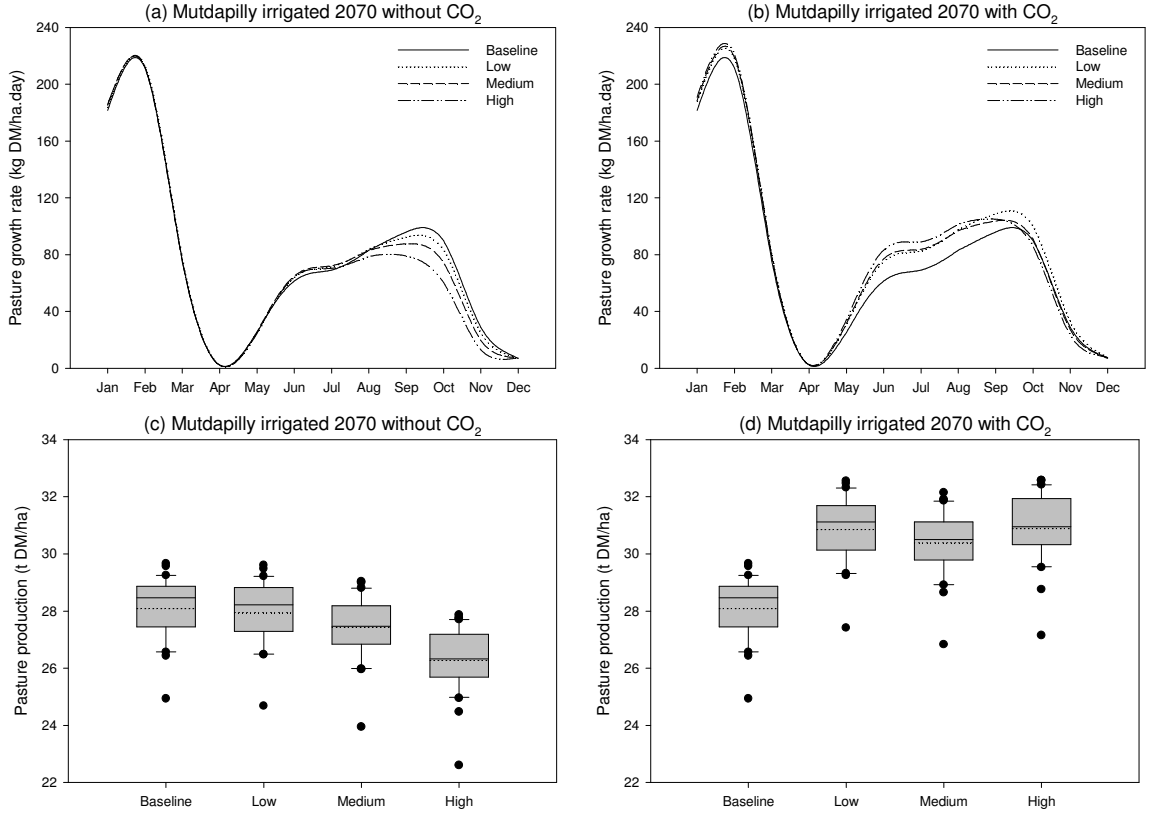

Figure 18. Irrigated pasture production at Mutdapilly in 2070. Mean monthly growth rates (a) without CO2 and (b) with CO_2, and annual production (c) without CO_2 and (d) with CO_2.

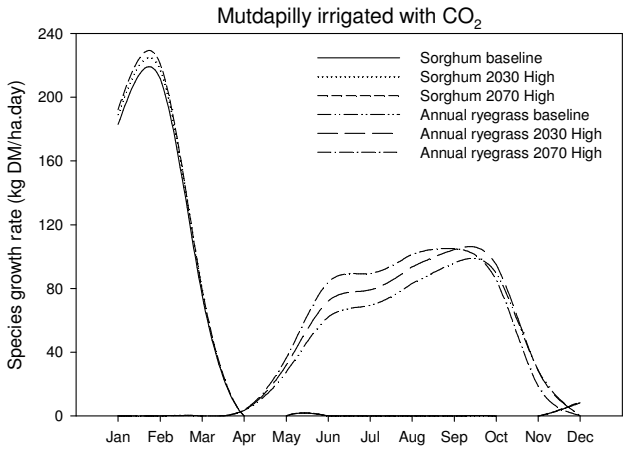

Figure 19. Growth rates of sorghum and irrigated annual ryegrass under baseline, 2030 High and 2070 High scenarios at Mutdapilly. CO_2 is included in these simulations.

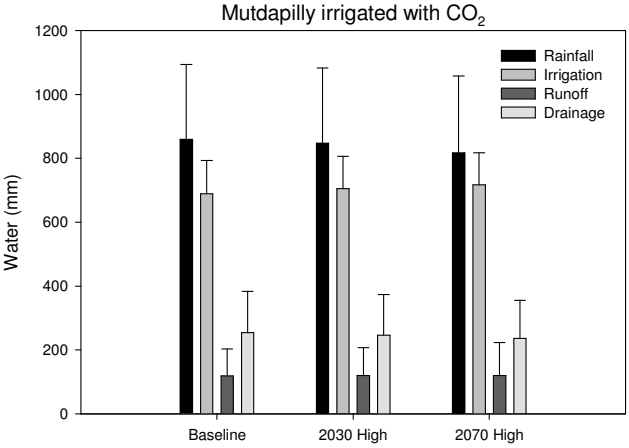

Figure 20. Rainfall, irrigation, runoff and drainage for irrigated pasture at Mutdapilly under baseline, 2030 High and 2070 High scenarios. CO_2 is included in these simulations (vertical bars indicate one SD).

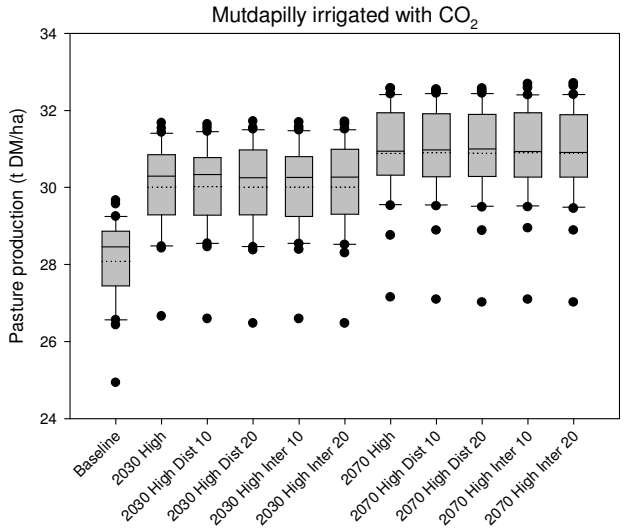

Figure 21. Annual irrigated pasture production at Mutdapilly for the baseline, 2030 and 2070 High scenarios including the rainfall distribution treatments.

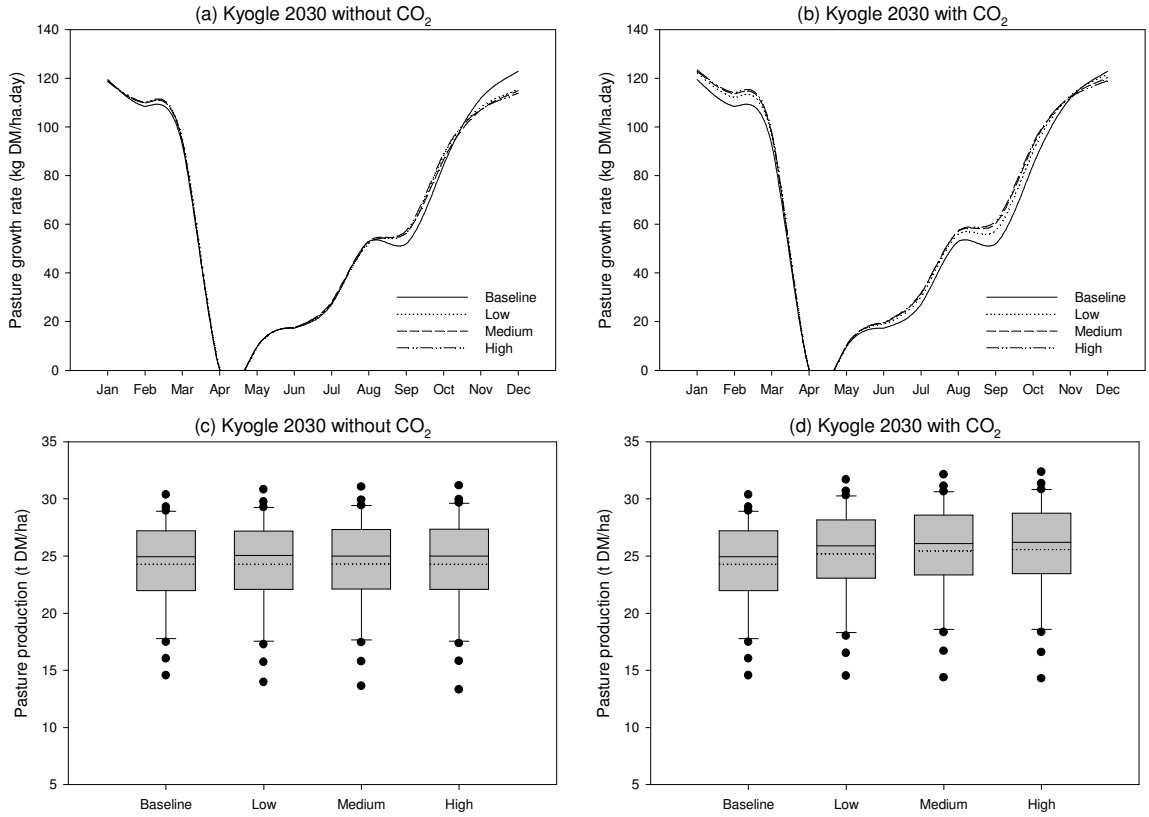

Figure 22. Dryland pasture production at Kyogle in 2030. Mean monthly growth rates (a) without CO_2 and (b) with CO_2, and annual production (c) without CO_2 and (d) with CO_2.

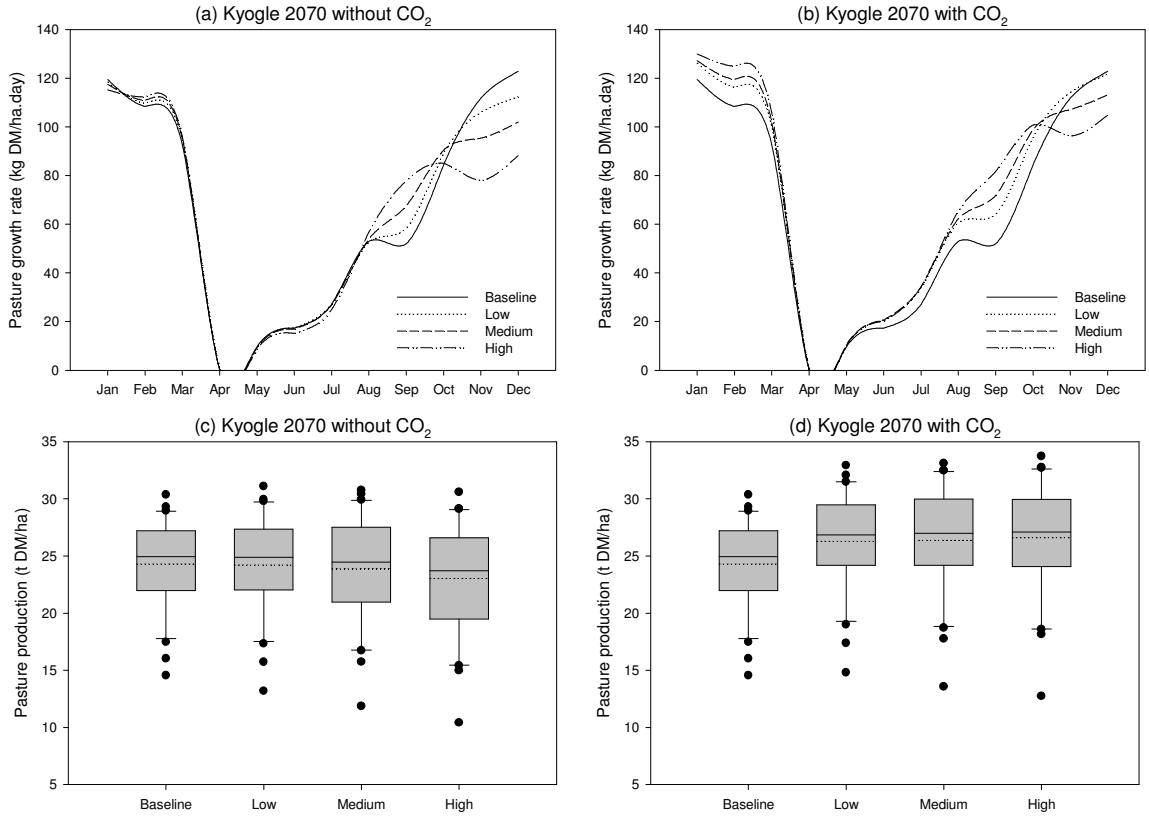

Figure 23. Dryland pasture production at Kyogle in 2070. Mean monthly growth rates (a) without CO_2 and (b) with CO_2, and annual production (c) without CO_2 and (d) with CO_2.

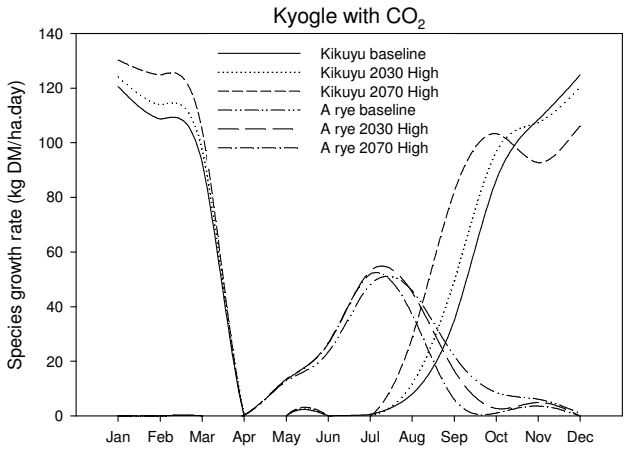

Figure 24. Growth rates of kikuyu and annual ryegrass at Kyogle under baseline, 2030 High and 2070 High scenarios. CO_2 is included in these simulations.

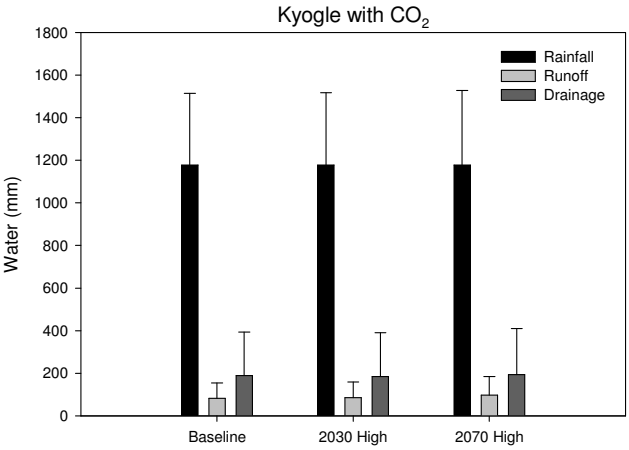

Figure 25. Rainfall, runoff and drainage at Kyogle under baseline, 2030 High and 2070 High scenarios. CO_2 is included in these simulations (vertical bars indicate one SD).

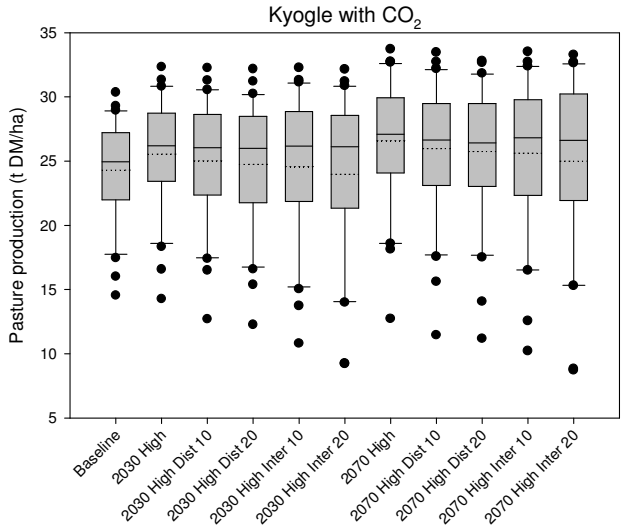

Figure 26. Annual pasture production at Kyogle for the baseline, 2030 and 2070 High scenarios including the rainfall distribution treatments.

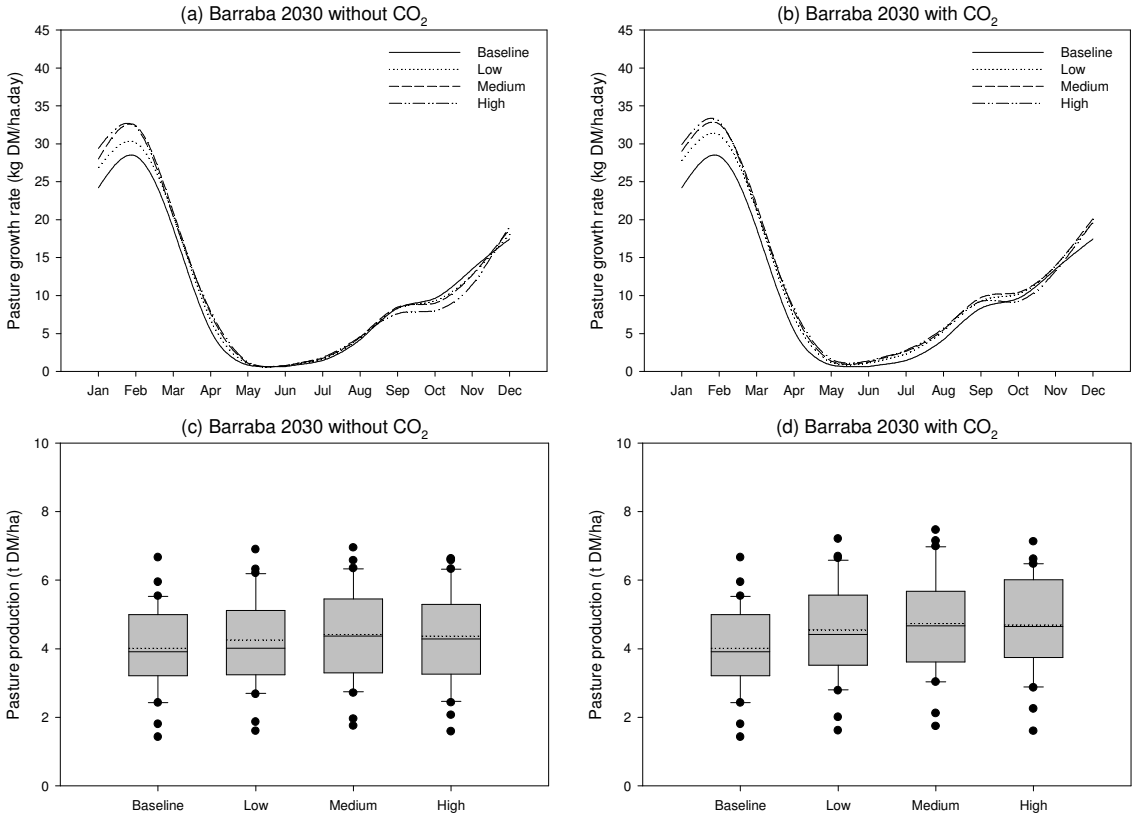

Figure 27. Pasture production at Barraba in 2030. Mean monthly growth rates (a) without CO_2 and (b) with CO_2, and annual production (c) without CO_2 and (d) with CO_2.

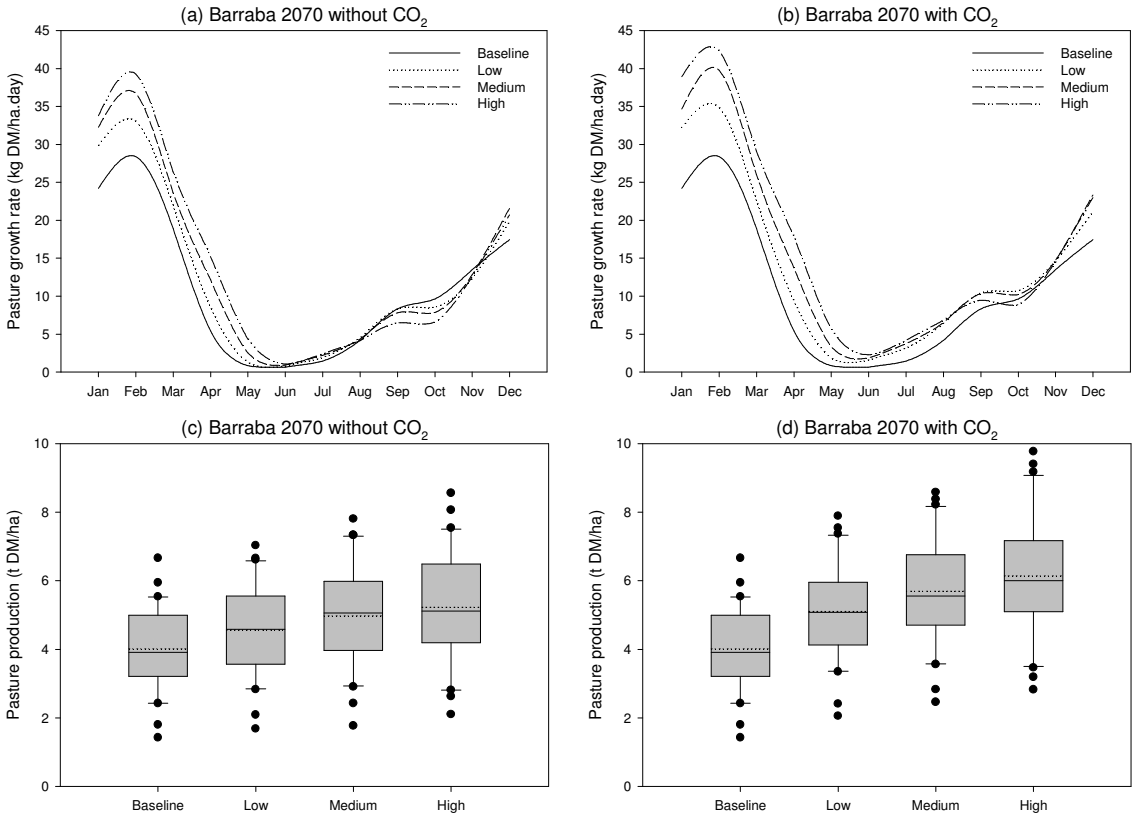

Figure 28. Pasture production at Barraba in 2070. Mean monthly growth rates (a) without CO_2 and (b) with CO_2, and annual production (c) without CO_2 and (d) with CO_2.

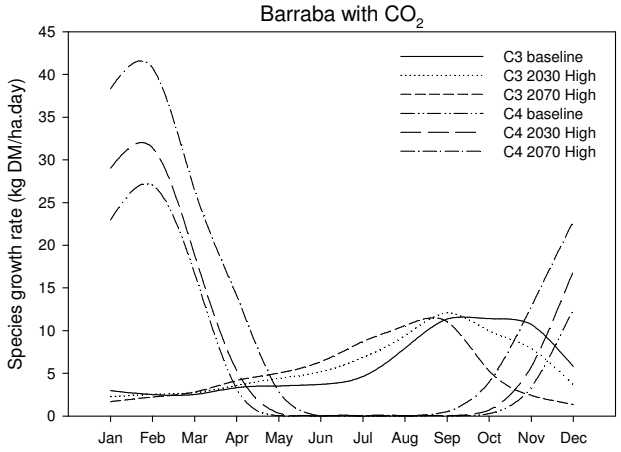

Figure 29. Growth rates of C_3 and C_4 native grasses at Barraba under baseline, 2030 High and 2070 High scenarios. CO_2 is included in these simulations.

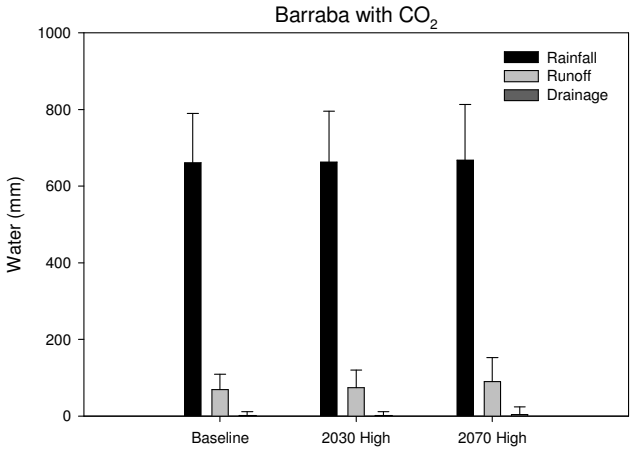

Figure 30. Rainfall, runoff and drainage at Barraba under baseline, 2030 High and 2070 High scenarios. CO_2 is included in these simulations (vertical bars indicate one SD).

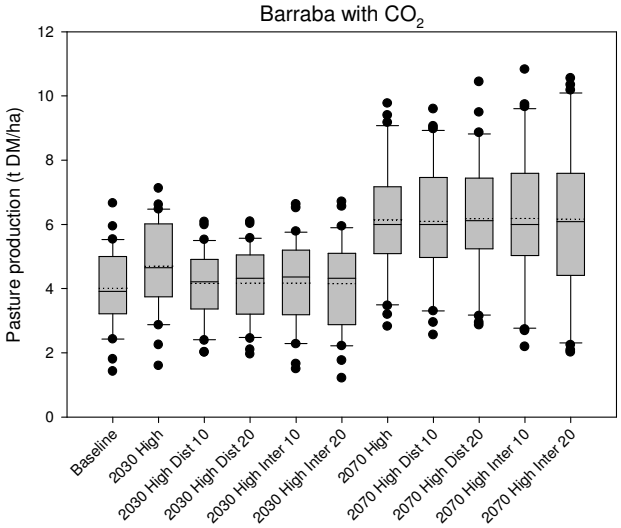

Figure 31. Annual pasture production at Barraba for the baseline, 2030 and 2070 High scenarios including the rainfall distribution treatments.

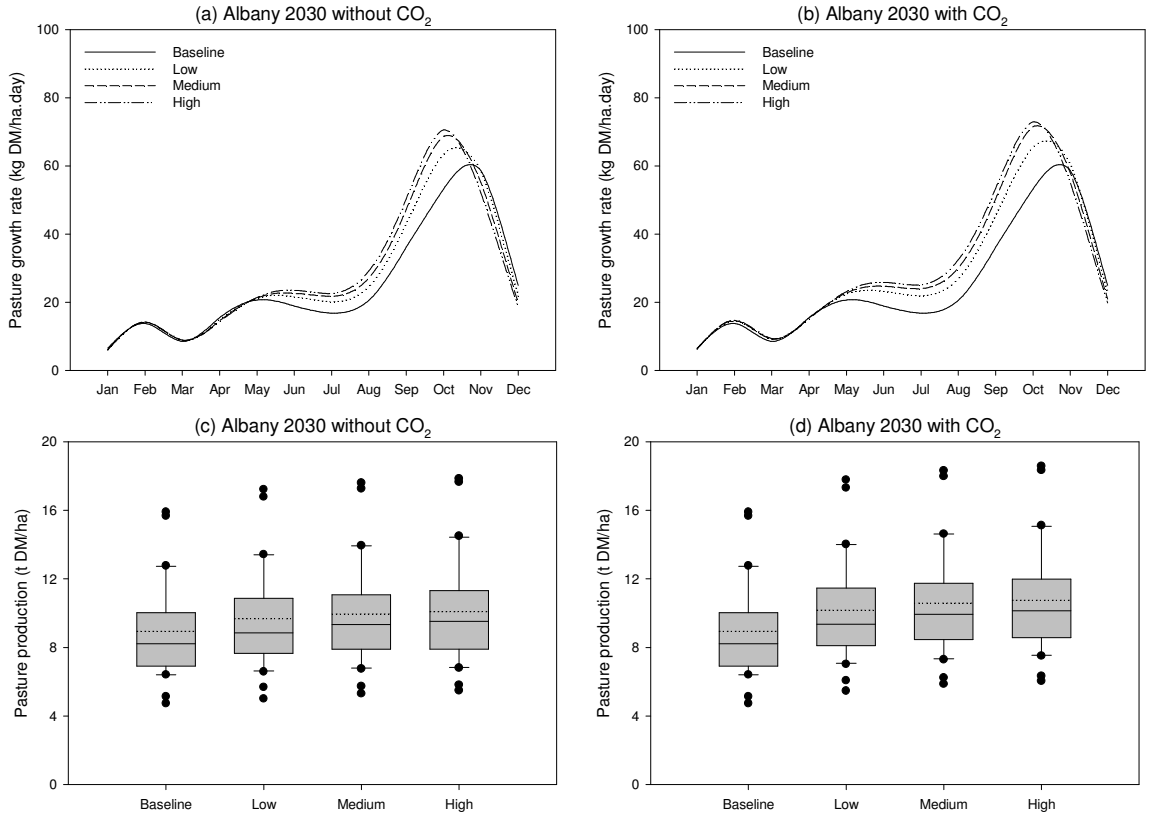

Figure 32. Pasture production at Albany in 2030. Mean monthly growth rates (a) without CO_2 and (b) with CO_2, and annual production (c) without CO_2 and (d) with CO_2.

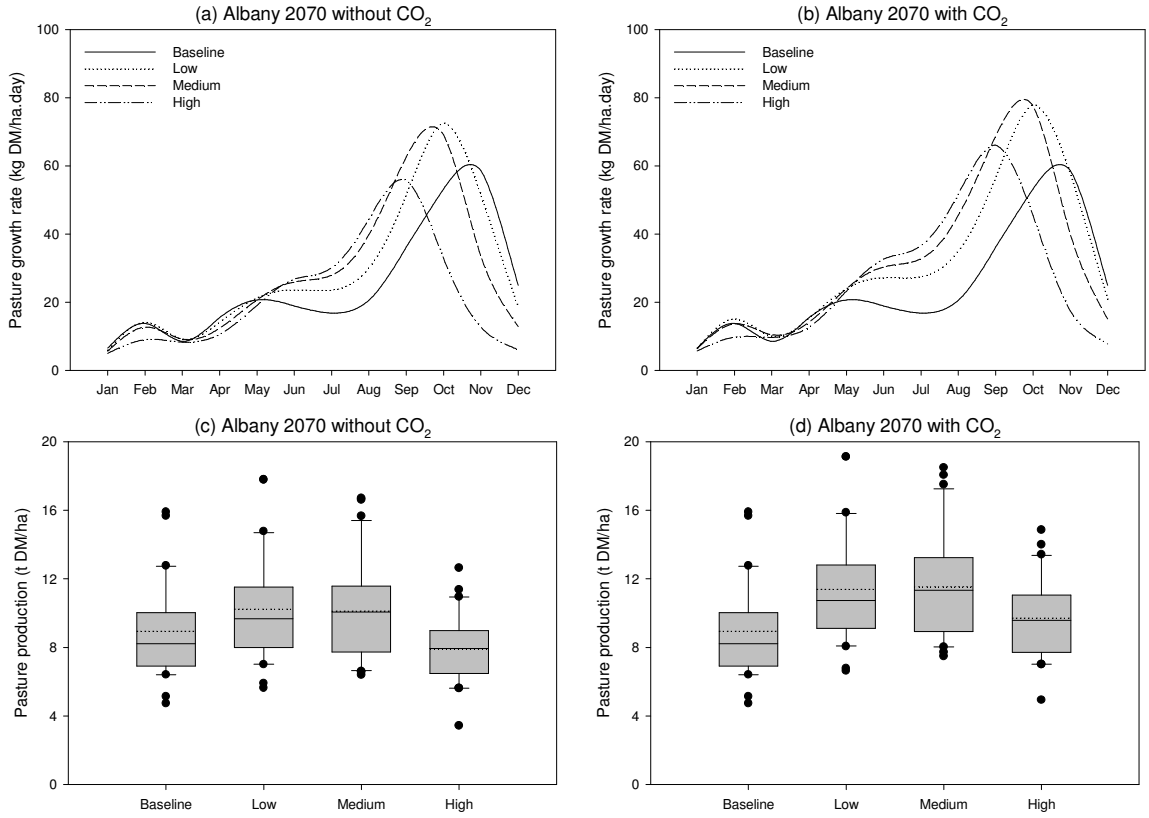

Figure 33. Pasture production at Albany in 2070. Mean monthly growth rates (a) without CO_2 and (b) with CO_2, and annual production (c) without CO_2 and (d) with CO_2.

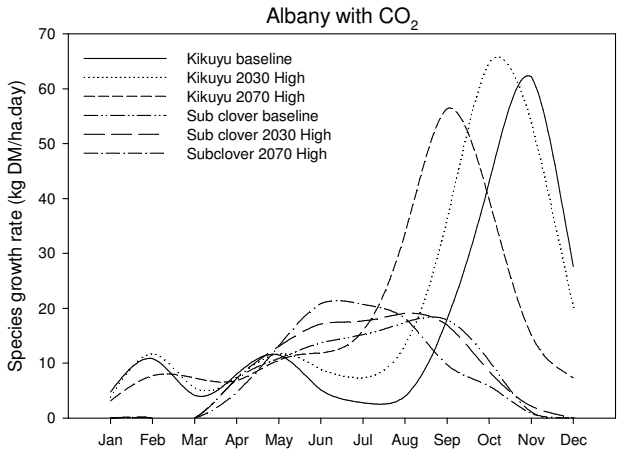

Figure 34. Growth rates of kikuyu and sub clover at Albany under baseline, 2030 High and 2070 High scenarios. CO_2 is included in these simulations.

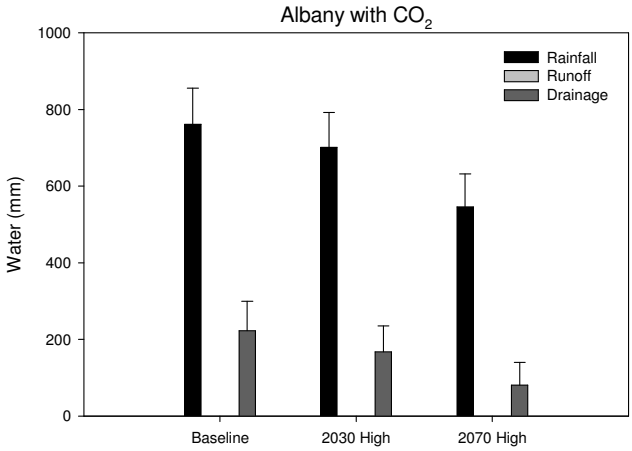

Figure 35. Rainfall, runoff and drainage at Albany under baseline, 2030 High and 2070 High scenarios. CO_2 is included in these simulations (vertical bars indicate one SD).

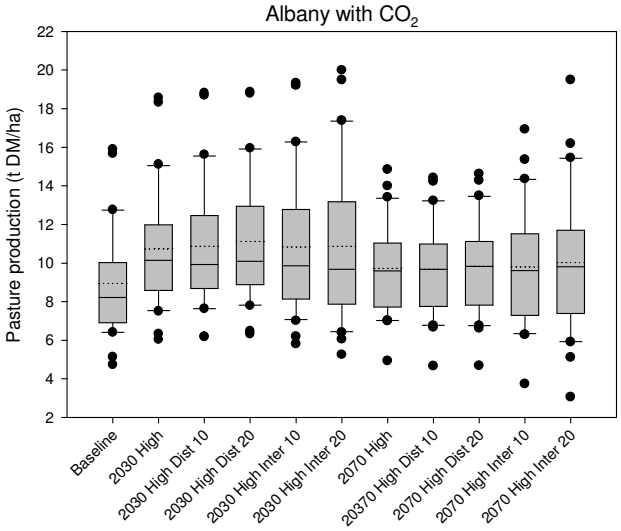

Figure 36. Annual pasture production at Albany for the baseline, 2030 and 2070 High scenarios including the rainfall distribution treatments.

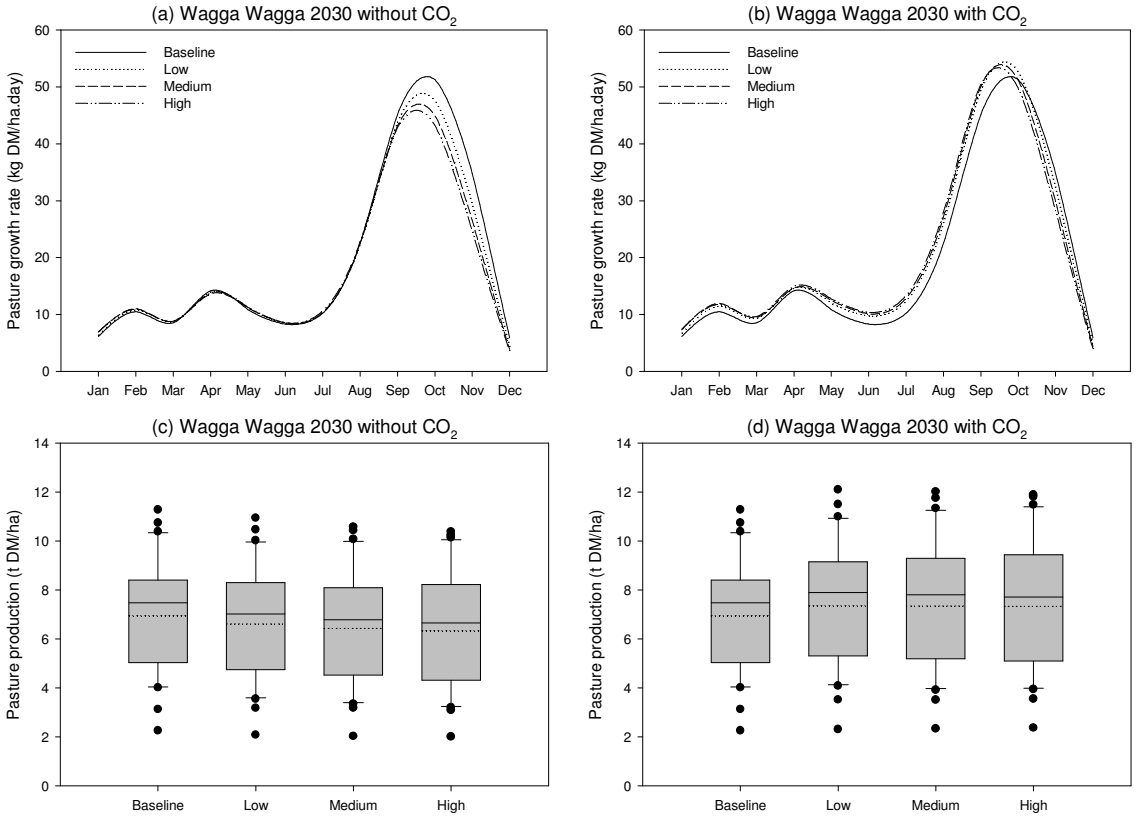

Figure 37. Pasture production at Wagga Wagga in 2030. Mean monthly growth rates (a) without CO_2 and (b) with CO_2, and annual production (c) without CO_2 and (d) with CO_2.

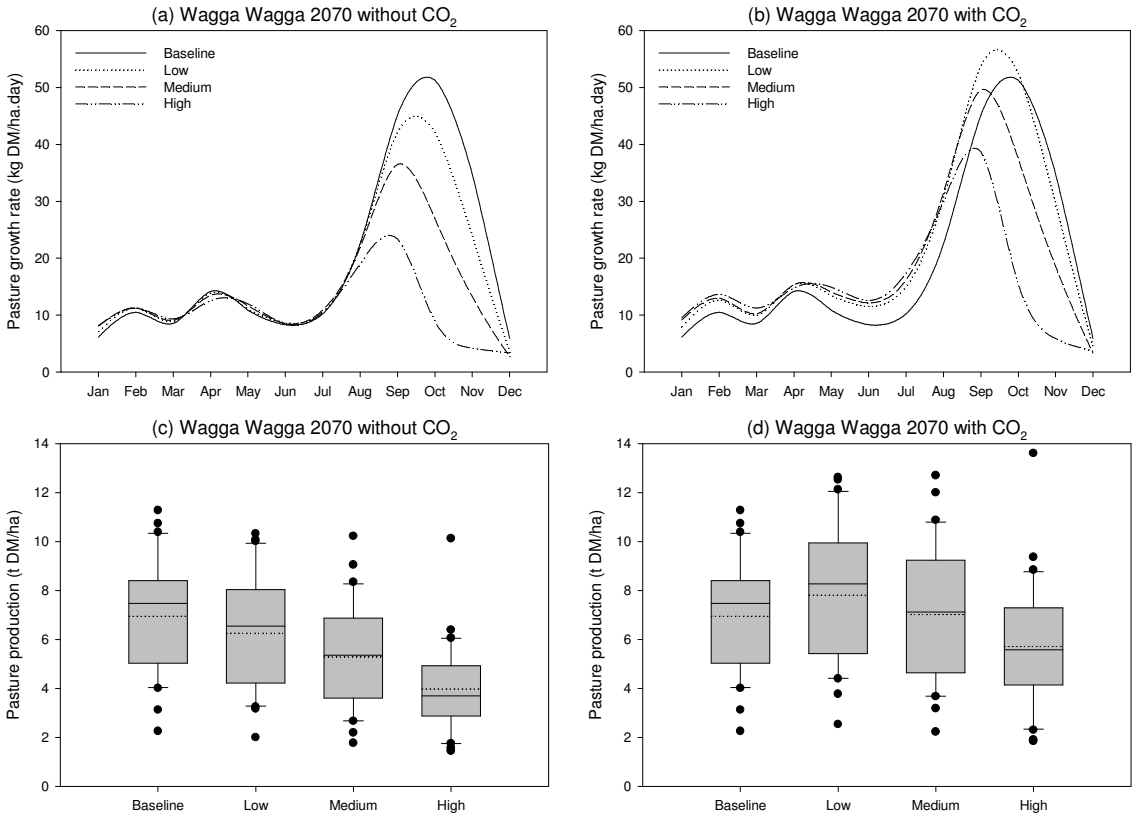

Figure 38. Pasture production at Wagga Wagga in 2070. Mean monthly growth rates (a) without CO_2 and (b) with CO_2, and annual production (c) without CO_2 and (d) with CO_2.

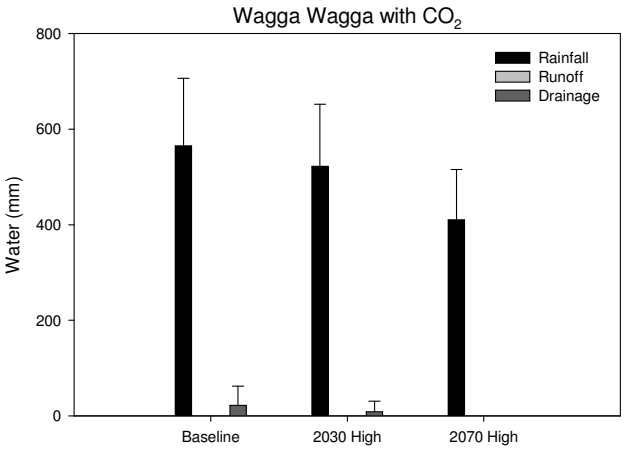

Figure 39. Rainfall, runoff and drainage at Wagga Wagga under baseline, 2030 High and 2070 High scenarios. CO_2 is included in these simulations (vertical bars indicate one SD).

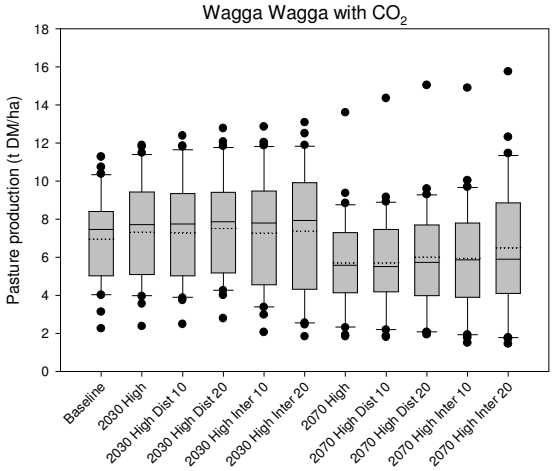

Figure 40. Annual pasture production at Wagga Wagga for the baseline, 2030 and 2070 High scenarios including the rainfall distribution treatments.

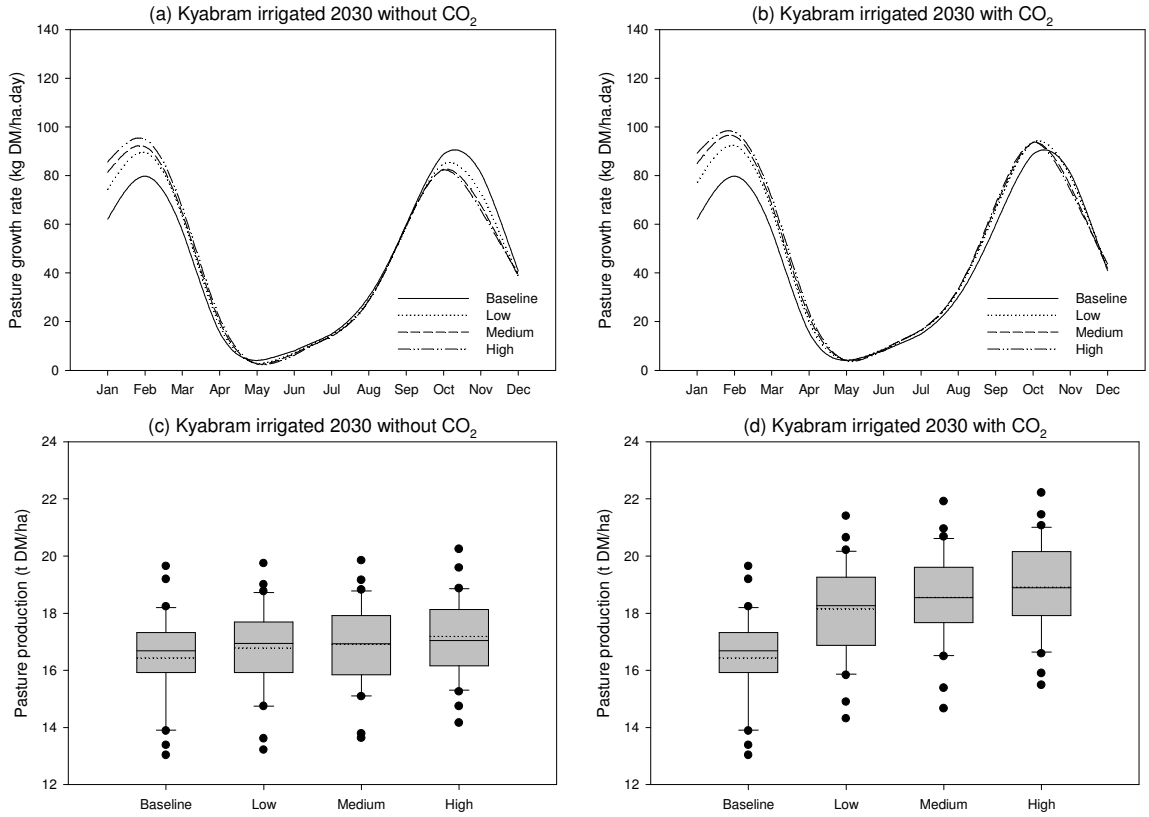

Figure 41. Irrigated pasture production at Kyabram in 2030. Mean monthly growth rates (a) without CO_2 and (b) with CO_2, and annual production (c) without CO_2 and (d) with CO_2.

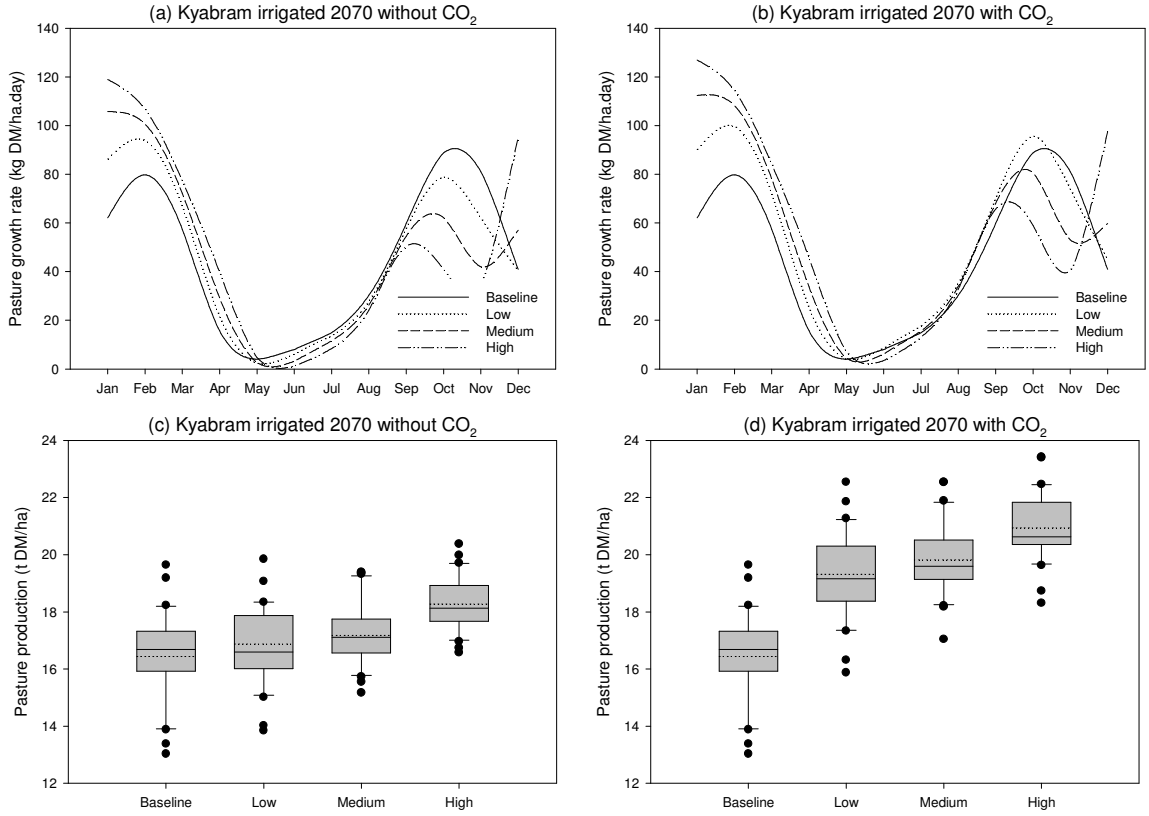

Figure 42. Irrigated pasture production at Kyabram in 2070. Mean monthly growth rates (a) without CO_2 and (b) with CO_2, and annual production (c) without CO_2 and (d) with CO_2.

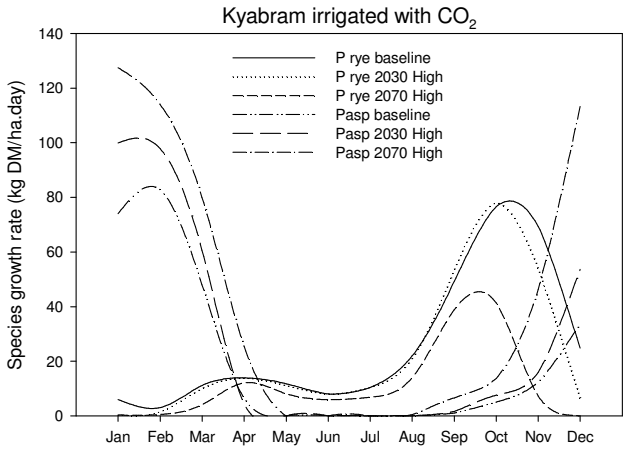

Figure 43. Growth rates of irrigated perennial ryegrass and paspalum at Kyabram under baseline, 2030 High and 2070 High scenarios. CO_2 is included in these simulations.

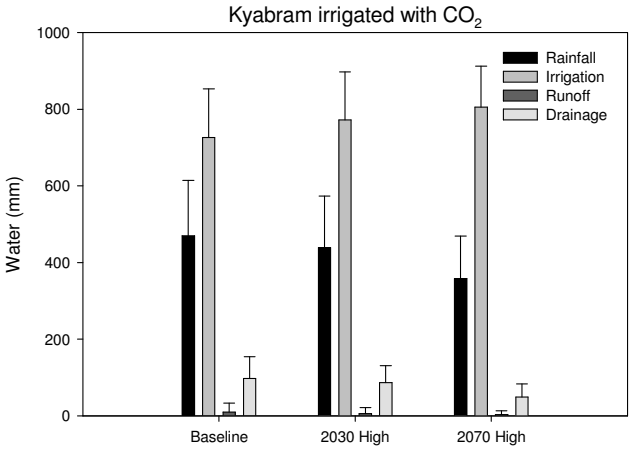

Figure 44. Rainfall, irrigation, runoff and drainage for irrigated pasture at Kyabram under baseline, 2030 High and 2070 High scenarios. CO_2 is included in these simulations (vertical bars indicate one SD).

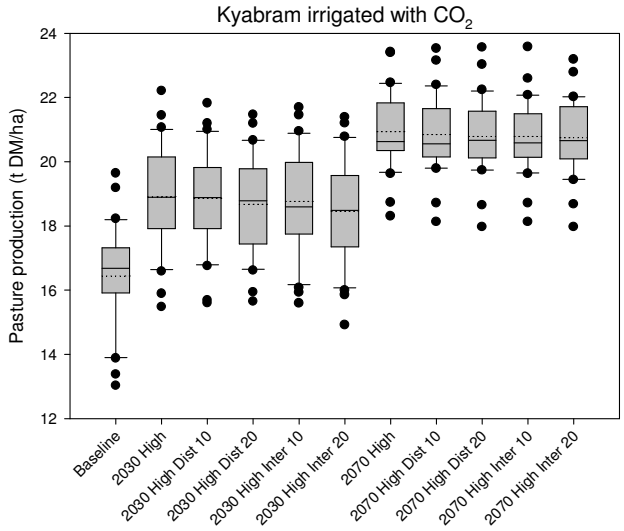

Figure 45. Annual irrigated pasture production at Kyabram for the baseline, 2030 and 2070 High scenarios including the rainfall distribution treatments.

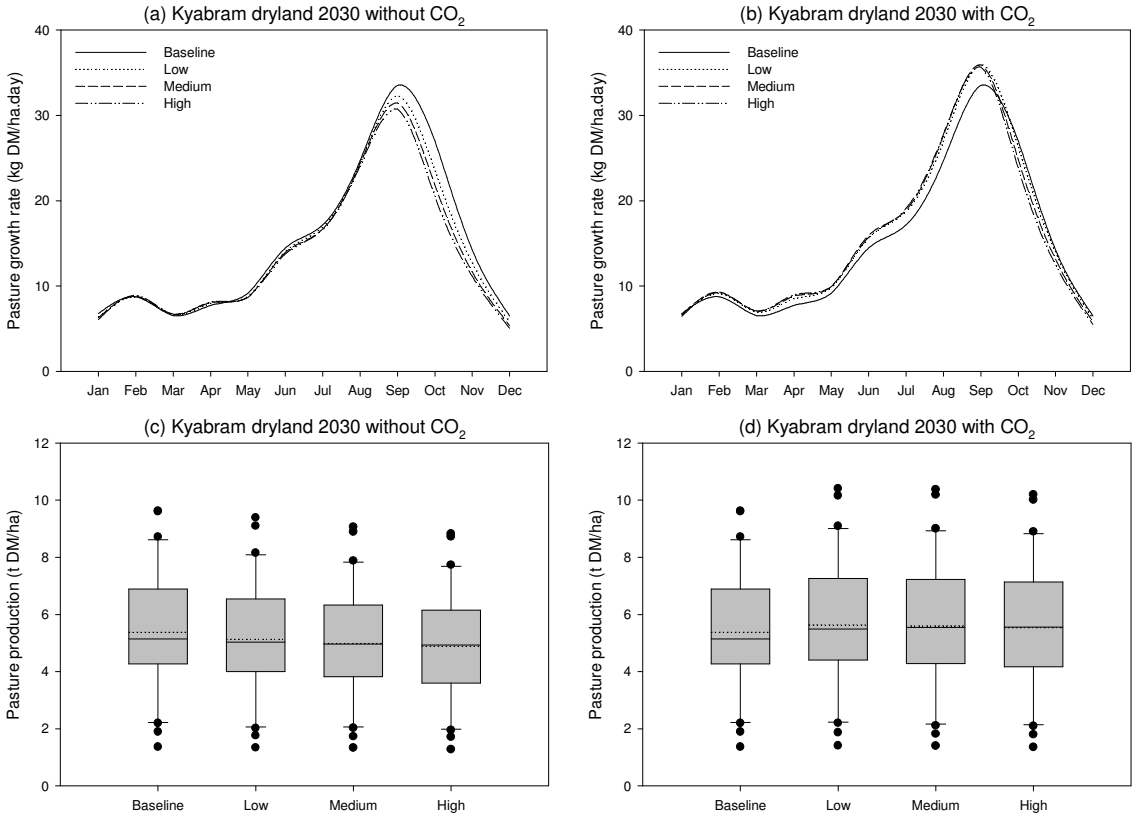

Figure 46. Dryland pasture production at Kyabram in 2030. Mean monthly growth rates (a) without CO_2 and (b) with CO_2, and annual production (c) without CO_2 and (d) with CO_2.

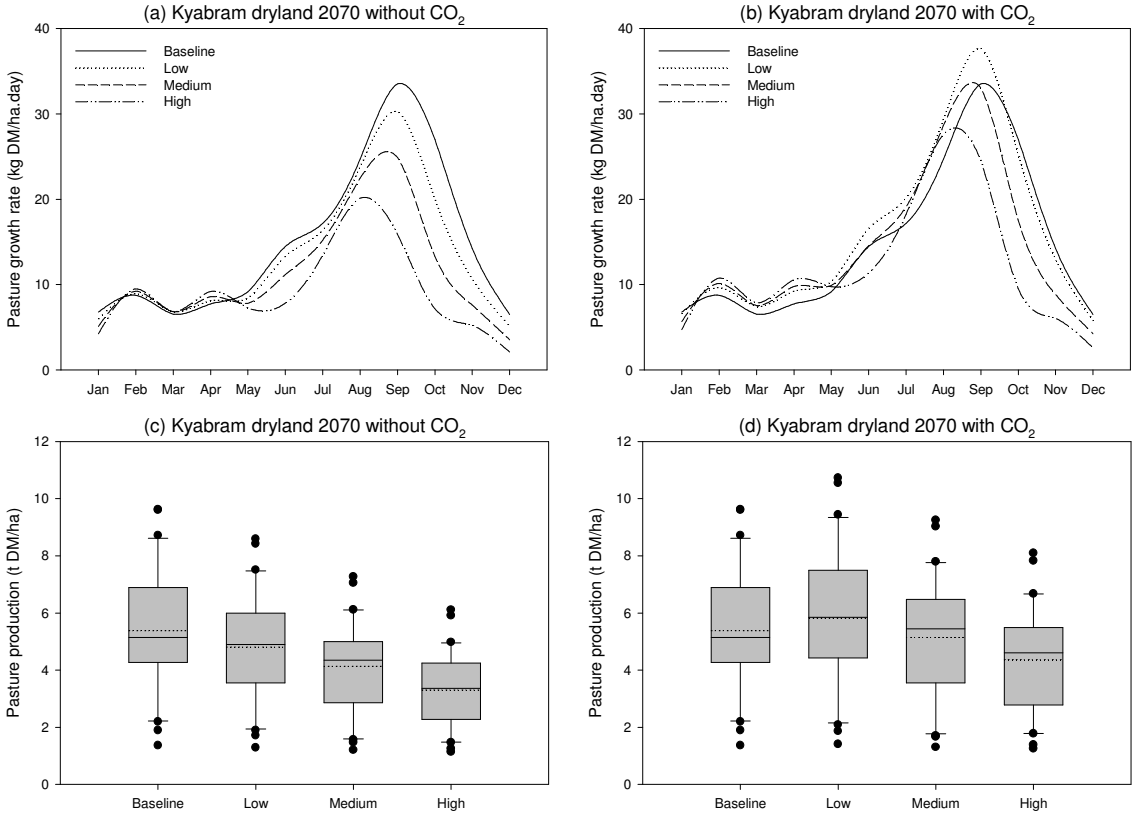

Figure 47. Dryland pasture production at Kyabram in 2070. Mean monthly growth rates (a) without CO_2 and (b) with CO_2, and annual production (c) without CO_2 and (d) with CO_2.

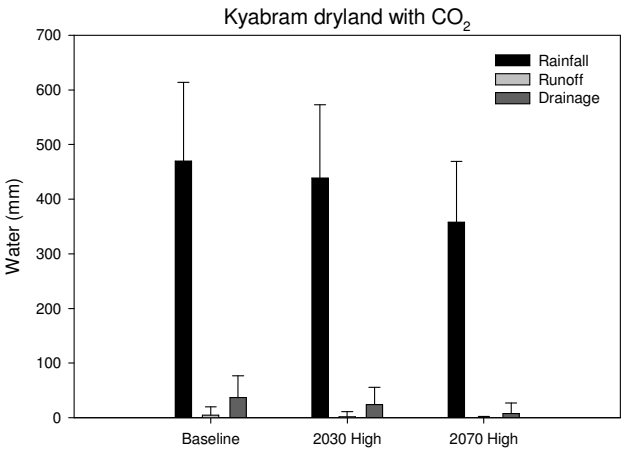

Figure 48. Rainfall, irrigation, runoff and drainage for dryland pasture at Kyabram under baseline, 2030 High and 2070 High scenarios. CO_2 is included in these simulations (vertical bars indicate one SD).

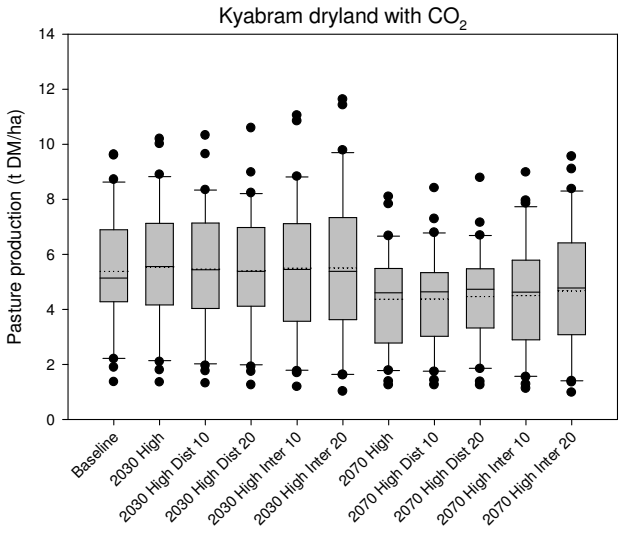

Figure 49. Annual dryland pasture production at Kyabram for the baseline, 2030 and 2070 High scenarios including the rainfall distribution treatments.

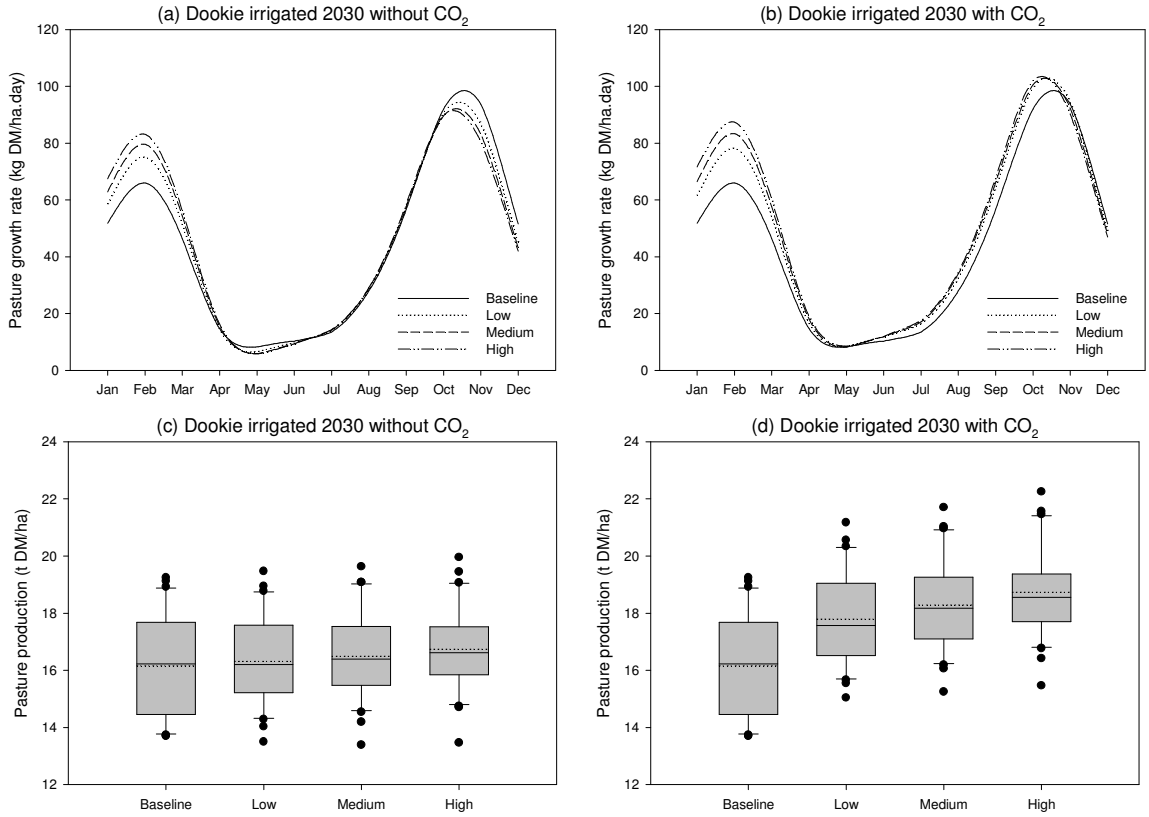

Figure 50. Pasture production at Dookie in 2030. Mean monthly growth rates (a) without CO_2 and (b) with CO_2, and annual production (c) without CO_2 and (d) with CO_2.

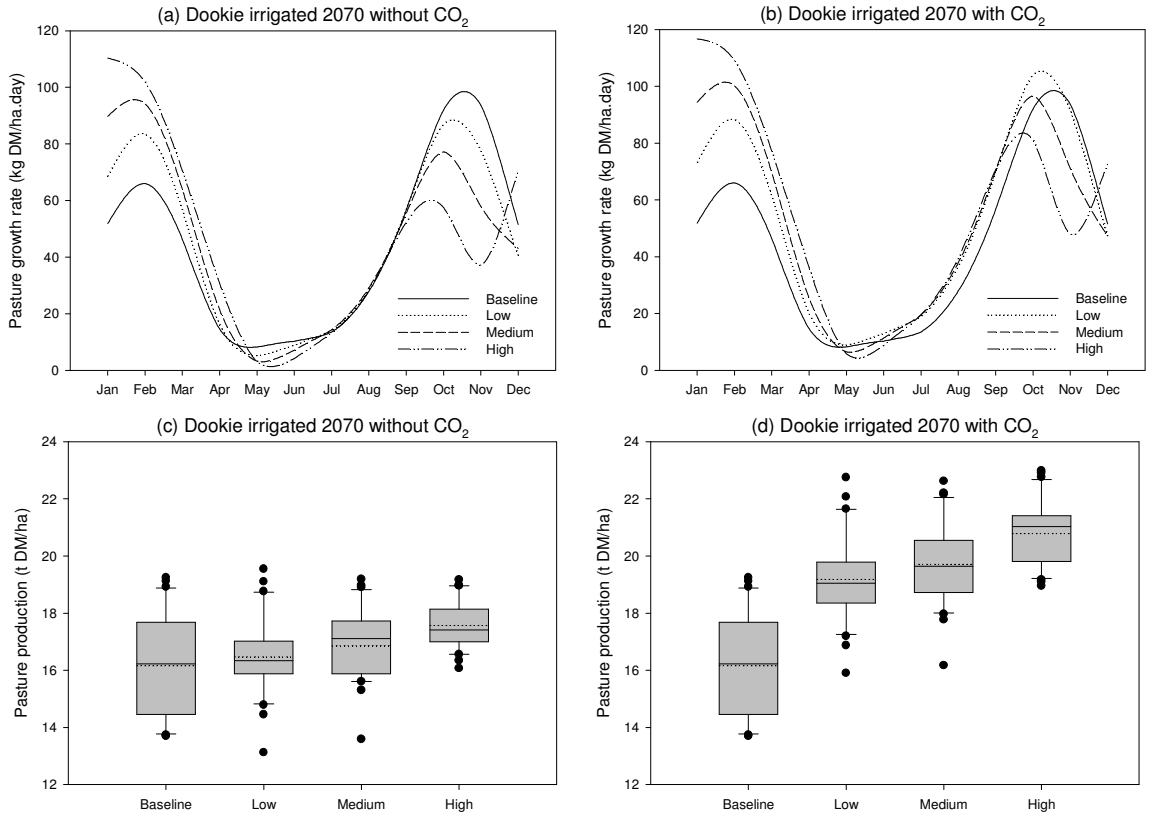

Figure 51. Pasture production at Dookie in 2070. Mean monthly growth rates (a) without CO_2 and (b) with CO_2, and annual production (c) without CO_2 and (d) with CO_2.

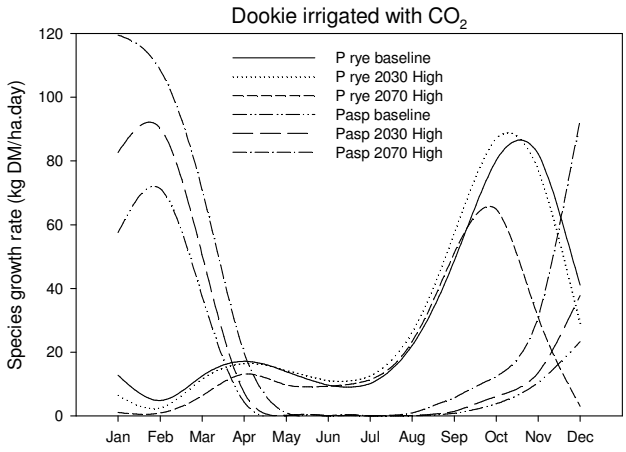

Figure 52. Growth rates of perennial ryegrass and paspalum at Dookie under baseline, 2030 High and 2070 High scenarios. CO_2 is included in these simulations.

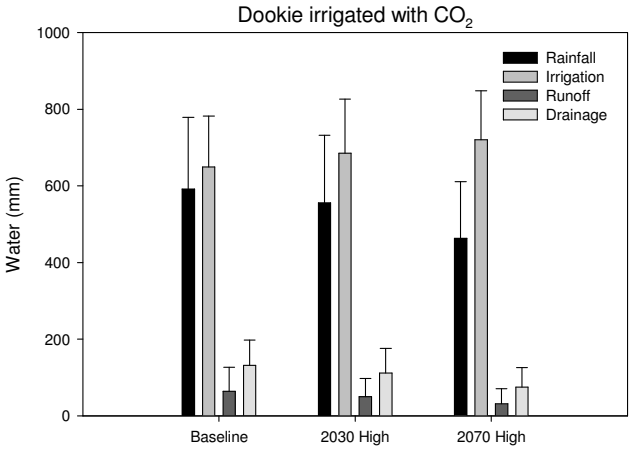

Figure 53. Rainfall, irrigation, runoff and drainage at Dookie under baseline, 2030 High and 2070 High scenarios. CO_2 is included in these simulations (vertical bars indicate one SD).

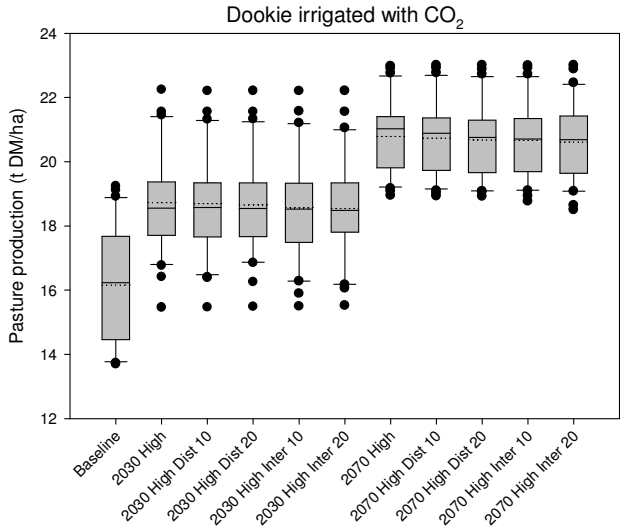

Figure 54. Annual pasture production at Dookie for the baseline, 2030 and 2070 High scenarios including the rainfall distribution treatments.

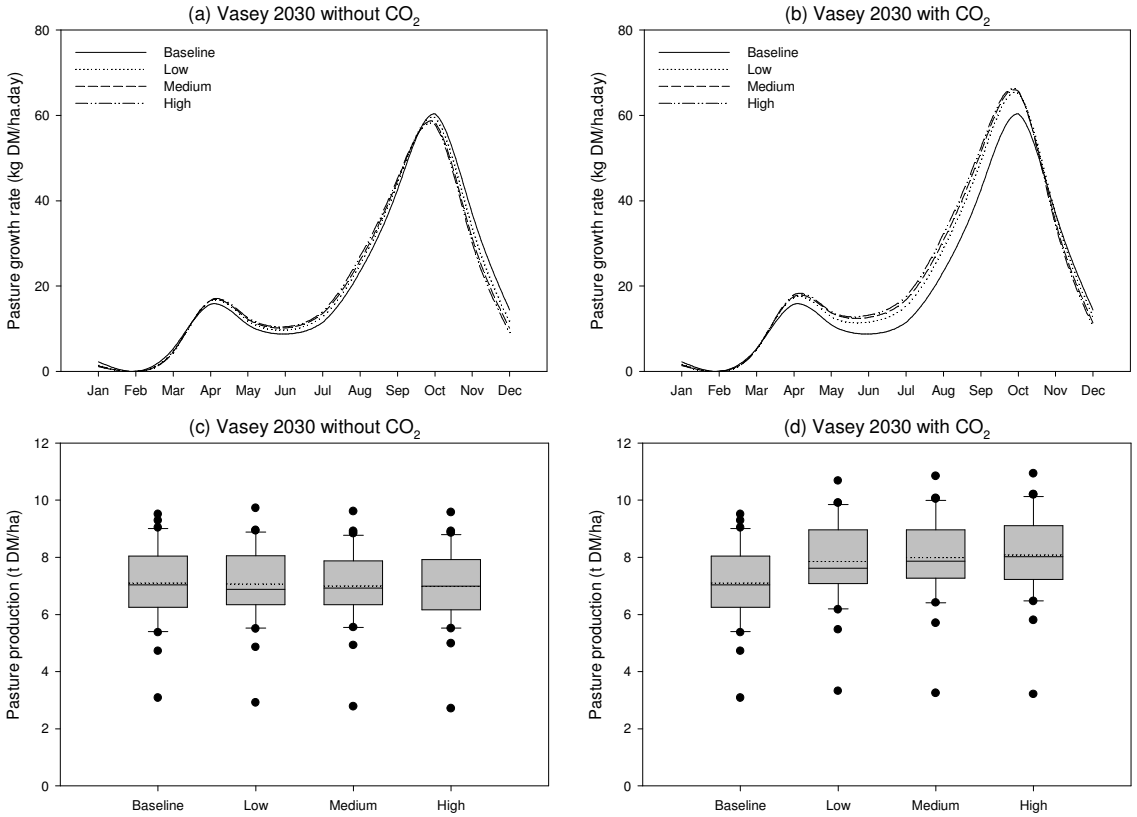

Figure 55. Pasture production at Vasey in 2030. Mean monthly growth rates (a) without CO_2 and (b) with CO_2, and annual production (c) without CO_2 and (d) with CO_2.

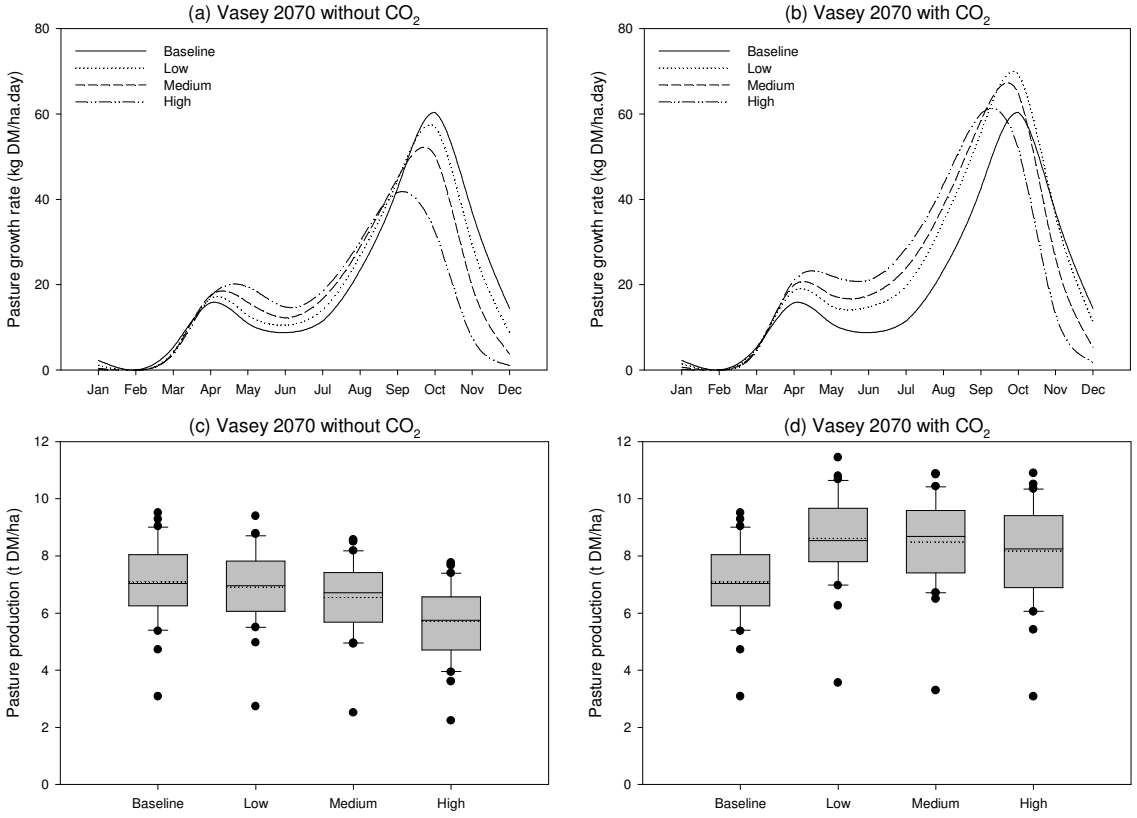

Figure 56. Pasture production at Vasey in 2070. Mean monthly growth rates (a) without CO_2 and (b) with CO_2, and annual production (c) without CO_2 and (d) with CO_2.

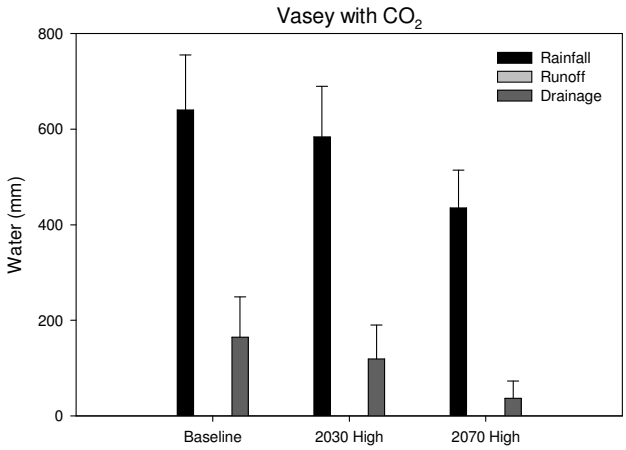

Figure 57. Rainfall, runoff and drainage at Vasey under baseline, 2030 High and 2070 High scenarios. CO_2 is included in these simulations (vertical bars indicate one SD).

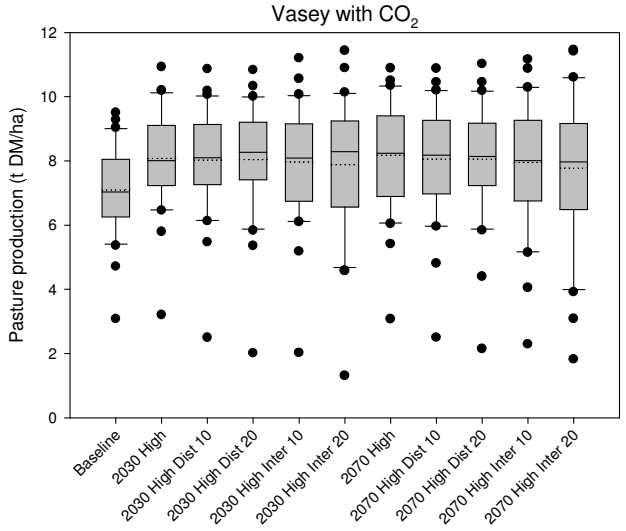

Figure 58. Annual pasture production at Vasey for the baseline, 2030 and 2070 High scenarios including the rainfall distribution treatments.

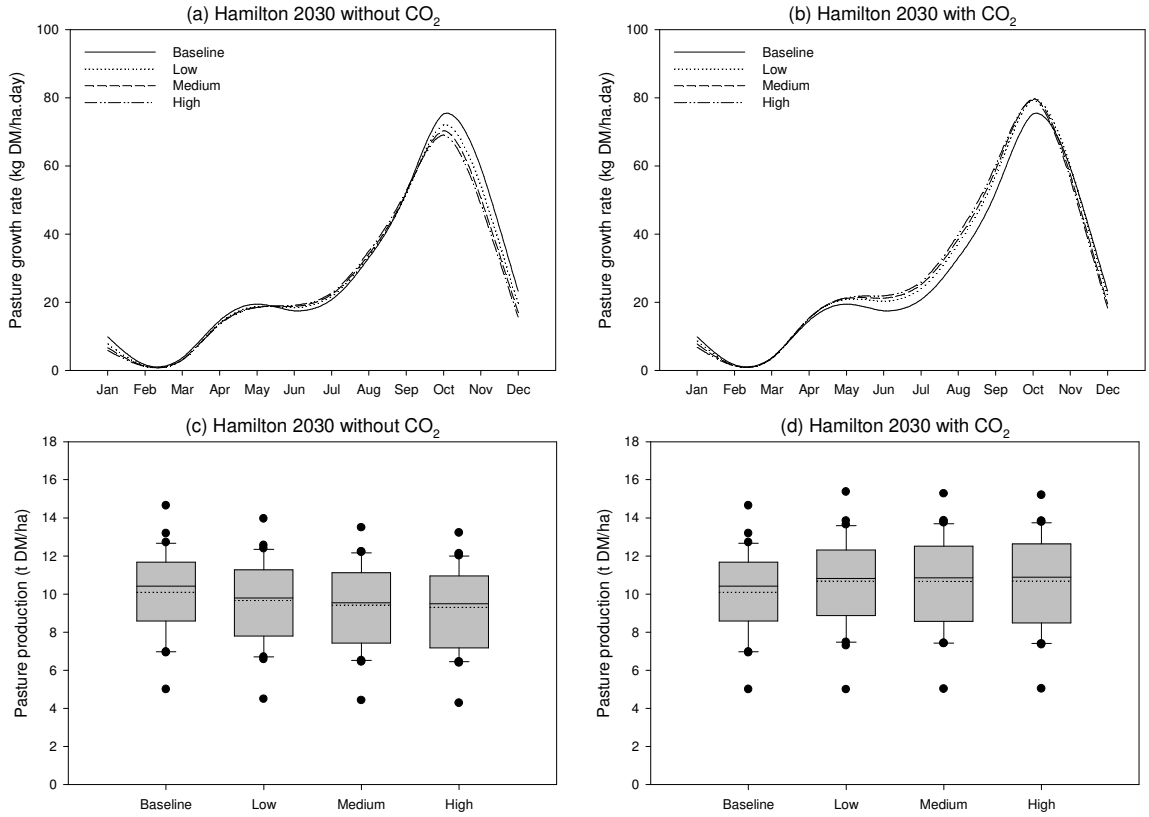

Figure 59. Pasture production at Hamilton in 2030. Mean monthly growth rates (a) without CO_2 and (b) with CO_2, and annual production (c) without CO_2 and (d) with CO_2.

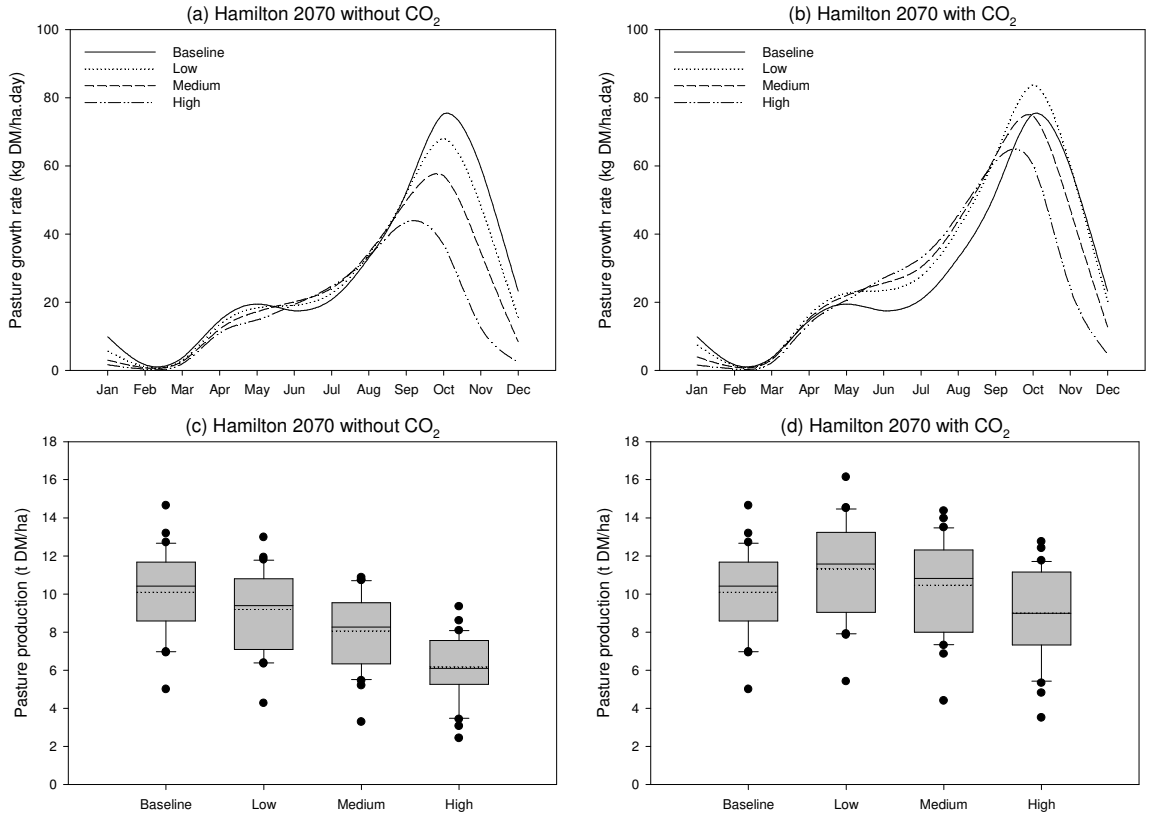

Figure 60. Pasture production at Hamilton in 2070. Mean monthly growth rates (a) without CO_2 and (b) with CO_2,and annual production (c) without CO_2 and (d) with CO_2.

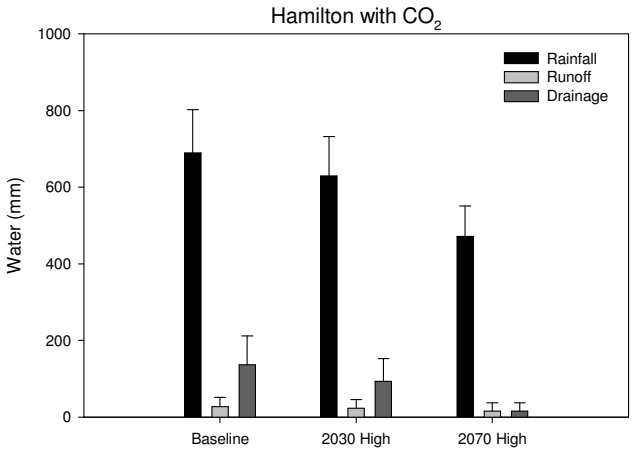

Figure 61. Rainfall, runoff and drainage at Hamilton under baseline, 2030 High and 2070 High scenarios. CO_2 is included in these simulations (vertical bars indicate one SD).

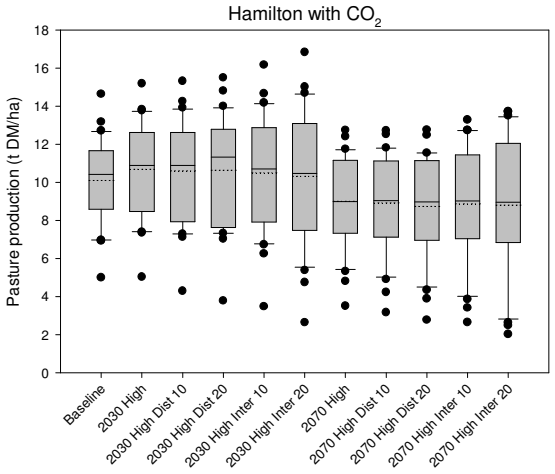

Figure 62. Annual pasture production at Hamilton for the baseline, 2030 and 2070 High scenarios including the rainfall distribution treatments.

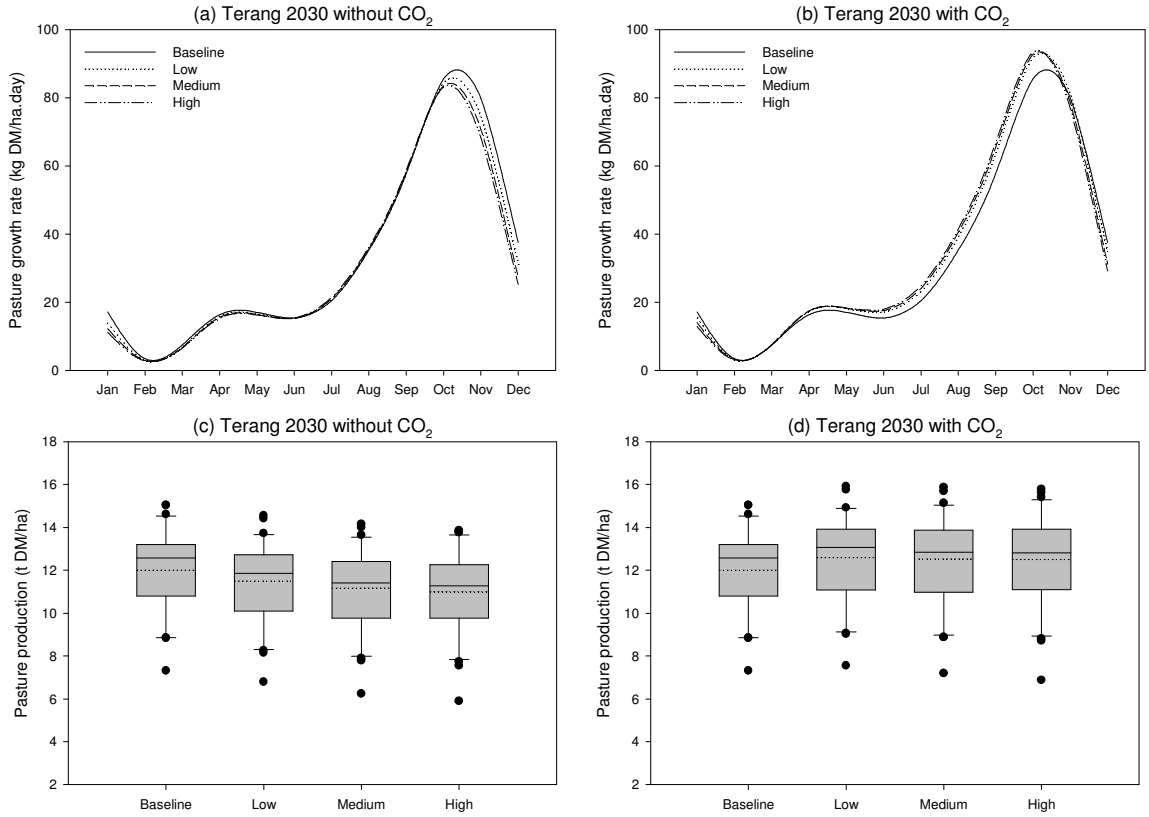

Figure 63. Pasture production at Terang in 2030. Mean monthly growth rates (a) without CO_2 and (b) with CO_2, and annual production (c) without CO_2 and (d) with CO_2.

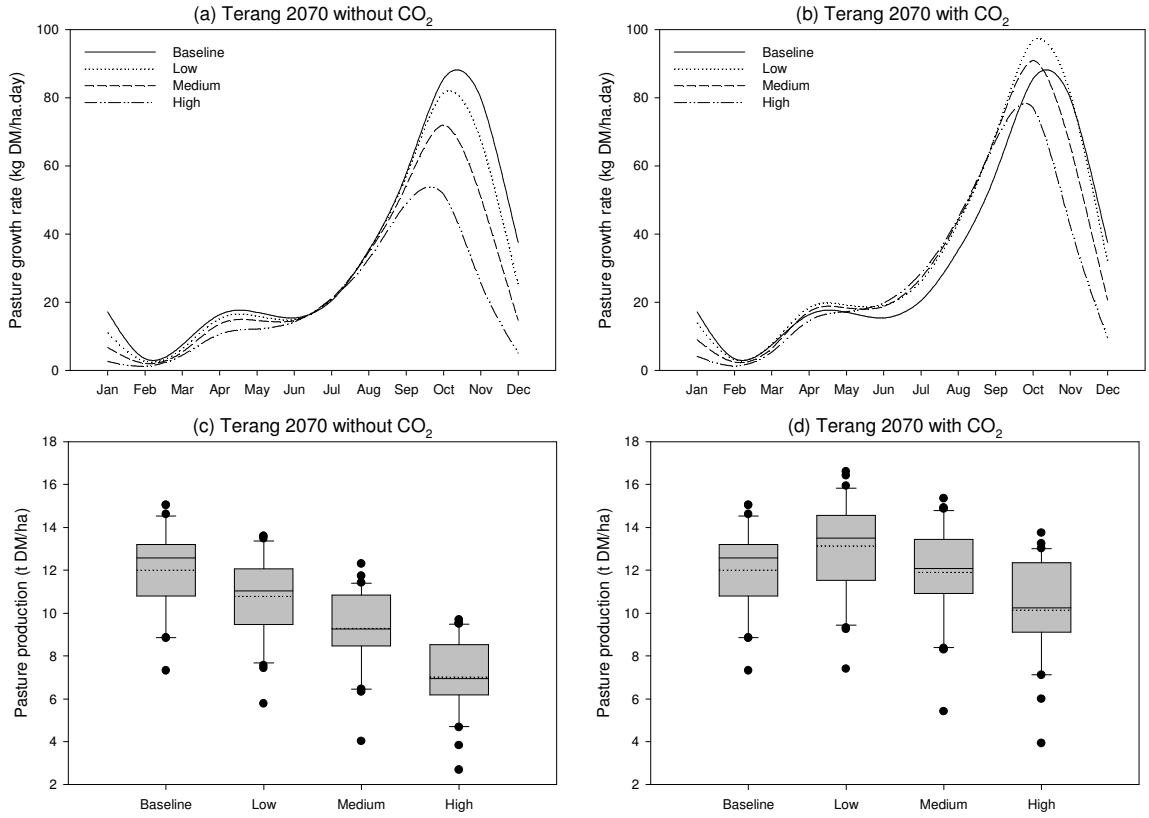

Figure 64. Pasture production at Terang in 2070. Mean monthly growth rates (a) without CO_2 and (b) with CO_2, and annual production (c) without CO_2 and (d) with CO_2.

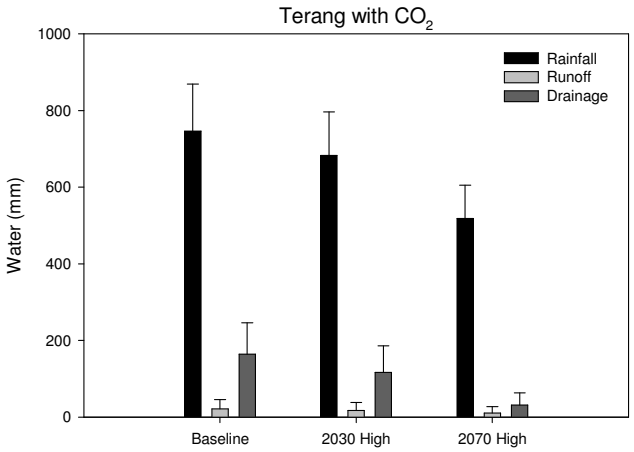

Figure 65. Rainfall, runoff and drainage at Terang under baseline, 2030 High and 2070 High scenarios. CO_2 is included in these simulations (vertical bars indicate one SD).

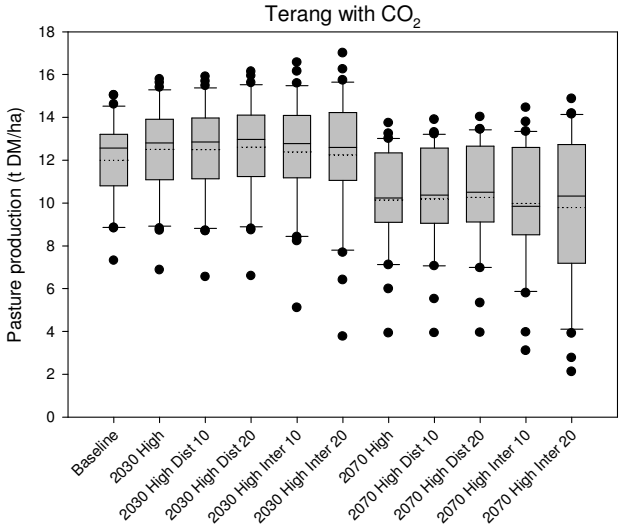

Figure 66. Annual pasture production at Terang for the baseline, 2030 and 2070 High scenarios including the rainfall distribution treatments.

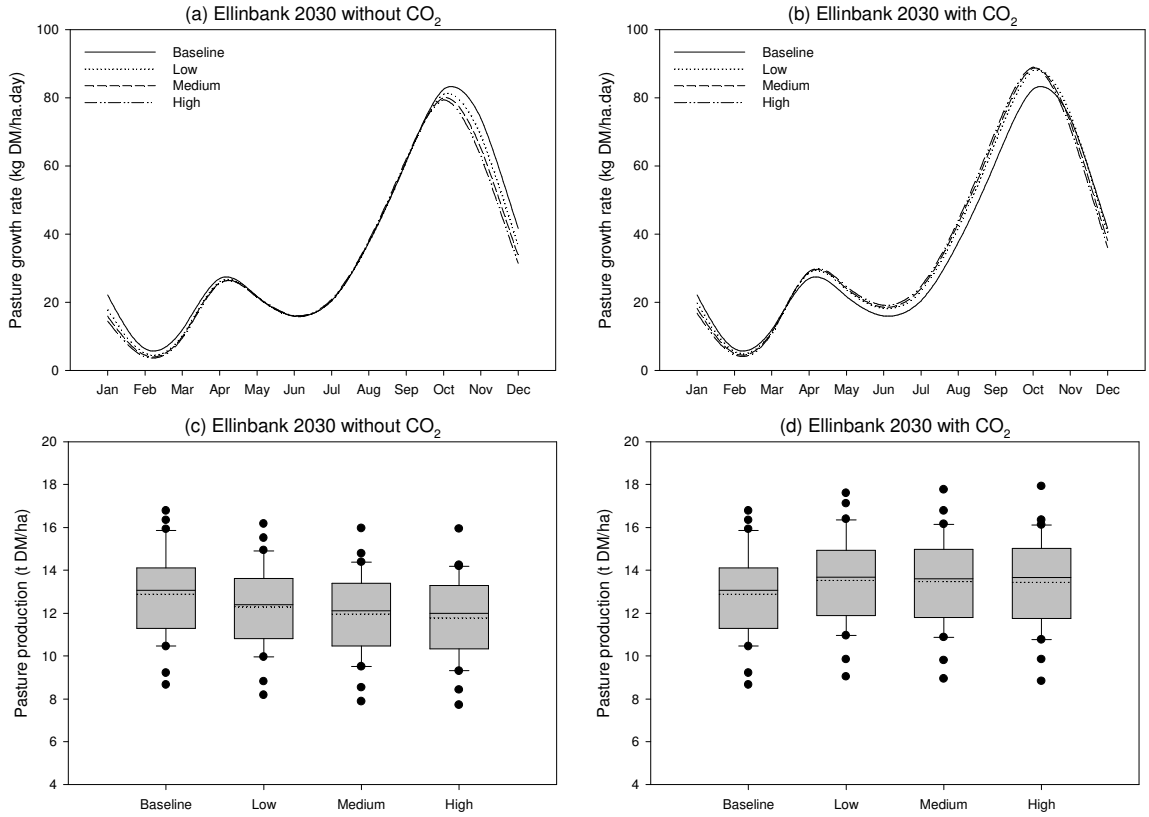

Figure 67. Pasture production at Ellinank in 2030. Mean monthly growth rates (a) without CO_2 and (b) with CO_2, and annual production (c) without CO_2 and (d) with CO_2.

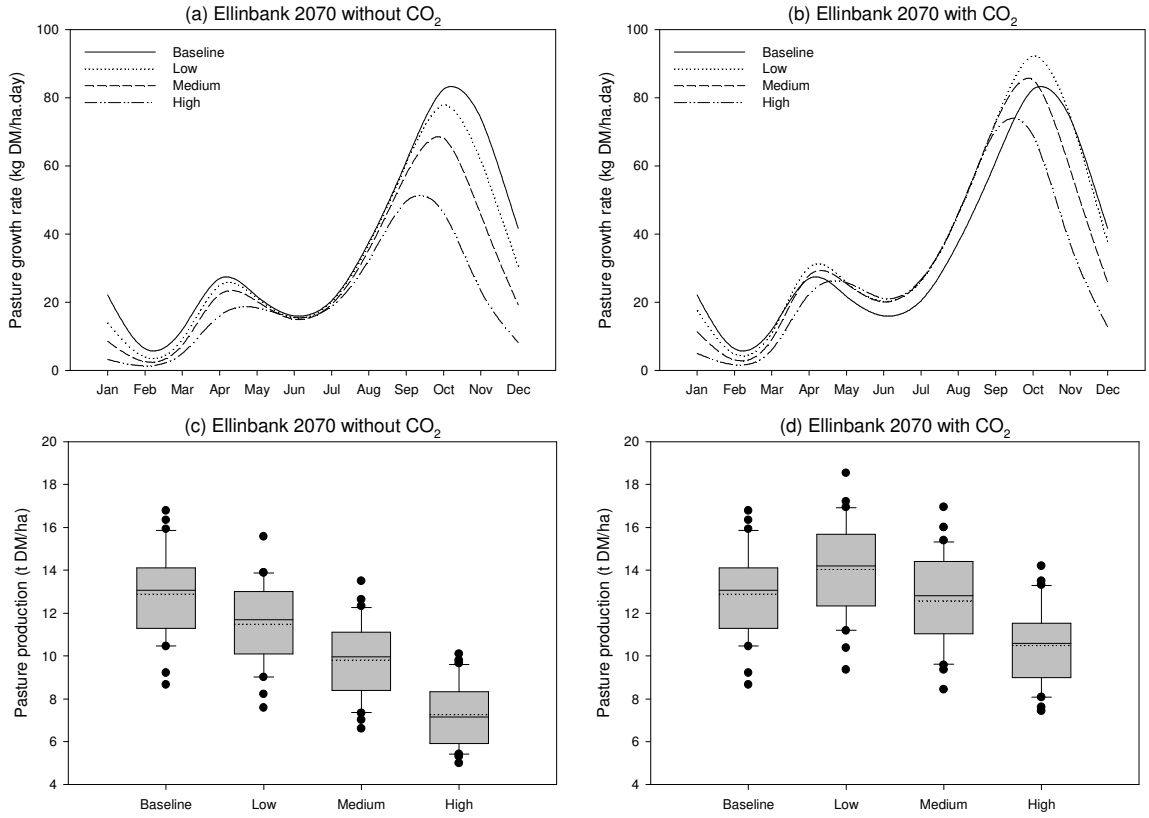

Figure 68. Pasture production at Ellinbank in 2070. Mean monthly growth rates (a) without CO_2 and (b) with CO_2, and annual production (c) without CO_2 and (d) with CO_2.

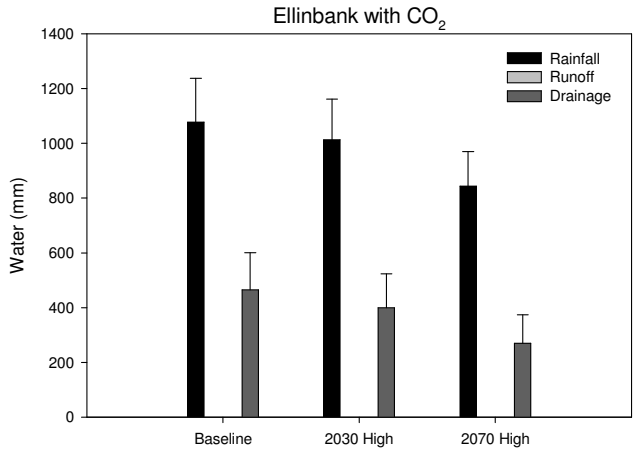

Figure 69. Rainfall, runoff and drainage at Ellinbank under baseline, 2030 High and 2070 High scenarios. CO_2 is included in these simulations (vertical bars indicate one SD).

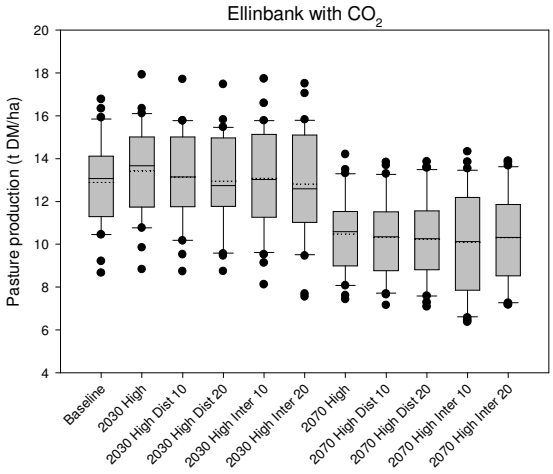

Figure 70. Annual pasture production at Ellinbank for the baseline, 2030 and 2070 High scenarios including the rainfall distribution treatments.

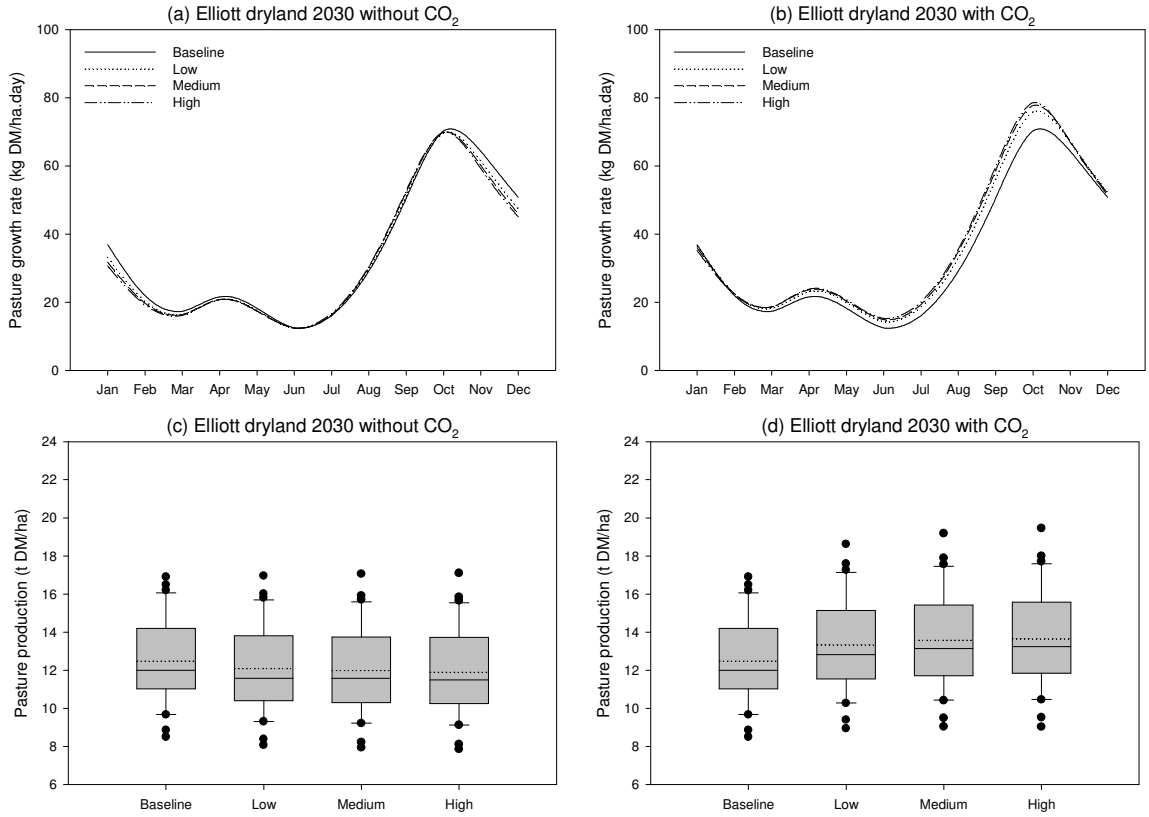

Figure 71. Dryland pasture production at Elliott in 2030. Mean monthly growth rates (a) without CO_2 and (b) with CO_2, and annual production (c) without CO_2 and (d) with CO_2.

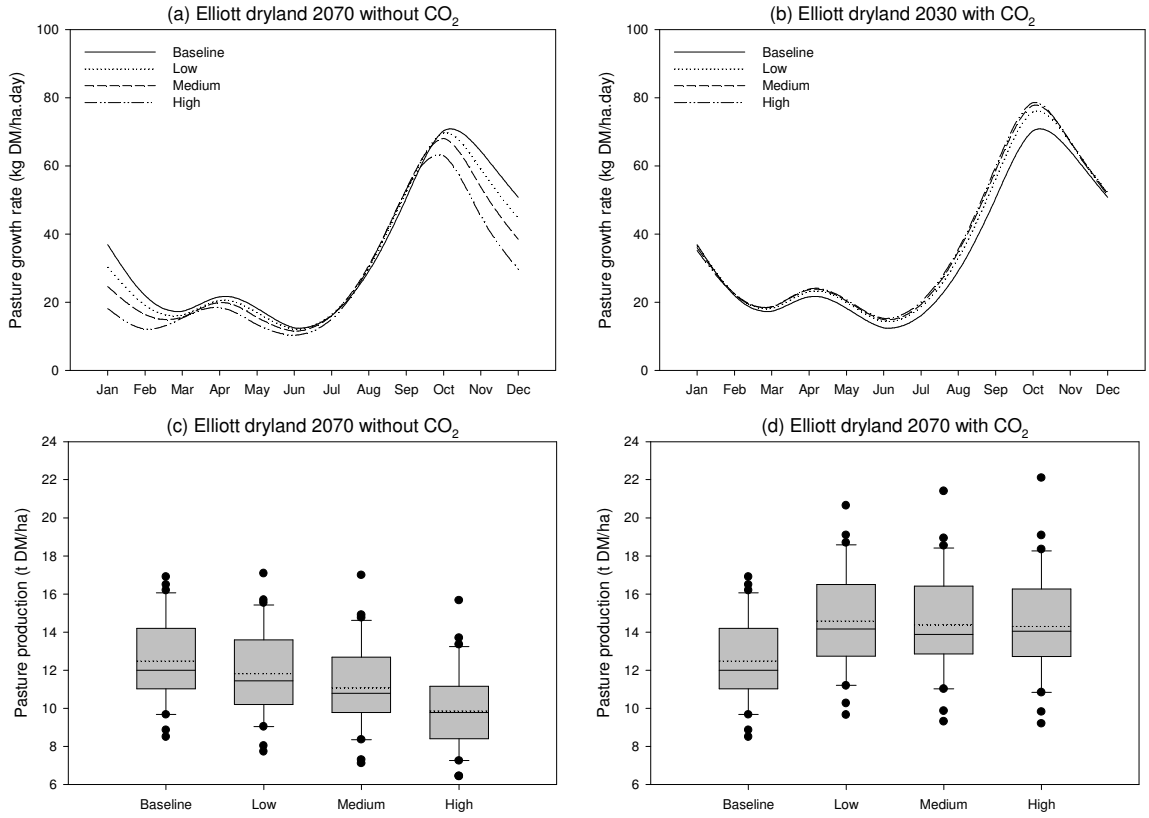

Figure 72. Dryland pasture production at Elliott in 270. Mean monthly growth rates (a) without $CO_2$and (b) with CO_2 and annual production (c) without CO_2 and (d) with CO_2.

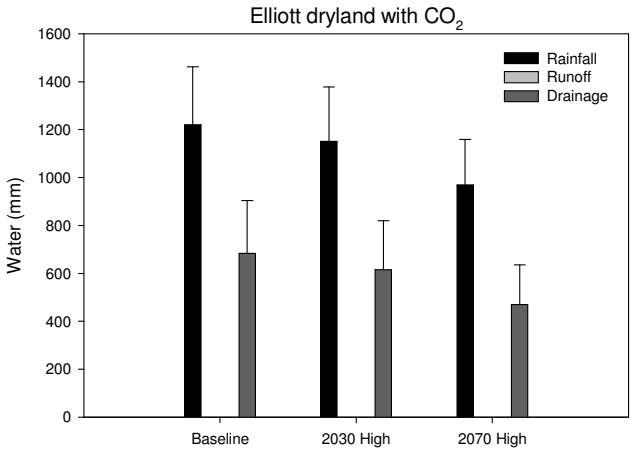

Figure 73. Rainfall, runoff and drainage for dryland pasture at Elliott under baseline, 2030 High and 2070 High scenarios. CO_2 is included in these simulations (vertical bars indicate one SD).

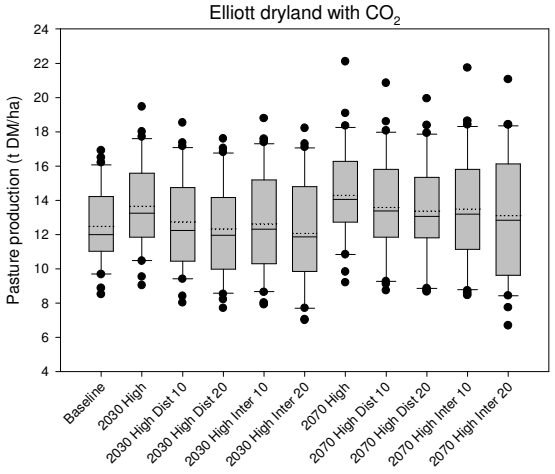

Figure 74. Annual dryland pasture production at Elliott for the baseline, 2030 and 2070 High scenarios including the rainfall distribution treatments.

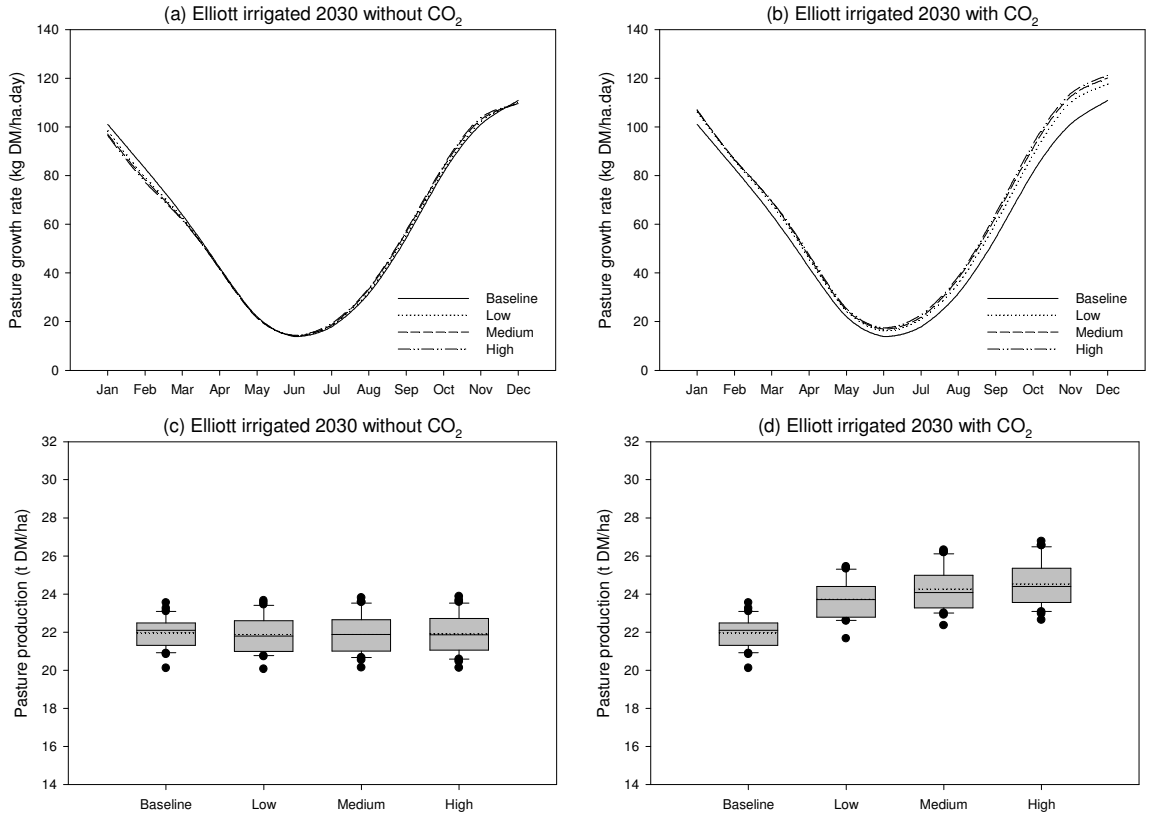

Figure 75. Irrigated pasture production at Elliott in 2030. Mean monthly growth rates (a) without CO_2 and (b) with CO_2, and annual production (c) without CO_2 and (d) with CO_2.

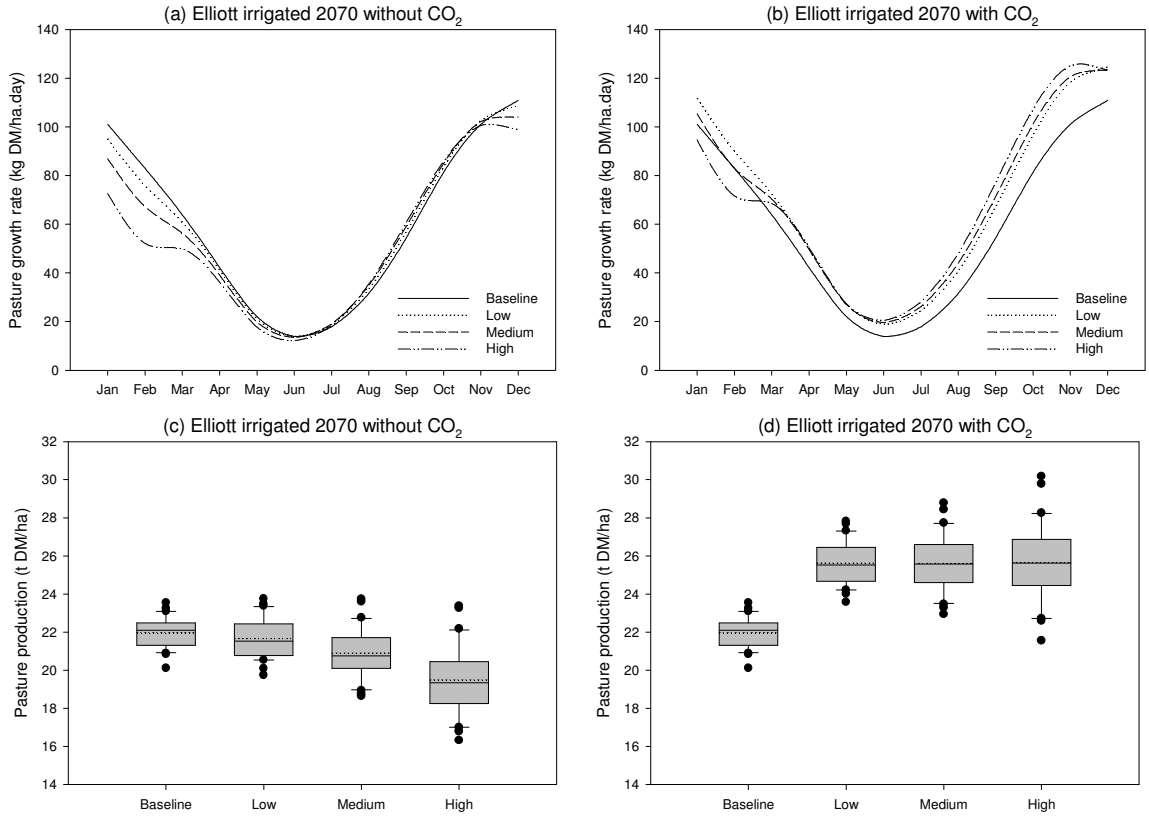

Figure 76. Irrigated pasture production at Elliott in 2070. Mean monthly growth rates (a) without CO_2 and (b) with CO_2, and annual production (c) without CO_2 and (d) with CO_2.

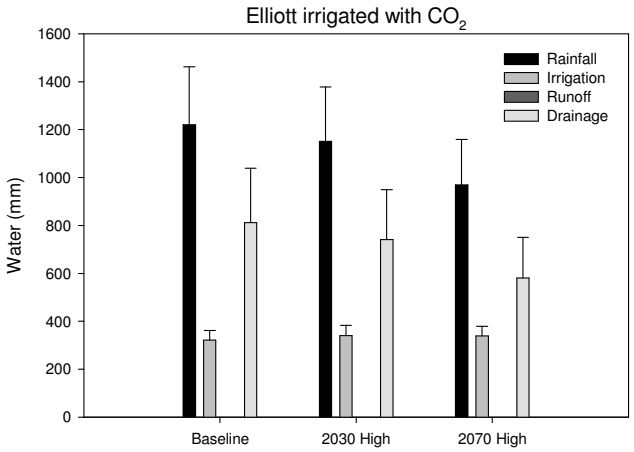

Figure 77. Rainfall, irrigation, runoff and drainage for irrigated pasture at Elliott under baseline, 2030 High and 2070 High scenarios. CO_2 is included in these simulations (vertical bars indicate one SD).

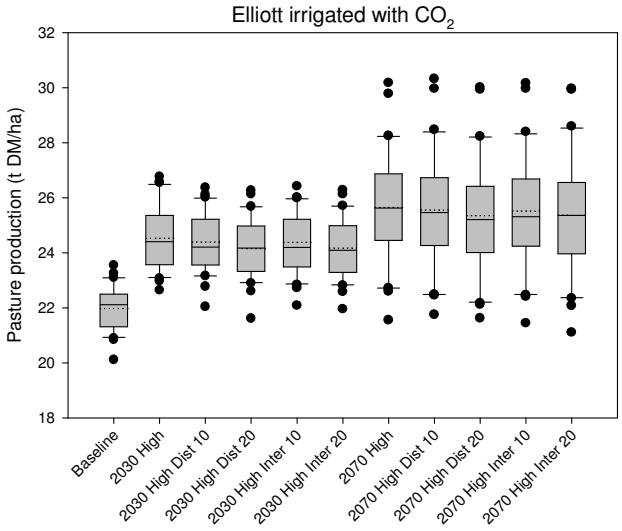

Figure 78. Annual irrigated pasture production at Elliott for the baseline, 2030 and 2070 High scenarios including the rainfall distribution treatments.

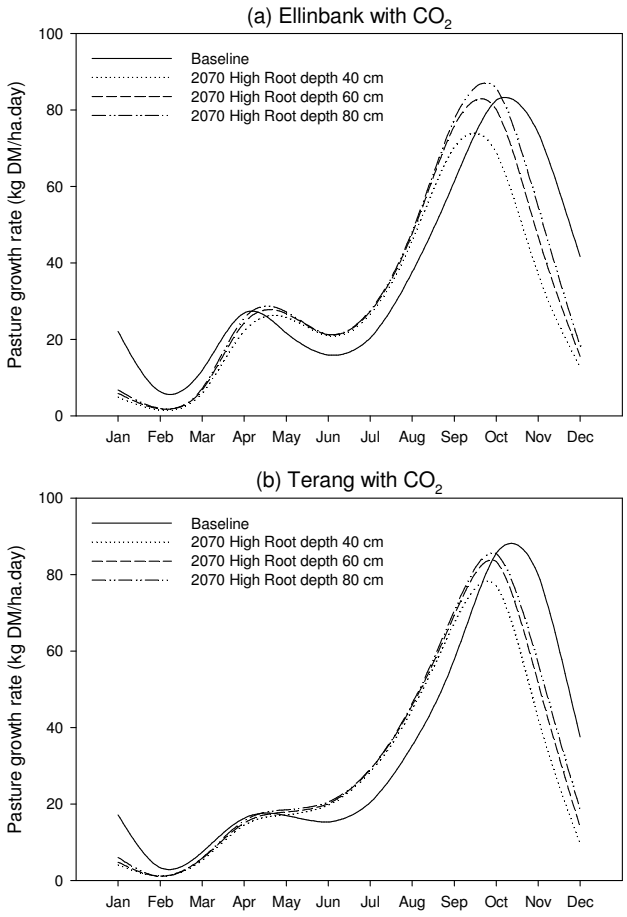

Figure 79. Effect of increasing root depth on monthly pasture growth rate under the 2070 High future climate scenario at (a) Ellinbank and (b) Terang. The baseline pasture growth rate is also shown for comparison.

Discussion

The simulated impact of future climate scenarios on forage production and quality for a range of pasture systems across Australia was determined by the interactions between the climate scenario modelled, location and pasture type. The climate scenario, including both the emission scenario and the year in the future selected, and location determined the amount of climatic shift (ie. temperature and rainfall change). For each location, existing well-adapted pasture types were modelled, with responses to future climate scenarios determined by the species ability to cope with increasing temperature and changes in rainfall patterns. In this respect, the photosynthetic pathway (C_3 or C_4) and rooting depth were important plant attributes.

In 2030 there was little difference between the Low, Medium and High climate change statistics (Table 2) and simulated pasture production at each site (Table 5). Under the 2030 scenarios with CO_2 included in the simulation, annual yields where increased at all sites above the baseline (by up to 20% at Albany, Table 5). This suggests that the grazing systems modelled in northern Australia are resilient to 1.2^{o}C temperature increases with little change in rainfall, and southern grazing systems are resilient to temperature increase of 0.8^{o}C and rainfall reduction up to 9%.

However in the 2070 scenarios, differences between the climate change projections were more apparent (Table 2), and important changes in pasture production were observed particularly under the Medium and High change scenarios (Table 5). At southern Australian sites, these 2070 Medium and High scenarios corresponded with a 1.5-3.7^{o}C temperature increase and 11-30% annual rainfall decrease, with reductions concentrated in spring. In C_3 dominant pastures, increased winter and early spring growth rates were observed under these conditions however the length of the spring growing season contracted so that annual production declined (eg. Wagga Wagga, Hamilton, Terang and Ellinbank sites, Table 5). At other sites dominated by C_3 species under the 2070 High scenario, production was greater than the baseline but less than the 2070 Low and Medium climate change scenarios (eg. Vasey and Elliott dryland, Table 5). A similar pattern was observed in the kikuyu/subclover system at Albany where annual production was maintained above the baseline under the 2070 High scenario that simulated a temperature increase of 3.3^{o}C and 20% rainfall decline. However, there was a change in species composition under these conditions with kikuyu becoming the dominant species for an extra two months per year (Fig 34). C_3 species are expected to remain of higher forage quality than C_4 species at elevated CO_2 concentrations despite some changes in protein and carbohydrate levels (Barbehenn *et al.* 2004), so this modelled change in species composition has important implications for animal production potential, in the absence of balancing supplementation.

In the subtropical regions, the 2070 High impact scenarios suggest a temperature increase of 4.2-4.4^{o}C and, though there is little change in annual rainfall, a shift towards more summer rainfall dominance is predicted. Under these conditions mixed C_3/C_4 pastures were able to increase annual production (eg. Kyogle, Mutdapilly and Barraba sites), but with a shift towards C_4 species dominance. A similar pattern was observed in the

irrigated pastures of northern Victoria, where rainfall declines were compensated for by increased irrigation requirements. This shift towards C_4 species dominance will reduce forage quality resulting in lower ruminant animal production and increased methane emissions (Howden *et al.* 2008). The specific implications for livestock production systems require further analysis on a case-by-case basis.

The influence of elevated atmospheric CO_2 concentrations on pasture growth (via leaf photosynthetic potential and canopy conductance) was particularly important in C_3 pastures (eg. Wagga Wagga, Vasey, Hamilton, Terang and Elliott sites). Howden *et al.* (2008) argued that the overall impact of climate change on pasture production in southern Australia would be determined by the balance between increased production through higher atmospheric CO_2 and decreased production caused by lower rainfall and higher evaporation, with these effects balancing at approximately 10% rainfall reduction. This study confirms that finding in the Mediterranean and temperate environments (eg. Wagga Waaga, Hamilton, Terang and Ellinbank sites). In these environments, there was little change or a small increases in annual pasture production modelled where rainfall decrease by up to 10%, but reduced pasture production when the rainfall reductions were larger. However the modelling for dryland production at Elliott suggests that high rainfall cool temperate environments can cope with larger rainfall declines (>20%) before production is limited.

The main impacts of the future climate scenarios on the water balance were at the southern Australian sites where there were large reductions in rainfall (Table 2). At these sites, there was a significant reduction in drainage of water below the root zone (eg. Albany, Vasey, Hamilton, Terang, Ellinbank and Elliott dryland sites). This has implications for dryland salinity, with less water entering the watertable. Similar reductions in deep drainage were modelled in wheat cropping systems in Western Australia (van Ittersum *et al.* 2003). There was a general reduction in the amount of runoff generated, which suggests a reduced erosion risk, however it is important to note that changes in rainfall intensity have not been taken into account in these climate scenarios. While modelling irrigation water availability was not the focus of this study, the reduced runoff that was simulated together with the increases in irrigation requirements that were modelled at the Elliott, Kyabram and Dookie sites suggest an increasingly limited water supply. At a catchment scale, Jones *et al.* 2006 showed that each 1% change in annual rainfall relates to runoff change of 1.8-4.1%, depending on the catchments characteristics and the hydrological model used for analysis. The implications of a range of climate change scenarios for irrigation inflows and land use changes in the Murray-Darling basin are explored by Quiggan *et al.* (2008).

Irrigated farming systems are significantly more complex to understand and model than rainfed systems. For the purpose of this project, we have taken one site (Kyabram in northern Victoria) and combined the predicted increases in irrigation requirement (due to higher temperatures and evapotranspiration) with the predicted decreases in irrigation water supply. Under a 2030 climate scenario, CSIRO (2008) estimated that runoff in the Goulburn-Broken catchment would be reduced by 13% (range -44 to -2%), corresponding to a 5% reduction in water availability for use. Quiggan *et al.* (2008)

projected a 7% reduction (range -15 to +2%) in irrigation inflows in the same catchment. In both studies the range in projections is large due to uncertainties about future rainfall patterns. This reduced water supply, together with an average 6% increase in water required to irrigate pastures in the 2030 High future climate scenario (Fig 44), suggests a 10% decrease in irrigated pasture area. In 2070 unmitigated climate change scenarios, Quiggan *et al.* (2008) estimated a 22% reduction in irrigation inflows (range -84 to +5%). When this is combined with a 9% increase in water required to irrigate pastures in 2070 (Fig 44), a 29% decrease in irrigated pasture area is estimated.

If we take a hypothetical dairy farm that during the baseline period (1971 to 2000) had 100 ha of irrigated perennial pasture, and 25 ha of dryland pasture, then in 2030 this farm would only be able to irrigate 90 ha (with 35 ha of dryland pasture) and in 2070, the area of irrigated pasture would be reduced to 71 ha (Figure 80a). At Kyabram, dryland pasture produces approximately one third as much dry matter as irrigated pasture in the baseline climate scenario (Table 5). In the 2030 scenario, higher growth rates for irrigated and dryland pastures (Table 5) compensate for the reduced area of irrigated pasture area and total farm pasture production was increased by 3% compared to the baseline (Figure 80b). However in the 2070 scenario lower dryland pasture growth rates (Table 5) and reduced irrigated pasture area result in total farm pasture production being 5% less than the baseline (Figure 80b).

It is likely that these estimates of irrigation water availability used here are optimistic because the baseline period had historically high irrigation water availability, with inflows into the Murray Darling Basin over the last 10 years being lower than the models predict for 2070 (CSIRO 2008), and competition for irrigation water from other industries (where the demand per ha will also increase), for urban users and for increased environmental flows will make water either more expensive for dairy farmers, less available, or both. On the positive side, strategies are available (or will be developed) that farmers can use to increase the amount of forage grown per unit of irrigation water and/or to introduce more flexibility to adapt to changing water availability. A more focused project is needed to explore the implications for irrigated dairy farming from changes in climate.

In dryland systems, deeper rooted perennial plants have the potential to overcome some of the reduced spring growth by intercepting more of the available water (ie. further reducing drainage) at the Ellinbank and Terang sites (Fig 79). Breeding for deeper rooted plants is therefore an effective means of reducing the impact of climate change in southern Victoria, however in pasture systems where there is little drainage (eg. the Wagga Wagga site) deeper rooted plant will merely dry out the root profile earlier in the season. Other adaptation options, such as improving heat tolerance of perennial ryegrass and changing planting time for annual ryegrass, need to be analysed. The Elliott irrigated simulation provides an example of heat stress impacts on pasture production with reduced January-March growth rates under the 2070 future climate scenarios (Fig 76).

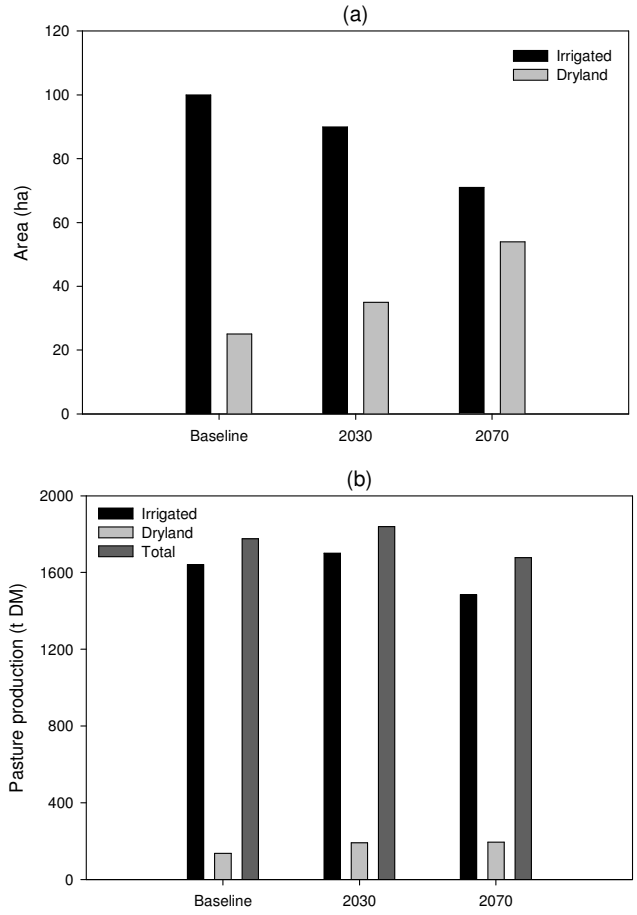

Figure 80. Hypothetical Kyabram farm under the historical baseline, 2030 and 2070 climate scenarios; (a) average area (ha) allocated to irrigated and dryland pasture production, and (b) total average annual pasture production (t DM) from irrigated and dryland areas together with the total farm pasture production.

In assessing the impacts of these future climate scenarios on pasture production it is important to recognise the limitations of the future climate scenarios, and be aware that climate change projections will change as global circulation models improve in their depiction of climatic systems. The method used to create the future climate scenarios reflects the changes in mean climate, but does not account for projected increases in extreme climate events, such as heat waves and high intensity rainfall. The rainfall variability treatments included in this analysis are an attempt to investigate the impact of changes in the rainfall pattern, however there was, in general, little impact on annual pasture production. More work needs to be carried out to assess the impacts of these scenarios on the water balance, and further quantification of extreme events is required from climate scientists before their effects on pasture systems can be adequately modelled. We must also recognise that our grazing system model does not model plant persistence, so increased temperature or drought effects on plant mortality have not been captured in this analysis. Increased plant mortality could have important management consequences such as the need to re-sow pasture more frequently. Finally, there are still

some uncertainties about responses to elevated CO_2, for example in the Swiss and New Zealand FACE experiment there was evidence of progressive N and P nutrient limitations developing, and associated increases in legume content of the pasture (Hartwig and Sadowsky 2006; Newton *et al.* 2006).

Conclusion

Climate change impacts on pasture production were predicted to be minor under the 2030 scenarios, associated with temperature increases of up to 1.2^{o}C and rainfall reductions up to 9%. However, under High climate change projections for 2070, with up to 4.4^{o}C warming and 30% annual rainfall declines, increased growth and a shift towards C_4 species dominance was modelled in mixed C_3/C_4 swards in summer dominant rainfall regions or where irrigation was applied, while declines up to 19% of annual production of C_3 dominant pastures in southern Australia were predicted. In these pastures, the decline in pasture production was moderated by reduced drainage below the root zone, and employing deeper rooted plant systems was an effective means of mitigating some of the impact of lower rainfall. This analysis reflects the performance of current systems in future climates. Undoubtedly farmers will 'incrementally' adapt to mitigate the impact of climate change using technologies such as plant breeding and seasonal climate forecasting systems, however this analysis also points to scenarios where production is outside of the range of previous experience and suggests that 'transformational' adaptation, such as changing land use, may be required. It is unlikely that it will be the physical impacts of climate change that determine tipping points for transformational changes in agricultural systems in the next 20 years, rather policy issues related to climate change mitigation, including carbon and water trading schemes, will impact on farm economics and drive decisions about land use.

Acknowledgements

The Whole Farms Systems Analysis and Tools (WFSAT) project was funded by Dairy Australia, Meat & Livestock Australia and AgResearch, New Zealand.

References

Ainsworth EA, Long SP (2005) What have we learned from 15 years of free-air CO_2 enrichment (FACE)? A meta-analytical review of the responses of photosynthesis, canopy properties and plant production to rising CO_2. *New Phytologist* **165**, 351-372.

Anwar MR, O'Leary G, McNeil D, Hossain H, Nelson R (2007) Climate change impact on rainfed wheat in south-eastern Australia. *Field Crop Research* **104**, 139-147.

Barbehenn RV, Chen Z, Karowe DN, Spickard A (2004) C_3 grasses have higher nutritional quality than C_4 grasses under ambient and elevated atmospheric CO_2. *Global Change Biology* **10**, 1565-1575.

CSIRO (2007) Climate change in Australia. Technical report 2007. (Eds KB Pearce, PN Holper, M Hopkins, WJ Bouma, PH Whetton, KJ Hensessy, SB Power) p. 148. (CSIRO Marine and Atmospheric Research: Aspendale) http://www.climatechangeinaustralia.gov.au/

CSIRO (2008) Water availability in the Goulburn-Broken. A Report to the Australian Government from the CSIRO Murray-Darling Basin Sustainable Yields Project. CSIRO Australia. 132 pp. http://www.csiro.au/partnerships/MDBSYReports.html (accessed 21st October 2008)

Cullen BR, Eckard RJ, Callow MN, Johnson IR, Chapman DF, Rawnsley RP, Garcia SC, White T, Snow VO (2008) Simulating pasture growth rates in Australian and New Zealand grazing systems. *Australian Journal of Agricultural Research* **59**, 761-768.

Hartwig UA, Sadowsky MJ (2006) Biological nitrogen fixation: a key process for the response of grassland ecosystems to elevated atmospheric [CO_2]. In 'Managed ecosystems and CO2: case studies processes and perspectives. Ecological studies 187'. (Eds J Nösberger, SP Long, RJ Norby, M Stitt, GR Hendrey, H Blum) pp. 325-336. (Springer-Verlag: Berlin, Heidelberg)

Howden SM, Crimp SJ, Stokes CJ (2008) Climate change and Australian livestock systems: impacts, research and policy issues. *Australian Journal of Experimental Agriculture* **48**, 780-788.

Hennessy KJ (2007) Climate change in Australian dairy regions. CSIRO Atmospheric Research: Aspendale

Isbell RF (1996) 'Australian soil and land survey handbook: the Australian soil classification.' (CSIRO Publishing: Collingwood, Victoria)

IPCC (2001) Summary for policy makers. In: Houghton JT, Ding Y, Griggs DJ, Noguer M, van der Linden PJ, Xioaosu D (Eds) Climate change 2001: The scientific basis. Contribution of working group I to the third assessment report of the Intergovernmental Panel on Climate Change. Cambridge University Press, Cambridge, 944 pp.

Jeffrey SJ, Carter JO, Moodie KM, Beswick AR (2001) Using spatial interpolation to construct a comprehensive archive of Australian climate data. *Environmental Modelling and Software* **16**, 309-330.

Johnson IR, Chapman DF, Snow VO, Eckard RJ, Parsons AJ, Lambert MG, Cullen BR (2008) DairyMod and EcoMod: Biophysical pastoral simulation models for Australia and New Zealand. *Australian Journal of Experimental Agriculture* **48**, 621-631.

Johnson IR, Lodge GM, White RE (2003) The Sustainable Grazing Systems Pasture Model: description, philosophy and application to the SGS National Experiment. *Australian Journal of Experimental Agriculture* **43**, 711-728.

Johnson IR, Riha SG, Wilks DS (1995) Modelling daily net canopy photosynthesis and its adaptation to irradiance and atmospheric CO_2 concentration. *Agricultural Systems* **50,** 1-35.

Jones R, Chiew FHS, Broughton WC, Zhang L (2006) Estimating of mean annual runoff to climate change using selected hydrological models. *Advances in Water Resources* **29**, 1419-1429.

Long SP, Ainsworth EA, Rogers A, Ort DR (2004) Rising atmospheric carbon dioxide: plants FACE the future. *Annual Review of Plant Biology* **55**, 591-628.

Lüsher A, Aeschlimann U, Schneider MK, Blum H (2006) Short- and long-term responses of fertile grassland to elevated [CO_2]. In 'Managed ecosystems and CO2: case studies processes and perspectives. Ecological studies 187'. (Eds J Nösberger, SP Long, RJ Norby, M Stitt, GR Hendrey, H Blum) pp.139-155. (Springer-Verlag: Berlin, Heidelberg)

Newton PCD, Allard V, Carran RA, Lieffering M (2006) Impacts of elevated CO_2 on a grassland grazed by sheep: the New Zealand FACE experiment. In 'Managed ecosystems and CO_2: case studies processes and perspectives. Ecological studies 187'. (Eds J Nösberger, SP Long, RJ Norby, M Stitt, GR Hendrey, H Blum) pp. 157-171. (Springer-Verlag: Berlin, Heidelberg)

Quiggin J, Adamson D, Schrobback P, Chambers S (2008) Garnaut climate change review: the implications for irrigation in the Murray-Darling basin. http://www.garnautreview.org.au/CA25734E0016A131/WebObj/01-AMDBasin/$File/01-A%20MDBasin.pdf (Accessed 26th August 2008)

Tubiello FN, Amthor JS, Boote KJ, Donatelli M, Easterling W, Fischer G, Gifford RM, Howden M, Rielly J, Rosenzweig C (2007) Crop response to elevated CO_2 and world food supply. A comment on "Food for thought…" by Long et al Science 312: 1918-1921, 2006. *European Journal of Agronomy* **26**, 215-223.

Thornley JHM, Johnson IR (2000) 'Plant and Crop Modelling'. (The Blackburn Press)

van Ittersum MK, Howden SM, Asseng S (2003) Sensitivity of productivity and deep drainage of wheat cropping systems in a Mediterranean environment to changes in CO_2, temperature and precipitation. *Agriculture, Ecosystems and Environment* **97**, 255-273.

White TA, Johnson IR, Snow VO (2008) Comparison of outputs of a biophysical simulation model for pasture growth and composition with measured data under dryland and irrigated conditions in New Zealand. *Grass and Forage Science* **63**, 339-349.

Appendix 1. WFSAT Future Climate Scenarios – Users guide.

Brendan Cullen, University of Melbourne
Email: bcullen@unimelb.edu.au

Overview

Future climate scenarios were based on historical climate data and climate change projections for each site. A 30-year climate 'baseline' (1971-2000) was used to capture inherent climate variability at each site. This 'baseline' was also used to create 30-year realisations of future climate scenarios. A 10-year lead-in period (1961-1970) was modelled prior to the 'baseline' to allow the initial conditions of the model to settle out.

Six future climate scenarios were developed based on Low, Medium and High climate change projections for 2030 and 2070.

Step-by-step guide to generating future climate scenarios

1. Historical climate data. Data for the 30-year baseline and 10-year 'lead-in' period (1/1/1961-31/12/2000 in total) were obtained from the Bureau of Meteorology SILO database (http://www.bom.gov.au/silo/). The Patched Point dataset was used if the site was adjacent to a weather station, if not then the DataDrill was used. Climate data was obtained in the 'Standard including ET_o' format.
2. De-trending historical data to 1990 baseline. Climate change statistics are usually expressed relative to 1990, so de-trending of historical data to 1990 levels is required. For example, if January minimum temperatures had a trend showing 0.1 ^oC temperature increase per year over the 1971-2000 period then, to de-trend to 1990 levels, minimum temperatures for January 1971 would be adjusted up by 0.1*20 years= 2 ^oC, 1972 by 0.1*19 years = 1.9 ^oC, … 2000 by -0.1*10 years = -1 ^oC.

   Trends in monthly average minimum/maximum temperature and rainfall were investigated over the 30-year baseline climate. However, few significant trends were observed (as measured by r^2 correlation), so de-trending of the data was not performed. The reason for the few significant trends was probably due to the relatively short (ie. 30 year) dataset examined.
3. Climate change statistics. The monthly climate change statistics for mean temperature change (^oC) and rainfall (%) were based on output from the CSIRO Mk3 global circulation model, obtained from the OzClim database (www.csiro.au/ozclim). The Low, Medium and High climate change impact scenarios were based on B1 emission scenario with low climate sensitivity, A1B emission scenario with medium climate sensitivity and A1FI emission scenario with high climate sensitivity respectively. The annual and monthly change statistics for each site are sown in Tables A3-A15.

A scalar factor was used to convert mean temperature changes from OzClim to maximum and minimum temperature changes. These scalar factors were read off Fig 5.10 (CSIRO 2007, p. 60).

Annual change statistics for radiation and relative humidity were adapted for each site from the nearest site reported in 'Appendix B – City Summaries' (CSIRO 2007, p. 130-136).

4. Scaling 'baseline' data. The daily 'baseline' climate data was directly scaled according to the climate change statistic outlined in point 3.

   An example, using the climate at Ellinbank on the 1st of January 1991, is shown in Table A1.

Variable	Baseline	Scaling	2070 High Impact
Rainfall (mm)	10.2	* Jan rain % Δ = *-17.9%	8.4
Min Temp (^oC)	10	+ (Jan Mean T Δ * Jan Min T scalar) = + 3.9*0.9	13.5
Max Temp (^oC)	17	+ (Jan Mean T Δ * Jan Max T scalar) = + 3.9*1	20.9
Radiation (MJ/m^2)	16	* Annual radiation % Δ = +2.6%	16.4
Rel Humidity Min (%)	77.5	* Annual relative humidity % Δ = -2.3%	75.7
Rel Humidity Max (%)	100	Relative humidity = 100 = no change	100

Table A1. An example of daily scaling of baseline climate data to produce future climate scenarios for the 2070 High impact scenario using the 1st January 1971 at Ellinbank.

5. Changing rainfall distribution. Climate change projections suggest that there is likely to be a change in the distribution of rainfall events, such that large rainfall events are increased volume and small rainfall events become less important. To simulate this change in rainfall distribution two rainfall distribution treatments were created, whereby rainfall events greater than the average event were scaled to increase by 10 and 20% respectively, with reductions to rainfall events less than the average made to keep the long-term average annual rainfall the same.

   For example, in the Ellinbank 'baseline' climate data the average rainfall event was 6.18 mm. To create the 'Rainfall distribution 10 and 20%' treatments, rain events greater than 6.18 mm where increased by 10% and 20%, with reductions of 33 and 66% for below average rainfall events imposed to keep the long-term average annual rainfall the same. Imposing this treatment did create a small increase in inter-annual rainfall variability (Table A2.)

Climate scenario	Variability treatment	Rainfall (mm)	CV %
Baseline	None	1078	14.7
	Rainfall dist. 10%	1082	15.4
	Rainfall dist. 20%	1083	16.2
	Inter-annual 10%	1090	21.4
	Inter-annual 20%	1105	28.2
2030 High impact	None	1013	14.7
	Rainfall dist. 10%	1012	15.5
	Rainfall dist. 20%	1014	16.4
	Inter-annual 10%	1024	21.4
	Inter-annual 20%	1032	28.3
2070 High impact	None	844	14.9
	Rainfall dist. 10%	840	16.0
	Rainfall dist. 20%	839	17.1
	Inter-annual 10%	848	21.9
	Inter-annual 20%	856	28.9

Table A2. 30-year average rainfall and the coefficient of variation of annual rainfall (%) at Ellinbank for the baseline, 2030 High impact and 2070 High impact climate scenarios with the changes in rainfall distribution and inter-annual variability applied.

6. Increasing inter-annual rainfall variability. Climate change projections also suggest more 'extreme' events. This was simulated by increasing the inter-annual rainfall variability. This was achieved by making the wettest 7 years in the 30-year baseline wetter by increasing rainfall by 10 and 20% and making the driest 7 years in the baseline climate were made drier by 10 and 20%, to create the 'Inter-annual 10 and 20%' treatments. The 'Inter-annual 10%' treatment was applied to the 'Rainfall distribution 10%' data-set and the 'Inter-annual 20%' treatment was applied to the 'Rainfall distribution 20%' data-set so that both rainfall distribution and inter-annual variability was altered. These treatments produced a small increase in mean rainfall but a large increase in inter-annual rainfall variability (Table A2).
7. Use of future climate data in the SGS Pasture model. The daily climate datasets produced were used as inputs into the SGS Pasture model (along with Vapour pressure, which was not scaled). From these climate inputs potential evapotranspiration was calculated by the model using the Penman-Monteith equation.

The baseline scenario monthly average minimum/ maximum temperatures and rainfall, together with the temperature and rainfall climate change statistics applied for each of the future climate scenarios, are shown for each site in the Tables A3-A15.

Table A3. The baseline monthly average minimum (Tmin, °C) and maximum (Tmax, °C) temperature and rainfall (mm), together with temperature (°C) and rainfall (%) climate change statistics applied for the six future scenarios at Malanda, Queensland (-17.35, 145.59).

	Baseline			2030 Low		2030 Medium		2030 High		2070 Low		2070 Medium		2070 High	
	Tmin (°C)	Tmax (°C)	Rain (mm)	Temp (°C)	Rain (%)	Temp (°C)	Rain (%)	Temp (°C)	Rain (%)	Temp (°C)	Rain (%)	Temp (°C)	Rain (%)	Temp (°C)	Rain (%)
Annual				0.5	-1	0.8	-1.5	1	-1.9	1.1	-2.1	2.2	-4.2	3.6	-6.8
Jan	19.1	28.1	260.9	0.6	-2.4	0.9	-3.6	1.1	-4.4	1.3	-4.9	2.5	-9.7	4.1	-15.8
Feb	19.3	27.2	338.9	0.6	2.6	0.9	3.9	1.1	4.7	1.2	5.3	2.4	10.4	4	17.1
Mar	18.4	26.1	330.5	0.6	-0.2	0.9	-0.2	1.1	-0.3	1.2	-0.3	2.5	-0.7	4	-1.1
Apr	17.1	24.2	180.5	0.5	-4.8	0.8	-7.2	1	-8.8	1.1	-9.8	2.1	-19.4	3.4	-31.7
May	15.0	22.4	117.4	0.5	-2.3	0.8	-3.4	1	-4.1	1.1	-4.7	2.1	-9.2	3.5	-15
Jun	11.9	20.9	58.9	0.5	1.9	0.8	2.8	0.9	3.5	1	3.9	2.1	7.7	3.4	12.6
Jul	11.2	20.7	47.1	0.5	-8	0.8	-11.9	0.9	-14.5	1	-16.3	2.1	-32.1	3.4	-52.6
Aug	11.8	22.1	45.1	0.5	-0.1	0.7	-0.2	0.9	-0.2	1	-0.3	2	-0.5	3.3	-0.8
Sep	13.3	24.4	39.7	0.5	1.6	0.7	2.3	0.9	2.8	1	3.2	1.9	6.3	3.1	10.3
Oct	15.4	26.7	46.0	0.5	-1.6	0.8	-2.5	1	-3	1.1	-3.4	2.1	-6.6	3.5	-10.9
Nov	17.4	28.2	108.1	0.6	0.2	0.8	0.4	1	0.5	1.1	0.5	2.2	1	3.7	1.6
Dec	18.5	28.4	159.7	0.6	-5	0.9	-7.5	1.1	-9.2	1.2	-10.3	2.4	-20.2	4	-33.2

Table A4. The baseline monthly average minimum (Tmin, °C) and maximum (Tmax, °C) temperature and rainfall (mm), together with temperature (°C) and rainfall (%) climate change statistics applied for the six future scenarios at Mutdapilly, Queensland (-27.63, 152.71).

	Baseline			2030 Low		2030 Medium		2030 High		2070 Low		2070 Medium		2070 High	
	Tmin (°C)	Tmax (°C)	Rain (mm)	Temp (°C)	Rain (%)	Temp (°C)	Rain (%)	Temp (°C)	Rain (%)	Temp (°C)	Rain (%)	Temp (°C)	Rain (%)	Temp (°C)	Rain (%)
Annual				0.7	-0.2	1	-0.3	1.2	-0.4	1.3	-0.4	2.6	-0.8	4.3	-1.3
Jan	19.7	31.0	120.6	0.6	4.6	0.9	6.8	1.1	8.4	1.2	9.4	2.5	18.5	4	30.3
Feb	19.4	30.3	112.5	0.6	2.3	0.9	3.4	1.1	4.2	1.2	4.7	2.4	9.3	4	15.2
Mar	17.5	29.5	73.0	0.6	3.8	0.9	5.7	1.1	7	1.2	7.9	2.4	15.5	3.9	25.3
Apr	14.0	27.1	70.0	0.5	-2.1	0.8	-3.1	1	-3.8	1.1	-4.3	2.2	-8.4	3.6	-13.8
May	10.9	24.1	68.5	0.6	-4.5	0.9	-6.7	1.1	-8.2	1.2	-9.2	2.4	-18.1	3.9	-29.7
Jun	6.7	21.5	33.6	0.7	-0.1	1	-0.2	1.2	-0.2	1.4	-0.2	2.7	-0.4	4.5	-0.7
Jul	5.4	21.2	39.0	0.7	-1.8	1.1	-2.7	1.3	-3.3	1.5	-3.7	2.9	-7.2	4.8	-11.8
Aug	6.2	22.6	27.8	0.7	-3	1.1	-4.5	1.3	-5.5	1.5	-6.2	2.9	-12.1	4.8	-19.9
Sep	9.4	25.7	31.0	0.7	-3.3	1	-4.9	1.2	-6	1.4	-6.8	2.7	-13.3	4.4	-21.9
Oct	13.2	27.6	72.2	0.7	-4.3	1	-6.4	1.3	-7.8	1.4	-8.8	2.8	-17.2	4.6	-28.2
Nov	16.1	29.3	92.3	0.7	-6.1	1.1	-9.1	1.3	-11.2	1.4	-12.6	2.9	-24.7	4.7	-40.6
Dec	18.3	30.9	118.5	0.7	-1.1	1	-1.7	1.3	-2.1	1.4	-2.3	2.8	-4.6	4.6	-7.6

Table A5. The baseline monthly average minimum (Tmin, °C) and maximum (Tmax, °C) temperature and rainfall (mm), together with temperature (°C) and rainfall (%) climate change statistics applied for the six future scenarios at Kyogle, NSW (-28.62, 153.00).

	Baseline			2030 Low		2030 Medium		2030 High		2070 Low		2070 Medium		2070 High	
	Tmin (°C)	Tmax (°C)	Rain (mm)	Temp (°C)	Rain (%)	Temp (°C)	Rain (%)	Temp (°C)	Rain (%)	Temp (°C)	Rain (%)	Temp (°C)	Rain (%)	Temp (°C)	Rain (%)
Annual				0.6	0.2	1	0.3	1.2	0.3	1.3	0.4	2.6	0.7	4.2	1.2
Jan	19.0	30.2	143.4	0.6	4.9	0.9	7.2	1.1	8.9	1.2	10	2.3	19.6	3.9	32.1
Feb	18.8	29.2	162.8	0.6	2.5	0.9	3.7	1.1	4.6	1.2	5.2	2.4	10.1	3.9	16.6
Mar	17.4	28.2	167.6	0.6	2.9	0.9	4.3	1.1	5.3	1.2	5.9	2.3	11.6	3.8	19.1
Apr	14.2	26.0	107.8	0.5	-0.7	0.8	-1.1	1	-1.3	1.1	-1.5	2.1	-2.9	3.5	-4.7
May	11.4	22.9	109.1	0.6	-5.1	0.9	-7.6	1.1	-9.3	1.2	-10.5	2.4	-20.6	3.9	-33.8
Jun	8.0	20.5	63.1	0.7	0.3	1	0.4	1.2	0.5	1.4	0.6	2.7	1.2	4.5	1.9
Jul	6.6	20.3	59.2	0.7	-0.6	1.1	-0.8	1.3	-1	1.5	-1.1	2.9	-2.2	4.7	-3.7
Aug	7.1	21.9	31.9	0.7	-1.6	1.1	-2.3	1.3	-2.8	1.5	-3.2	2.9	-6.3	4.7	-10.3
Sep	10.0	24.9	41.4	0.7	-3.1	1	-4.6	1.2	-5.6	1.4	-6.4	2.7	-12.5	4.4	-20.5
Oct	13.1	26.9	73.0	0.7	-3.8	1	-5.6	1.3	-6.9	1.4	-7.7	2.8	-15.2	4.6	-24.9
Nov	15.7	28.4	99.2	0.7	-4.9	1.1	-7.3	1.3	-8.9	1.4	-10	2.8	-19.7	4.7	-32.3
Dec	17.7	30.0	118.6	0.7	0.1	1	0.2	1.2	0.2	1.3	0.3	2.6	0.5	4.3	0.9

Table A6. The baseline monthly average minimum (Tmin, °C) and maximum (Tmax, °C) temperature and rainfall (mm), together with temperature (°C) and rainfall (%) climate change statistics applied for the six future scenarios at Barraba, NSW (-30.55, 150.65).

	Baseline			2030 Low		2030 Medium		2030 High		2070 Low		2070 Medium		2070 High	
	Tmin (°C)	Tmax (°C)	Rain (mm)	Temp (°C)	Rain (%)	Temp (°C)	Rain (%)	Temp (°C)	Rain (%)	Temp (°C)	Rain (%)	Temp (°C)	Rain (%)	Temp (°C)	Rain (%)
Annual				0.7	0.8	1	1.2	1.2	1.4	1.4	1.6	2.7	3.2	4.4	5.2
Jan	16.6	31.1	99.9	0.6	6	0.9	9	1.1	11	1.2	12.4	2.4	24.3	4	39.8
Feb	16.3	30.4	72.7	0.6	4.3	0.9	6.3	1.1	7.8	1.2	8.7	2.4	17.2	3.9	28.1
Mar	13.7	28.7	42.6	0.6	4.7	0.9	7	1.1	8.5	1.2	9.6	2.3	18.8	3.8	30.9
Apr	9.3	24.5	37.0	0.5	-0.4	0.8	-0.7	1	-0.8	1.1	-0.9	2.2	-1.8	3.6	-2.9
May	6.1	20.2	49.8	0.6	-1.8	0.9	-2.6	1.1	-3.2	1.2	-3.6	2.4	-7.1	3.9	-11.7
Jun	2.7	16.2	32.8	0.6	-2.2	0.9	-3.3	1.1	-4	1.3	-4.5	2.5	-8.9	4.1	-14.6
Jul	1.6	15.5	44.4	0.7	-2.8	1	-4.2	1.2	-5.2	1.4	-5.8	2.7	-11.4	4.4	-18.7
Aug	2.3	17.4	33.8	0.7	-3.2	1	-4.7	1.3	-5.8	1.4	-6.5	2.8	-12.7	4.6	-20.9
Sep	5.2	20.9	41.8	0.8	0.1	1.2	0.1	1.4	0.1	1.6	0.1	3.1	0.2	5.1	0.4
Oct	9.1	24.3	58.1	0.8	-5.9	1.2	-8.8	1.5	-10.7	1.7	-12.1	3.3	-23.7	5.4	-38.9
Nov	12.3	27.2	73.0	0.8	-3.1	1.3	-4.6	1.5	-5.6	1.7	-6.3	3.4	-12.5	5.6	-20.4
Dec	15.1	30.4	74.9	0.7	-0.4	1.1	-0.7	1.3	-0.8	1.5	-0.9	3	-1.8	4.9	-2.9

Table A7. The baseline monthly average minimum (Tmin, °C) and maximum (Tmax, °C) temperature and rainfall (mm), together with temperature (°C) and rainfall (%) climate change statistics applied for the six future scenarios at Albany, WA (-34.90, 117.80).

	Baseline			2030 Low		2030 Medium		2030 High		2070 Low		2070 Medium		2070 High	
	Tmin (°C)	Tmax (°C)	Rain (mm)	Temp (°C)	Rain (%)	Temp (°C)	Rain (%)	Temp (°C)	Rain (%)	Temp (°C)	Rain (%)	Temp (°C)	Rain (%)	Temp (°C)	Rain (%)
Annual				0.5	-3.2	0.7	-4.7	0.9	-5.8	1	-6.5	2	-12.8	3.3	-20.9
Jan	13.9	25.1	27.4	0.4	6.3	0.6	9.3	0.8	11.4	0.9	12.8	1.7	25.2	2.8	41.4
Feb	14.5	25.3	23.7	0.5	5.2	0.7	7.8	0.8	9.6	0.9	10.8	1.9	21.2	3.1	34.7
Mar	13.6	24.2	33.2	0.5	-6.8	0.8	-10.2	0.9	-12.4	1.1	-14	2.1	-27.5	3.4	-45
Apr	11.7	22.2	49.3	0.6	3.2	0.9	4.7	1.1	5.8	1.2	6.5	2.3	12.8	3.8	21
May	9.9	19.0	95.2	0.5	-0.8	0.7	-1.1	0.9	-1.4	1	-1.6	2	-3.1	3.3	-5.1
Jun	8.1	16.8	92.8	0.5	-4.7	0.7	-7	0.9	-8.5	1	-9.6	1.9	-18.9	3.1	-30.9
Jul	7.6	15.9	115.4	0.5	-6.4	0.7	-9.5	0.8	-11.7	1	-13.1	1.9	-25.8	3.1	-42.2
Aug	7.6	16.2	99.9	0.5	-6.5	0.7	-9.7	0.9	-11.8	1	-13.3	2	-26.1	3.3	-42.8
Sep	8.1	17.6	82.8	0.5	-9.9	0.7	-14.7	0.9	-18	1	-20.3	1.9	-39.9	3.1	-65.4
Oct	9.1	18.9	70.4	0.5	-6.3	0.8	-9.4	0.9	-11.5	1.1	-12.9	2.1	-25.5	3.4	-41.7
Nov	10.8	21.0	48.4	0.5	-7.8	0.7	-11.7	0.9	-14.3	1	-16	1.9	-31.5	3.1	-51.7
Dec	12.6	23.5	22.3	0.5	2.3	0.8	3.5	0.9	4.2	1.1	4.8	2.1	9.3	3.4	15.3

Table A8. The baseline monthly average minimum (Tmin, °C) and maximum (Tmax, °C) temperature and rainfall (mm), together with temperature (°C) and rainfall (%) climate change statistics applied for the six future scenarios at Wagga Wagga, NSW (-35.10, 147.30).

	Baseline			2030 Low		2030 Medium		2030 High		2070 Low		2070 Medium		2070 High	
	Tmin (°C)	Tmax (°C)	Rain (mm)	Temp (°C)	Rain (%)	Temp (°C)	Rain (%)	Temp (°C)	Rain (%)	Temp (°C)	Rain (%)	Temp (°C)	Rain (%)	Temp (°C)	Rain (%)
Annual				0.4	-4.6	0.6	-6.9	0.7	-8.4	0.8	-9.5	1.5	-18.6	2.5	-30.5
Jan	16.5	31.4	43.9	0.3	-1.2	0.5	-1.7	0.6	-2.1	0.7	-2.4	1.4	-4.7	2.2	-7.7
Feb	16.9	31.2	37.3	0.3	4.8	0.5	7.2	0.6	8.8	0.6	9.9	1.3	19.5	2.1	31.9
Mar	13.9	27.8	35.7	0.3	-2.4	0.5	-3.6	0.6	-4.4	0.7	-5	1.3	-9.7	2.2	-16
Apr	9.7	22.6	44.7	0.4	-2.6	0.6	-3.9	0.7	-4.8	0.8	-5.4	1.5	-10.7	2.4	-17.5
May	7.1	17.8	54.8	0.4	-4.7	0.6	-7	0.7	-8.5	0.8	-9.6	1.5	-18.9	2.5	-31
Jun	4.2	13.9	46.7	0.4	-6.8	0.6	-10.1	0.7	-12.3	0.8	-13.9	1.6	-27.3	2.7	-44.7
Jul	3.2	12.9	54.9	0.4	-4.9	0.6	-7.3	0.8	-8.9	0.9	-10	1.8	-19.7	2.9	-32.3
Aug	4.2	14.7	52.6	0.4	-6.6	0.6	-9.8	0.8	-12	0.9	-13.5	1.7	-26.6	2.8	-43.6
Sep	6.0	17.6	51.5	0.4	-8.5	0.6	-12.7	0.8	-15.5	0.9	-17.4	1.7	-34.3	2.8	-56.2
Oct	8.4	21.5	58.9	0.4	-6.1	0.6	-9.1	0.7	-11.2	0.8	-12.6	1.6	-24.7	2.7	-40.5
Nov	11.3	25.8	41.3	0.4	-2.5	0.6	-3.7	0.7	-4.5	0.8	-5.1	1.5	-9.9	2.5	-16.3
Dec	14.4	29.6	42.5	0.4	-4.3	0.5	-6.4	0.7	-7.9	0.7	-8.8	1.5	-17.4	2.4	-28.5

Table A9. The baseline monthly average minimum (Tmin, °C) and maximum (Tmax, °C) temperature and rainfall (mm), together with temperature (°C) and rainfall (%) climate change statistics applied for the six future scenarios at Kyabram, Victoria (-36.34, 145.06).

	Baseline			2030 Low		2030 Medium		2030 High		2070 Low		2070 Medium		2070 High	
	Tmin (°C)	Tmax (°C)	Rain (mm)	Temp (°C)	Rain (%)	Temp (°C)	Rain (%)	Temp (°C)	Rain (%)	Temp (°C)	Rain (%)	Temp (°C)	Rain (%)	Temp (°C)	Rain (%)
Annual				0.6	-3	0.8	-4.4	1	-5.4	1.2	-6.1	2.3	-11.9	3.7	-19.5
Jan	14.2	29.5	37.7	0.7	-1.5	1	-2.2	1.2	-2.7	1.3	-3	2.6	-5.9	4.3	-9.7
Feb	14.7	29.6	26.7	0.6	4.3	0.9	6.4	1.1	7.8	1.2	8.8	2.4	17.3	3.9	28.4
Mar	12.4	26.3	27.8	0.6	-0.8	0.8	-1.2	1	-1.4	1.1	-1.6	2.2	-3.1	3.7	-5.1
Apr	8.6	21.4	38.0	0.5	-0.7	0.8	-1.1	1	-1.3	1.1	-1.5	2.2	-2.9	3.6	-4.7
May	6.3	17.2	47.5	0.5	-4.8	0.7	-7.2	0.9	-8.8	1	-9.9	1.9	-19.5	3.1	-32
Jun	3.8	13.8	41.3	0.4	-5.9	0.7	-8.8	0.8	-10.8	0.9	-12.2	1.8	-23.9	2.9	-39.2
Jul	2.9	13.0	46.0	0.5	-2.6	0.7	-3.8	0.9	-4.7	1	-5.3	1.9	-10.3	3.1	-16.9
Aug	3.9	14.7	46.8	0.5	-4.6	0.8	-6.8	0.9	-8.4	1.1	-9.4	2.1	-18.5	3.4	-30.3
Sep	5.5	17.2	46.7	0.6	-6.8	0.9	-10.1	1.1	-12.4	1.3	-13.9	2.5	-27.4	4.1	-44.8
Oct	7.6	20.7	46.7	0.6	-6.3	1	-9.4	1.2	-11.5	1.3	-13	2.6	-25.5	4.2	-41.8
Nov	10.2	24.4	36.8	0.6	-3.9	0.9	-5.8	1.1	-7.1	1.3	-8	2.5	-15.7	4.1	-25.7
Dec	12.4	27.8	28.0	0.6	-5.3	1	-7.8	1.2	-9.6	1.3	-10.8	2.6	-21.2	4.3	-34.8

Table A10. The baseline monthly average minimum (Tmin, °C) and maximum (Tmax, °C) temperature and rainfall (mm), together with temperature (°C) and rainfall (%) climate change statistics applied for the six future scenarios at Dookie, Victoria (-36.37, 145.70).

	Baseline			2030 Low		2030 Medium		2030 High		2070 Low		2070 Medium		2070 High	
	Tmin (°C)	Tmax (°C)	Rain (mm)	Temp (°C)	Rain (%)	Temp (°C)	Rain (%)	Temp (°C)	Rain (%)	Temp (°C)	Rain (%)	Temp (°C)	Rain (%)	Temp (°C)	Rain (%)
Annual				0.6	-2.6	0.8	-3.9	1	-4.7	1.2	-5.3	2.3	-10.5	3.7	-17.2
Jan	13.7	28.9	44.4	0.6	-0.8	1	-1.2	1.2	-1.4	1.3	-1.6	2.6	-3.1	4.3	-5.2
Feb	14.1	29.1	31.5	0.6	5.2	0.9	7.8	1.1	9.5	1.2	10.7	2.4	21	3.9	34.5
Mar	11.7	25.6	37.3	0.5	-1.1	0.8	-1.6	1	-2	1.1	-2.2	2.2	-4.3	3.6	-7.1
Apr	8.0	20.4	48.0	0.5	-0.8	0.8	-1.2	1	-1.5	1.1	-1.7	2.2	-3.4	3.6	-5.5
May	5.7	16.0	56.9	0.5	-4.3	0.7	-6.3	0.9	-7.8	1	-8.7	1.9	-17.2	3.1	-28.1
Jun	3.3	12.5	52.4	0.4	-5.4	0.7	-8	0.8	-9.8	0.9	-11.1	1.8	-21.7	2.9	-35.6
Jul	2.4	11.4	60.8	0.5	-2.1	0.7	-3.2	0.9	-3.9	1	-4.4	1.9	-8.6	3.1	-14.1
Aug	3.4	13.1	62.9	0.5	-4.5	0.8	-6.7	0.9	-8.2	1.1	-9.2	2.1	-18.1	3.4	-29.6
Sep	5.1	15.9	60.0	0.6	-6.5	0.9	-9.7	1.1	-11.9	1.3	-13.3	2.5	-26.2	4.1	-43
Oct	7.1	19.4	54.2	0.7	-6.5	1	-9.7	1.2	-11.9	1.3	-13.4	2.7	-26.3	4.3	-43.1
Nov	9.5	23.4	45.6	0.6	-3.3	0.9	-4.9	1.2	-5.9	1.3	-6.7	2.5	-13.1	4.2	-21.5
Dec	11.8	26.9	38.5	0.7	-4.8	1	-7.1	1.2	-8.7	1.4	-9.8	2.7	-19.3	4.4	-31.6

Table A11. The baseline monthly average minimum (Tmin, °C) and maximum (Tmax, °C) temperature and rainfall (mm), together with temperature (°C) and rainfall (%) climate change statistics applied for the six future scenarios at Vasey, Victoria (-37.40, 141.90).

	Baseline			2030 Low		2030 Medium		2030 High		2070 Low		2070 Medium		2070 High	
	Tmin (°C)	Tmax (°C)	Rain (mm)	Temp (°C)	Rain (%)	Temp (°C)	Rain (%)	Temp (°C)	Rain (%)	Temp (°C)	Rain (%)	Temp (°C)	Rain (%)	Temp (°C)	Rain (%)
Annual				0.4	-4.4	0.7	-6.6	0.8	-8.1	0.9	-9.1	1.8	-17.9	2.9	-29.3
Jan	11.1	26.5	28.6	0.5	-2.5	0.7	-3.7	0.9	-4.5	1	-5.1	2	-10	3.2	-16.5
Feb	11.4	27.4	21.7	0.5	0.2	0.7	0.3	0.9	0.4	1	0.4	1.9	0.8	3.1	1.4
Mar	10.1	24.1	31.2	0.4	1.3	0.6	2	0.8	2.4	0.9	2.7	1.7	5.3	2.7	8.7
Apr	7.8	19.5	45.6	0.4	-3	0.6	-4.5	0.8	-5.6	0.9	-6.2	1.7	-12.3	2.8	-20.1
May	6.3	15.6	64.2	0.4	-5.8	0.6	-8.7	0.7	-10.6	0.8	-12	1.6	-23.5	2.6	-38.5
Jun	4.3	12.6	71.5	0.4	-6.7	0.6	-10	0.7	-12.3	0.8	-13.8	1.6	-27.1	2.6	-44.5
Jul	3.8	12.0	79.0	0.4	-3.6	0.6	-5.4	0.7	-6.6	0.8	-7.5	1.7	-14.7	2.7	-24
Aug	4.4	13.2	80.0	0.4	-4.2	0.6	-6.2	0.8	-7.6	0.9	-8.6	1.7	-16.9	2.8	-27.7
Sep	5.4	15.2	75.4	0.5	-8.5	0.7	-12.7	0.8	-15.5	0.9	-17.5	1.8	-34.3	3	-56.3
Oct	6.4	17.9	63.3	0.5	-6.2	0.7	-9.2	0.8	-11.3	0.9	-12.7	1.9	-24.9	3	-40.8
Nov	7.8	21.0	45.0	0.5	-5.1	0.7	-7.6	0.8	-9.3	0.9	-10.5	1.8	-20.6	3	-33.8
Dec	9.6	24.3	34.6	0.5	-5.9	0.7	-8.8	0.8	-10.7	0.9	-12.1	1.9	-23.7	3	-38.9

Table A12. The baseline monthly average minimum (Tmin, °C) and maximum (Tmax, °C) temperature and rainfall (mm), together with temperature (°C) and rainfall (%) climate change statistics applied for the six future scenarios at Hamilton, Victoria (-37.83, 142.06).

	Baseline			2030 Low		2030 Medium		2030 High		2070 Low		2070 Medium		2070 High	
	Tmin (°C)	Tmax (°C)	Rain (mm)	Temp (°C)	Rain (%)	Temp (°C)	Rain (%)	Temp (°C)	Rain (%)	Temp (°C)	Rain (%)	Temp (°C)	Rain (%)	Temp (°C)	Rain (%)
Annual				0.4	-4.5	0.6	-6.7	0.8	-8.2	0.9	-9.2	1.7	-18.2	2.8	-29.8
Jan	10.4	25.1	35.1	0.5	-2.9	0.7	-4.3	0.9	-5.2	1	-5.9	1.9	-11.6	3.1	-19
Feb	10.8	26.1	24.8	0.5	0.1	0.7	0.2	0.8	0.2	0.9	0.3	1.8	0.5	3	0.9
Mar	9.7	23.2	39.2	0.4	1.4	0.6	2.1	0.7	2.5	0.8	2.8	1.6	5.6	2.6	9.1
Apr	7.8	19.0	51.2	0.4	-3.4	0.6	-5	0.8	-6.2	0.9	-6.9	1.7	-13.7	2.7	-22.4
May	6.4	15.4	62.3	0.4	-5.8	0.6	-8.7	0.7	-10.6	0.8	-11.9	1.5	-23.5	2.5	-38.5
Jun	4.6	12.6	70.7	0.4	-6.7	0.6	-9.9	0.7	-12.2	0.8	-13.7	1.6	-26.9	2.6	-44.1
Jul	4.2	12.1	80.8	0.4	-3.6	0.6	-5.4	0.7	-6.7	0.8	-7.5	1.6	-14.7	2.6	-24.1
Aug	4.8	13.1	80.5	0.4	-4.1	0.6	-6.1	0.8	-7.4	0.8	-8.4	1.7	-16.4	2.7	-26.9
Sep	5.6	14.8	80.3	0.4	-8.5	0.6	-12.6	0.8	-15.4	0.9	-17.4	1.7	-34.1	2.8	-55.9
Oct	6.3	17.0	67.7	0.4	-6	0.7	-8.9	0.8	-10.9	0.9	-12.3	1.8	-24.2	2.9	-39.6
Nov	7.4	19.6	52.5	0.4	-5.2	0.7	-7.7	0.8	-9.5	0.9	-10.7	1.8	-21	2.9	-34.4
Dec	9.0	22.7	44.1	0.4	-5.7	0.7	-8.5	0.8	-10.4	0.9	-11.7	1.8	-22.9	2.9	-37.6

Table A13. The baseline monthly average minimum (Tmin, °C) and maximum (Tmax, °C) temperature and rainfall (mm), together with temperature (°C) and rainfall (%) climate change statistics applied for the six future scenarios at Terang, Victoria (-38.15, 142.55).

	Baseline			2030 Low		2030 Medium		2030 High		2070 Low		2070 Medium		2070 High	
	Tmin (°C)	Tmax (°C)	Rain (mm)	Temp (°C)	Rain (%)	Temp (°C)	Rain (%)	Temp (°C)	Rain (%)	Temp (°C)	Rain (%)	Temp (°C)	Rain (%)	Temp (°C)	Rain (%)
Annual				0.4	-4.3	0.6	-6.5	0.8	-7.9	0.9	-8.9	1.7	-17.6	2.8	-28.8
Jan	12.0	24.1	40.2	0.5	-3.3	0.7	-5	0.9	-6.1	1	-6.9	2	-13.5	3.2	-22.1
Feb	12.4	24.9	28.4	0.5	0	0.7	-0.1	0.9	-0.1	1	-0.1	1.9	-0.1	3.1	-0.2
Mar	11.3	22.6	40.8	0.4	1.9	0.6	2.9	0.7	3.5	0.8	4	1.6	7.8	2.6	12.8
Apr	9.2	19.2	58.1	0.4	-3.8	0.6	-5.6	0.8	-6.9	0.9	-7.8	1.7	-15.2	2.8	-25
May	7.7	16.1	66.9	0.4	-5.7	0.6	-8.5	0.7	-10.4	0.8	-11.7	1.6	-23	2.6	-37.7
Jun	5.7	13.4	77.3	0.4	-6.2	0.6	-9.3	0.7	-11.3	0.8	-12.8	1.6	-25.1	2.6	-41.1
Jul	5.1	12.8	78.1	0.4	-3	0.6	-4.5	0.7	-5.5	0.8	-6.1	1.6	-12.1	2.7	-19.8
Aug	5.7	13.8	86.9	0.4	-3.4	0.6	-5.1	0.7	-6.2	0.8	-7	1.6	-13.7	2.6	-22.5
Sep	6.7	15.4	83.2	0.4	-8.4	0.6	-12.6	0.7	-15.4	0.8	-17.3	1.6	-34	2.7	-55.7
Oct	7.7	17.5	75.5	0.4	-5.5	0.6	-8.2	0.8	-10	0.9	-11.3	1.7	-22.2	2.8	-36.4
Nov	9.0	19.7	60.4	0.4	-5.9	0.7	-8.8	0.8	-10.8	0.9	-12.2	1.8	-23.9	2.9	-39.2
Dec	10.5	22.1	49.8	0.4	-6	0.7	-9	0.8	-11	0.9	-12.4	1.8	-24.4	3	-39.9

Table A14. The baseline monthly average minimum (Tmin, °C) and maximum (Tmax, °C) temperature and rainfall (mm), together with temperature (°C) and rainfall (%) climate change statistics applied for the six future scenarios at Ellinbank, Victoria (-38.25, 145.93).

	Baseline			2030 Low		2030 Medium		2030 High		2070 Low		2070 Medium		2070 High	
	Tmin (°C)	Tmax (°C)	Rain (mm)	Temp (°C)	Rain (%)	Temp (°C)	Rain (%)	Temp (°C)	Rain (%)	Temp (°C)	Rain (%)	Temp (°C)	Rain (%)	Temp (°C)	Rain (%)
Annual				0.5	-2.8	0.7	-4.2	0.9	-5.1	1	-5.7	2	-11.2	3.3	-18.4
Jan	12.7	24.4	65.5	0.6	-2.7	0.9	-4	1.1	-4.9	1.2	-5.6	2.4	-10.9	3.9	-17.9
Feb	13.2	25.5	45.8	0.5	0.8	0.8	1.2	1	1.4	1.1	1.6	2.2	3.2	3.5	5.2
Mar	11.9	22.8	63.6	0.5	1.8	0.7	2.6	0.9	3.2	1	3.6	1.9	7.1	3.2	11.7
Apr	9.5	19.0	81.7	0.5	-1.1	0.7	-1.7	0.8	-2.1	0.9	-2.3	1.8	-4.6	3	-7.6
May	7.6	15.8	97.0	0.4	-3.6	0.7	-5.4	0.8	-6.6	0.9	-7.5	1.8	-14.6	2.9	-24
Jun	5.5	13.0	103.8	0.5	-3.8	0.7	-5.7	0.8	-7	0.9	-7.8	1.8	-15.4	3	-25.3
Jul	4.7	12.4	107.7	0.5	-0.9	0.7	-1.4	0.8	-1.7	0.9	-1.9	1.9	-3.8	3	-6.2
Aug	5.5	13.6	107.3	0.5	-1.3	0.7	-2	0.8	-2.4	0.9	-2.7	1.8	-5.4	3	-8.8
Sep	6.6	15.5	114.0	0.5	-6.8	0.7	-10.2	0.9	-12.5	1	-14	1.9	-27.5	3.2	-45.1
Oct	8.1	17.8	111.7	0.5	-6.3	0.8	-9.4	0.9	-11.5	1.1	-13	2.1	-25.5	3.4	-41.8
Nov	9.6	19.9	92.9	0.5	-4.3	0.8	-6.4	1	-7.9	1.1	-8.9	2.2	-17.4	3.5	-28.5
Dec	11.2	22.4	86.9	0.5	-6.2	0.8	-9.3	1	-11.4	1.1	-12.8	2.2	-25.1	3.6	-41.2

Table A15. The baseline monthly average minimum (Tmin, °C) and maximum (Tmax, °C) temperature and rainfall (mm), together with temperature (°C) and rainfall (%) climate change statistics applied for the six future scenarios at Elliott, Tasmania (-41.08, 145.77).

	Baseline			2030 Low		2030 Medium		2030 High		2070 Low		2070 Medium		2070 High	
	Tmin (°C)	Tmax (°C)	Rain (mm)	Temp (°C)	Rain (%)	Temp (°C)	Rain (%)	Temp (°C)	Rain (%)	Temp (°C)	Rain (%)	Temp (°C)	Rain (%)	Temp (°C)	Rain (%)
Annual				0.4	-3.1	0.6	-4.6	0.7	-5.6	0.8	-6.3	1.5	-12.3	2.5	-20.2
Jan	11.1	20.3	59.7	0.5	-4.3	0.7	-6.4	0.9	-7.9	1	-8.9	1.9	-17.4	3.1	-28.6
Feb	11.6	20.7	47.5	0.5	1	0.7	1.5	0.9	1.9	1	2.1	1.9	4.1	3.1	6.7
Mar	10.4	19.1	57.5	0.4	0	0.5	0	0.7	0	0.7	0	1.5	0	2.4	0.1
Apr	8.4	16.4	101.0	0.4	-3.5	0.6	-5.2	0.7	-6.4	0.8	-7.2	1.5	-14.2	2.5	-23.2
May	7.0	14.0	125.8	0.4	-4	0.6	-6	0.7	-7.3	0.8	-8.2	1.5	-16.2	2.5	-26.6
Jun	5.0	11.8	129.1	0.4	-4.8	0.6	-7.1	0.7	-8.7	0.8	-9.8	1.6	-19.3	2.6	-31.6
Jul	4.3	11.2	161.6	0.4	-1.3	0.5	-1.9	0.7	-2.4	0.8	-2.7	1.5	-5.3	2.4	-8.6
Aug	4.6	11.7	141.8	0.3	-1.5	0.5	-2.2	0.6	-2.7	0.7	-3	1.4	-6	2.3	-9.8
Sep	5.4	13.1	128.5	0.3	-5	0.5	-7.5	0.6	-9.2	0.7	-10.3	1.3	-20.3	2.2	-33.2
Oct	6.4	15.0	105.2	0.3	-4.3	0.5	-6.4	0.6	-7.8	0.7	-8.8	1.3	-17.3	2.1	-28.4
Nov	8.1	16.9	81.6	0.4	-3.7	0.6	-5.6	0.7	-6.8	0.8	-7.6	1.5	-15	2.5	-24.6
Dec	9.5	18.7	80.8	0.4	-3.4	0.6	-5.1	0.7	-6.2	0.8	-7	1.7	-13.8	2.7	-22.6